Journal of CO2 Utilization 77 (2023) 102605

Contents lists available at ScienceDirect

Journal of CO2 Utilization

journal homepage: www.elsevier.com/locate/jcou

Review article

Compressed carbon dioxide as a medium in catalytic hydrogenations: Engineering and chemistry

Garima Garg [a,c,1], Montserrat Gómez [a], Anna M. Masdeu-Bultó [b,*], Yaocihuatl Medina González [c]

[a] Laboratoire Hétérochimie Fondamentale et Appliquée, UMR CNRS 5069, Université Toulouse 3 – Paul Sabatier, 118 route de Narbonne, 31062 Toulouse Cedex 9, France
[b] Department of Physical and Inorganic Chemistry, University Rovira i Virgili, 43007 Tarragona, Spain
[c] Laboratory of the Future, UMR 5258 CNRS Solvay Université de Bordeaux, 178 Avenue du Dr. Schweitzer, 33600 Pessac, France

ARTICLE INFO

Keywords:
Compressed carbon dioxide
Carbon dioxide expanded liquids
Homogeneous catalysis
Nanocatalysis
Solvent engineering
Hydrogenation

ABSTRACT

In the frame of designing eco-friendly chemical processes, solvents represent a crucial economic and environmental concern. Compressed carbon dioxide (CO_2) is an alternative green solvent for many industrial applications. Herein, we present the most relevant aspects of using compressed CO_2 in metal-catalyzed hydrogenation reactions. In the first part, we discuss engineering fundamentals for the description of processes in supercritical fluids, gas-expanded liquids, continuous-flow applications and process design, including safety aspects and examples of heterogeneous catalysis. In the second part, we focus on catalytic systems based on both metal complexes and nano-systems, emphasizing how the catalysts have been adapted to the specificity of CO_2. For this purpose, significant aspects such as the catalyst design, the reaction conditions and the use of co-solvents are considered. The main goal of this review is to show the advantages of using this green solvent in catalytic hydrogenations, including a critical analysis concerning its limitations.

1. Introduction

In the last decades, the concerns of society about environmental issues caused by chemical processes have undeniably increased. As a result, the called Green Chemistry ideology expressed and collected by Anastas emerged as the 12 Green Chemistry Principles [1]; shortly after, the Sandestin declaration established the principles of Green Engineering [2]. Catalysis can integrate many of these Green concepts such as lowering the energy of the processes, increasing the selectivity of the reactions avoiding by-products, decreasing the separation and purification steps compared with stoichiometric reactions, and adapting to engineering sustainable solutions, in particular maximizing efficiency as in the intensification of processes [1].

Another important issue of chemical transformations is the use of volatile organic solvents in different stages of the processes (e.g., reaction medium, separation and purification steps, analysis of products), most of them hazardous substances such as aromatic (toluene, xylenes) and chlorinated compounds. Non-toxic solvents, like compressed CO_2, have, thus, emerged as a green alternative to volatile organic compounds [3]. Besides, CO_2 is an abundant compound produced in industrial combustion processes and emitted into the atmosphere, contributing to global warming. Therefore, an increasing industrial interest in carbon dioxide capture and utilization has appeared as proven by the growing number of patents published in recent years related to this subject [4,5]. Using compressed CO_2 as a solvent is also a way to reassess this gas. In addition, CO_2, easily recycled after the reaction by simple depressurization-pressurization cycles, turns into an attractive solvent for chemical transformations at industrial scale [6].

Supercritical fluids are fully miscible with gases eliminating the mass transfer issue at the gas-liquid interface, thus, the rate of the reactions involving gases as reactants usually increases [7]. This is the case of the hydrogenation reactions in supercritical carbon dioxide ($scCO_2$) in which the concentration of hydrogen in the supercritical phase is much higher than using organic solvents with limited hydrogen solubility. This may be especially useful when the hydrogen solubility in the catalyst-containing phase or the mass transfer of hydrogen into the solid catalyst are the limiting factors [8]. Thus, it is essential to design a chemical process taking into account phases equilibria, and transport phenomena. In metal-based homogeneous catalysis, where the catalyst (a metal complex or nanoparticle-based system) is soluble or

* Corresponding author.
E-mail address: annamaria.masdeu@urv.cat (A.M. Masdeu-Bultó).
[1] Current adress: Department of Chemistry and Biochemistry, University of Windsor, 401 Sunset Avenue, Windsor N9B 3P4, Canada

https://doi.org/10.1016/j.jcou.2023.102605
Received 22 July 2023; Received in revised form 3 October 2023; Accepted 12 October 2023
Available online 19 October 2023

well-dispersed in the supercritical medium, the high solubility of hydrogen in $scCO_2$ usually triggers high reaction rate by increasing its concentration in the catalytic phase. Also, the properties of CO_2 can modify the equilibria of the different catalytic species causing changes in selectivity.

Moreover, the perspective of green production of H_2 using renewable energies opens new possibilities for this gas to obtain biomass-derived chemicals or to transform harmful substances such as aromatics, haloarenes and nitroarenes.

Other considerations are related to the use of other solvents combined with compressed CO_2 (e.g., alcohols, water or ionic liquids,[1] among the most used). The addition of these co-solvents leads to a plethora of properties that can be tuned for a specific catalytic system. In this way, a wide range of reaction media is possible, for example, CO_2-miscible co-solvents or biphasic systems with non-CO_2 soluble substances such as appropriate ionic liquids (ILs) [9–11].

CO_2 has not only been used as a solvent under the supercritical phase but, for some transformations, under subcritical conditions [12], requiring a deep optimization of parameters. The combination of compressed CO_2 with solvents under subcritical conditions leads to CO_2-expanded liquids [13,14].

It is noteworthy that compressed CO_2 as a solvent for hydrogenation reactions has important advantages but also some limitations. Advantages are related to its low toxicity compared with most current organic solvents. The availability of CO_2 is predicted to increase shortly, and thus, the price decrease, as the recovery technologies from the exhaust gases from power plants and thus industrial applications will grow. The possibility of being easily recycled by expansion/compression cycles in an accessible range of pressure and temperature ($Tc = 304.13$ K and $Pc = 7.375$ MPa) [15] may decrease the energy cost of separation from the excess hydrogen and the products from the hydrogenation reaction mixture. Additionally, in a gas reactant reaction like hydrogenation, the mass transfer issues in heterogeneous systems are drastically reduced by using a solvent in a supercritical phase and that affects the activity and also selectivity of the reaction. Unfortunately, there are also drawbacks, some of them associated to the low polarity of CO_2, which hampers the solubility of molecular polar catalysts and substrates. Another issue of the CO_2 recovered from the different processes is its low purity since other gases such as nitrogen, argon, oxygen or carbon monoxide can be present and interfere with catalytic materials [16]. Moreover, the costs associated to the use of a compressed medium may be an obstacle for industrial applications at a high scale. However, several industrial processes are currently applied using $scCO_2$ [17], such as the extraction of natural products for being applied in the production of drugs, cosmetics, food ingredients and also for biological purposes [18] as solvent for biorefinery [19–21] or for polymerization processes [22].

In this review, we focus on the most relevant aspects related to the use of compressed CO_2 as a medium in metal-catalyzed hydrogenation reactions. In previously published revisions, catalytic hydrogenation reactions under the dense CO_2 phase were included using homogeneous and heterogeneous catalysis [23–29], metal-based nanocatalysts [30] and continuous flow processes [31]. In this review, an update of results is presented, including an original approach regarding engineering aspects related to compressed fluids properties which are crucial for the performance of the catalysts, and highlighting processes involving substrates from biomass with relevant industrial applications.

In Table 1, selected catalysts (homogeneous, heterogeneous, nanocatalysts) and processes (batch, continuous flow…) involved in compressed carbon dioxide hydrogenations are listed. Each catalyst type and substrate has its own characteristics that have to be taken into account to perform efficient hydrogenation reactions in compressed carbon dioxide. When using heterogeneous catalysts (entries 1 and 2, Table 1), mass transfer is an issue and the solubility of the substrate and hydrogen in the medium can be also decisive. Solubility of H_2 in common organic solvents is limited [32] but full miscibility can be achieved when using $scCO_2$. The solubility of the substrates in $scCO_2$ depends on the nature of the interaction between solute and CO_2 including quadrupolar interactions, participation of its weak Lewis acidity or basicity and H-bond formation [33]. Furthermore, it can be tuned by introducing co-solvents [34] or in carbon dioxide-expanded systems (CXL, entry 2, Table 1). In some cases the expanded liquid is formed by the CO_2-liquid substrate and, although is desirable that substrate and hydrogen are in a single phase, some biphasic systems with partial insolubilized substrate are more active than when all the substrate is solubilized due to dilution effects [11]. Homogeneous systems based on organometallic complexes are excellent candidates for enantioselective hydrogenation of prochiral substrates with high added value for fine chemical industry (entry 3 and 4, Table 1). Nevertheless, the catalyst separation is costly using homogeneous catalytic systems; the catalyst heterogenization by immobilization on inorganic solids has led to efficient systems (entry 3, Table 1). Nanocatalysts can take advantage of the modulation capacity of molecular catalysts together with the surface reactivity of heterogeneous catalytic systems (entry 5, Table 1). Furthermore, heterogenized nanocatalysts supported on inorganic solids have led to highly active and selective systems (entry 6, Table 1). Examples of these systems are discussed all along the revision. Thus, in sections from 2 to 5, engineering fundamentals for the description of processes in supercritical fluids, gas-expanded liquids, continuous-flow applications, and process design including safety aspects are discussed. Examples mainly from heterogeneous catalysis which show how important is the knowledge of phase equilibrium and mass transfer, for example, in the performance of the catalyst thus affecting the activity and the selectivity of the reaction, are considered. The selected literature included in this part of the review will be in particular useful for readers willing to work with compressed carbon dioxide but less aware of engineering aspects.

Section 6 is devoted to hydrogenations involving organometallic complexes-based catalytic systems, focusing mostly on substrates obtained from biomass and/or exhibiting industrial applications. Critical issues in this section are the design of $scCO_2$ soluble systems, chemo- and (enantio)selectivity, and immobilization of the molecular catalysts to afford continuous-flow systems. In the last section, nanocatalysts as highly performance systems with potential in the selective hydrogenation of aromatic and renewable substrates are presented. In both cases, molecular and nano-catalysts, neat compressed CO_2 or CO_2 combined with other solvents in bi- or multiphasic systems are considered. The design of catalysts, the selection of reaction conditions, and the choice of co-solvents are discussed, highlighting the advantages and limitations of using CO_2 as a reaction medium.

2. Engineering aspects of catalytic hydrogenation reactions in supercritical fluids

This section aims to review the basic parameters that are key when chemical processes are developed, optimized or designed in supercritical fluids, in particular for hydrogenation reactions. This section is organized to present phases of equilibrium and mass and heat transfer, which are key phenomena in chemical engineering; then continuous chemical processes, reactor modeling, process design and safety issues, are discussed. Other key features that will be addressed concern potential sustainability advantages as well as the challenges for practical implementation of the innovations proposed in the literature.

It is worth noting that even if supercritical fluids and gas-expanded liquids are well present in chemistry literature and good efforts have been devoted to developing catalytic hydrogenation reactions in these fluids, engineering aspects are less well studied and discussed, in particular, those regarding gas-expanded liquids. It is then necessary to highlight the importance of obtaining data concerning mass and heat transfer in gas-expanded liquids, as it will increase the opportunity to develop entire industrial processes using these fluids that are

[1] Ionic liquids are generally organic salts having melting point below 373 K.

Table 1
Selected types of catalysts used in compressed carbon dioxide medium for hydrogenation purposes.

Entry	Type of catalysis	Medium	Range of total pressure and temperature	Process	Substrates	Selected references
1	Heterogeneous (Metal/C; M/alumina)	$scCO_2$	10–19 MPa 300–350 K	Continuous flow, fixed bed reactors	Phenol derivatives, citral, levulinic acid, cyclohexene.	[6,35,36]
2	Heterogeneous (M/alumina)	CXL: CO_2-IL, CO_2-water CO_2-substrate	8–14 MPa 283–473 K	Batch, Semi-batch (fixed bed)	Levulinic acid, nitroaromatics, limonene (terpenes)	[11,37-39]
3	Homogeneous supported catalysts Rh-complex/alumina	CO_2-IL CO_2-toluene	12–26 MPa 313–323 K	Continuous flow	Levodopa precursor, heteroaromatic enamides, dimethyl itaconate,	[40–42]
4	Molecular (Rh-, Ru-; Ir-based complexes)	$scCO_2$	17–18 MPa 323 K	Batch	Cinnamaldehyde, α,β-unsaturated acids	[43,44]
5	Nanocatalysts (MNP, MNP/SWCNT)	$scCO_2$	10 MPa 383 K	Batch	Non-conjugate substrates (cyclohexene, norbornenes	[45,46]
6	Nanocatalyst supported (MNP-IL, MNP-dendrimers)	$scCO_2$-IL $scCO_2$-water	3–20 MPa 293–353 K	Batch	Ketones	[47,48]

CXL = CO_2 expanded liquid, IL = ionic liquid, MNP = metal nanoparticles, SWCNT = single walled carbon nanotubes.

demonstrated to be safer and environmentally friendlier for several applications than conventional processes. Finally, part of the analysis of the current literature will be devoted to the tunability of CO_2 properties, in particular its compressibility at the conditions used. The tunability is more important under temperature and pressure at subcritical conditions where enhancement of properties can give dramatic increases in yields and selectivities.

2.1. Phases equilibrium

Phase diagrams for mixtures are not the same as for pure fluids: a pure fluid presents only one critical point while for a mixture of fluids, more than one critical point is observed depending on the concentration [49]. Fig. 1a shows the phase diagram for CO_2 together with some other thermophysical properties of this compound such as density, specific-heat capacity at constant pressure, the Prandtl number (for more details on this number, refer to Section 2.2.3) and specific work for isentropic compression when a compression ratio of 2 is considered.

A classification of the phase diagrams thatcan be obtained when different binary mixtures are used was proposed by Privat and Jaubert [52]. Phase behavior of reactive mixtures in hydrogenation reactions can be complex since large differences in size and volatility of the molecules in the reacting mixture can result in multiphase behavior. On another hand, as the solubility of gases in liquids decreases with temperature, the concentration of hydrogen in the mixture will influence the behavior of the phase's equilibrium with pressure [53]. Mass transfer will be enhanced by the presence of only one phase in contact with the catalyst, on the contrary, the presence of multiple phases will lead to a decrease in mass transfer. The need for the presence of only one phase imposes that the solubility of reactants and products in the supercritical phase is achieved at the temperature and pressure desired for the reaction, this guiding the choice of the solvent.

By studying phases equilibrium between different gases and triglycerides, it is known now that CO_2 is not a good solvent for these compounds, as immiscibility zones are present even at pressures higher than 30 MPa, while other compounds such as dimethyl ether and propane allow complete miscibility at moderate pressures [53]; mixtures of CO_2 and n-paraffins containing more than 7 carbon atoms present a liquid-liquid separation, while paraffins of up to 30 carbon atoms are soluble in propane at moderate pressures [54]. Given the importance of phases equilibrium knowledge [55], much work has been performed by several research groups and a significant quantity of data is now available; some examples can be found in the works developed by the groups of Brunner [56], Nunes da Ponte [57] and Brignole [53,54] to cite some. The importance of the knowledge of phase equilibrium has been shown in a work reported by Tschan et al. [58] for the continuous hydrogenation of phenylacetylene in $scCO_2$ in a fixed-bed tubular reactor with a Pd-based catalyst. The authors concluded that the phase behavior of the reaction mixture, which includes the substrate, hydrogen and CO_2, is very different from the phase behavior of pure CO_2. Therefore, the presumption of similar behavior between pure CO_2 and the real mixture would result in major flaws in the interpretation of reaction data.

A catalyzed hydrogenation reaction in supercritical conditions needs contact between the substrate, hydrogen and a solid catalyst present in a single-phase. It is then crucial to understand the behavior of the equilibrium between phases to develop hydrogenation chemical processes that meet the desired goals in terms of conversion, yield and selectivity since the passage of a monophasic to a multiphasic system can lead to dramatic decreases in reaction rates driven by mass transfer decrease. An example is shown for the hydrogenation of fatty acid methyl esters to

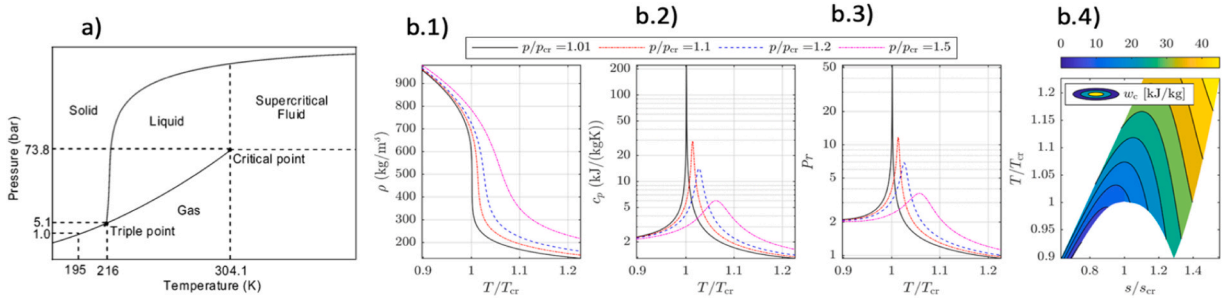

Fig. 1. a) Pressure-Temperature phases-equilibrium diagram for CO_2.
Reprinted with permission from Rayner [50], b) Thermodynamic behaviour of $scCO_2$ in the vicinity of the critical point (T_{cr}, p_{cr}): (b.1) density ρ; (b.2) specific-heat capacity at constant pressure Cp; (b.3) Prandtl number ($Pr = cp\ \mu/k$); (b.4) specific work for an isentropic compression for a compression ratio of 2, Wc.Reprinted with permission from White et al. [51]

obtain fatty alcohols by using propane as a solvent in supercritical conditions [55] (Scheme 1); the substrate concentration played a major role, as an increase in its concentration induced a phase splitting and a decrease in reaction rate.

When no experimental data is available, prediction can be performed by using different methods such as equations of state (EoS), molecular modeling or Monte Carlo methods among others. In particular, EoS have been long time developed, from the first cubic equation of state presented by van der Waals in 1873 to the more sophisticated equations involving attractive and repulsive terms or those based in perturbed hard chain theory [59] or in the statistical associating fluid theory [60,61] or even the ones using the group contribution-associating theory [62]. An example of calculations using this last model applied to the supercritical hydrogenation of vegetable oils was described by Pereda et al. and Rovetto et al. [53,54].

Phase equilibrium determination by experimental or modelling techniques can then be followed by a study of the different mechanisms of mass transfer present in a hydrogenation reaction; a non-exhaustive presentation of mass and heat transfer is presented in the next sections to give an idea to the reader of the importance of these mechanisms in hydrogenation reactions performed in supercritical conditions.

2.2. Transport phenomena in compressed fluids

2.2.1. Mass transfer in compressed carbon dioxide

Viscosity and density of compressed gases and in particular of compressed CO_2 can be broadly tuned when conditions of pressure and temperature are lower than the supercritical conditions; indeed, the compressibility factor (Z) of CO_2 greatly decreases with pressure before the critical point, which means that it is more compressible than an ideal gas. After the critical point, Z increases with pressure, meaning that the fluid becomes less compressible. Fick's first and second law of diffusion relates mass transport and concentration gradient. An increase in the viscosity of the solvent decreases mass transport [63].

Diffusion coefficients of chemical compounds in compressed gases decrease with pressure as density increases; in supercritical fluids, diffusion coefficients are higher than in liquids. Some experimental data on diffusivities are available in the literature and Table 2 collects some values for specific compounds. Self-diffusion values for CO_2 as a function of temperature and pressure have been reviewed by Cunico and Turner [64].

Diffusion coefficients can thus be obtained by using theories and models such as Enskog's kinetic theory of hard-sphere fluids [68]. Medina has presented data concerning diffusion coefficients for some solutes in compressed fluids and the correlation methods used for modelling the experimental data obtained [69]. The most used methods for these calculations are based on Stokes-Einstein equation and the Rough-Hard-Sphere models. Shenai et al. have discussed the validity of some models to obtain diffusivities when no experimental data exist [70], while Molecular Dynamics techniques can be used to calculate diffusion coefficients [71], especially when the validity of the equations and models cited before is in doubt.

Concerning hydrogenation reactions, they are usually performed in the presence of a gas phase in contact with the surface of a catalyst or in a three-phases system where a gas and a liquid phase are in contact with a solid catalyst (Fig. 2). Fig. 2a depicts the concentration profile of a reactant in the vicinity of a catalyst particle in a gas-solid system, Fig. 2b depicts these profiles for a gas-liquid-solid system, and Fig. 2c represents a supercritical phase-solid system.

Table 2
Diffusivities (D_{12}) of some compounds in $scCO_2$.

Compound	T (K)	P (MPa)	D_{12} (10^{-9} m^2s^{-1})	Reference
Anisole	313	15	11.78	[65]
	333	15	14.97	[65]
Nitrobenzene	313	15	10.66	[65]
	333	15	13.97	[65]
Methanol	313	9.5	28.17	[66]
	313	16	20.78	[66]
	313	21	18.44	[66]
Acetone	313	143	15.5	[67]
Toluene	308	116.1	13.8	[67]
	318	116.6	16.1	[67]
Ethyl acetate	308	80.4	27.1	[67]
	318	89.1	27.3	[67]
	328	88.1	32.3	[67]

Where gas and liquid phases are present, in particular during heterogeneous catalysis, some of the key steps that are affected by mass transport are: 1) diffusion of the gaseous reactants from the bulk to the interface between the gas and the liquid, 2) transfer of the reactants from the interface to the bulk of the liquid phase, 3) diffusion of the reactants from the liquid phase to the catalyst's surface, 4) internal diffusion of the reactants, 5) adsorption of reactants onto the active sites, 6) reaction and 7) diffusion of the products to the bulk. Diffusion, thus, plays a key role in the transfer of substrates and products during reaction, in particular when H_2 is present. The external or interphase transport effects or resistances are present outside of the catalyst particle, while internal or intraparticle transport effects occur inside the pores of the catalyst.

Given the low solubility of hydrogen in liquids, the mass transport of hydrogen is the limiting factor in catalylized hydrogenation reactions, so the concentration of hydrogen at the surface of the catalyst is in general low, which limits the reaction rates [8]. The diffusion of hydrogen inside the pores of a catalyst is often also hindered by the low diffusivity of this gas in liquids. Chemical processes to obtain fatty alcohols by hydrogenation of fatty acids generally operate at temperatures of 523–573 K and pressures of 20–30 MPa, and are performed by one of these three routes: (a) hydrogenation over a fixed bed catalyst in the gas phase, (b) hydrogenation over a fixed bed catalyst in the trickle phase, or (c) hydrogenation in the liquid phase with suspended catalyst [72].

To increase the concentration of hydrogen at the surface of the catalyst, the pressure of the system can be increased. Van den Hark and Härröd have proposed the catalytic hydrogenation of fatty acid methyl esters by using a supercritical phase formed by propane, hydrogen and the corresponding substrate because propane is an excellent solvent for vegetable oils [55,73]. A supercritical phase allowed for eliminating the mass transfer at the gas-liquid interface without depletion of hydrogen concentration at the surface of the catalyst [7], as demonstrated by the high hydrogenation rates obtained.

With the decrease of mass transfer issues, not only the activity increases but also the selectivity may be improved. One example of this effect was reported by Shirai et al. in the stereoselective hydrogenation of arenes using heterogeneous supported rhodium catalysts in $scCO_2$ [35]. In the hydrogenation of *tert*-butylphenol using Rh/C, when $scCO_2$ was used the selectivity in the desired product *cis*-4-*tert*-butylcyclohexanol, a starting material for fragrances, was higher than when 2-propanol was used a solvent. The authors proposed that $scCO_2$ produced an increase in the concentration of H_2 in the catalyst surface but produced a decrease of the concentration of the less soluble partially hydrogenated intermediates adsorbed on the catalyst. Since the partialy hydrogenated

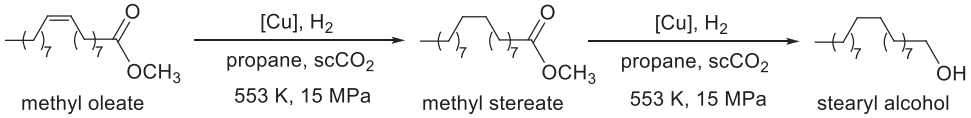

Scheme 1. Pathway for the Cu-catalyzed hydrogenation of methyl oleate into the corresponding fatty alcohol (stearyl alcohol) [55].

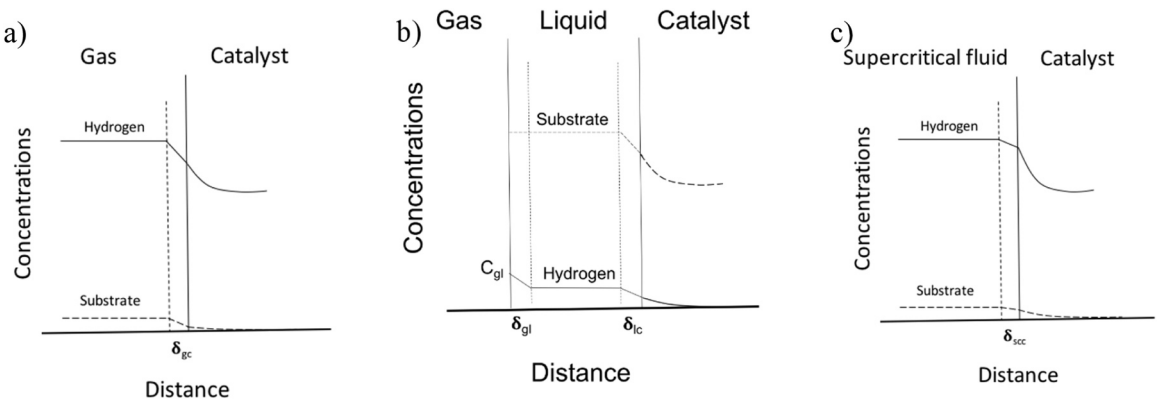

Fig. 2. Mass transfer resistances in a) gas-phase hydrogenation, b) gas-liquid phase hydrogenation, and c) hydrogenation in supercritical phase; all of them in the presence of a solid catalyst. δ_{gc} is the stagnant film layer at the gas-solid catalyst interface, δ_{gl} is the stagnant film layer at the gas-liquid interface, δ_{lc} is the stagnant film layer at the liquid-solid catalyst interface and δ_{scc} is the stagnant film layer at the supercritical-solid catalyst interface; C_{gl} is the equilibrium concentration of hydrogen in the liquid. Modified after Harröd [8].

aromatic intermediates are the responsible for the formation of the *trans* isomers an increase selectivity towards the desired *cis* isomer was obtained as a result of using the $scCO_2$ media.

Dynamic viscosity (η) of compressed and supercritical fluids is similar to the dynamic viscosity of a gas; however, as the density (ρ) of a compressed or supercritical fluid is close to that of a liquid, its kinematic viscosity (γ) is then very low ($\gamma = \eta/\rho$). Convection depends on γ and mass transfer is then enhanced in supercritical or compressed media [74]. When studying mass transfer effects, dimensionless numbers are useful to compare different effects such as diffusion, convection and inertial forces among others. Some of these numbers are cited in the following paragraphs.

The Schmidt number (*Sc*) represents the ratio of momentum diffusivity and mass diffusivity (*D* in m^2/s); in other words, it represents the ratio between the ability of a fluid to transport momentum to its ability to transport species by diffusion.

$$Sc = \frac{\nu}{D} = \frac{\mu}{\rho D} \tag{1}$$

Sc numbers of active compounds extracted from vegetal raw materials by using $scCO_2$ were calculated by López-Padilla et al. and the values obtained are between 4 and 10 [75].

The Grashof (*Gr*) number is defined as the ratio between the buoyancy forces and the viscous forces (Eq. 2):

$$Gr = \frac{g\beta\Delta T L^3 \rho^2}{\mu^2} \tag{2}$$

where g is the acceleration of gravity, β is the coefficient of thermal expansion, ΔT is the temperature difference. As CO_2 exhibits a liquid-like density and a gas-like density, the *Gr* number for CO_2-based processes can be significantly lower than that for analogous liquid processes [76].

A relationship between the Sherwood, Reynolds, Schimdt and Grashof numbers can be proposed (Eq. 3):

$$Sh \approx g(\mathrm{Re}, Sc, Gr) \tag{3}$$

The Damköhler number (*Da*) is useful to determine if diffusion rates or reaction rates are more important for defining a steady-state chemical distribution over the length and time scales of interest (Eq. 4):

$$Da = \frac{Reaction\ \ rate}{Diffusion\ \ rate} \tag{4}$$

If $Da >> 1$, the system is said to be diffusion-limited. If $Da << 1$, diffusion occurs much faster than the reaction. When the rate of diffusive mass transfer outpaces the reaction rate, the absence of mass transfer limitations may be assumed.

The following equation represents the expression to calculate Damköhler number *Da* for a first-order chemical reaction taking place at a surface (Eq. 5).

$$Da = \frac{kL}{D_{12}} \tag{5}$$

where *k* is the reaction rate and *L* is the characteristic length. Clearly, a large *Da*, implies great mass transfer limitations in the system. Guha et al. have studied the hydroformylation of 1-octene in CO_2-expanded solvents with great attention to mass transfer analysis [77]. Hydrogen and 1-octene concentration in the liquid phase were obtained as a function of time and of the *Da*. Reaction rates were obtained as function of stirring at different *Da* numbers. From this study, it has been concluded that mass transfer coefficients were increased through the introduction of gas by bubbling and by increasing stirring rates. At the conditions used during experiments, a stirring rate higher than 1000 rpm provoked a removal of mass transfer limitations, as well, the authors concluded that mass transfer of H_2 is faster than CO because of the higher diffusivity of H_2.

The diffusion of reactants or products in porous catalysts is highly dependent on the dimensions of the pores network. Transport of molecules through very large pores is essentially governed by molecular diffusion as collisions between molecules are more probable than collisions with the walls; this is called Fickian diffusion; when pores decrease in diameter, collisions with walls become more important; this regime is called Knudsen regime, in which diffusivity decreases with pore size reduction and collisions between gas molecules and pore walls play a major role. Further decrease in pore sizes results in a dramatic decrease of the diffusivity due to single-file diffusion of molecules; this phenomenon is called configurational diffusion. The interior becomes inaccessible for molecules of a bigger size than the pore opening (Fig. 3).

Hindered diffusion appears when a fluid is confined in porous media, this phenomenon is of interest in engineering applications, such as the utilization of molecular sieves, catalytic reactions with heterogenous catalyst as in most hydrogenation reactions or permeation through membranes. Adsorption and diffusion of CO_2 in sub- and supercritical conditions in slit carbon pores from 0.744 to 3.72 nm was studied by using a grand canonical Monte Carlo method combined with molecular dynamics [79]. The diffusion coefficients of molecules confined in slit pores in supercritical conditions are strongly dependent on the density in the pore. The diffusion coefficients generally decrease with increasing density at a constant temperature [79]. In another study, the flow of sub- and $scCO_2$ in coal was simulated by taking into account different diffusion regimes: Fick, Knudsen and transitional diffusion, which arises

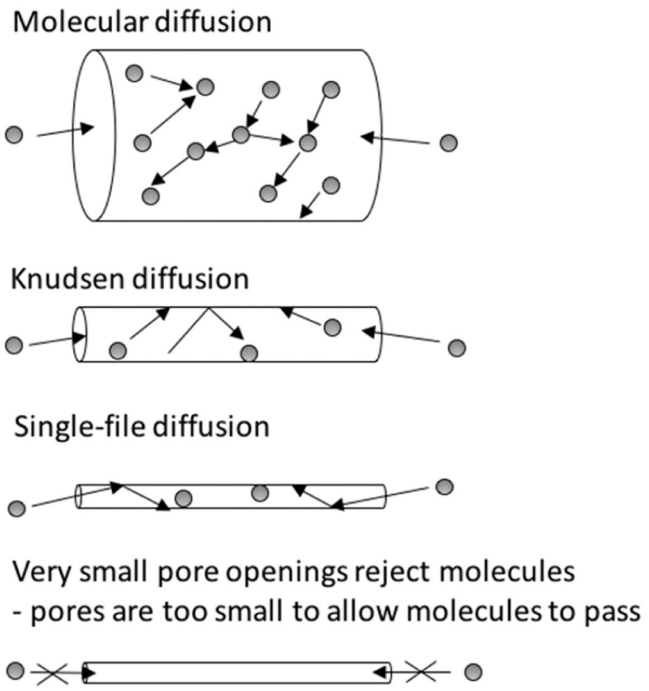

Fig. 3. Schema showing molecular, Knudsen and single-file diffusion regimes as well as the absence of diffusion. Modified after Davis and Davis [78].

when size or pore diameter and mean free path of gas molecules are almost the same; collisions between molecules and the pore walls are equally important [80]. From this study, it has been concluded that for pores of a micron or above, the diffusion effect can be ignored; however, advective flow due to pressure forces is much smaller than diffusion, and diffusion is the main transport mechanism and controls gas flow in nanosize pores. Concerning hydrogenation, Ramírez et al. measured the intraparticle diffusivities of triglycerides and hydrogen using propane as a supercritical solvent; intrinsic kinetic constants were obtained in small-size catalyst particles in absence of diffusional limitations; then, the use of these constants allowed obtaining diffusivities in diffusion-limited reactions [81]. Klaewkla et al. have reported a review about mass transfer controlling the reaction rate in heterogeneous catalysis [82].

Heat transfer plays a crucial role in chemical reactions; in exothermic reactions, effective evacuation of the heat produced is needed to keep high reaction rates. For endothermic processes, effective heat transfer from the exterior is required. A non-exhaustive treatment of thermophysical properties and heat transfer in systems concerning catalytic hydrogenation reactions is presented in the next section.

2.2.2. Thermophysical properties

The coefficient of isothermal compressibility (κ_T) of a pure fluid is given by Eq. 6. This property decreases with pressure; however, the isothermal compressibility of a pure compound presents a maximum value around the critical point. This behavior has been explained by the changes in density observed near the critical point [83].

$$\kappa_T = -\frac{1}{V}\left(\frac{\partial V}{\partial P}\right)_T \tag{6}$$

Clapeyron relationships (Eqs. 7 and 8) indicate how the thermal capacities depend on volume V and pressure P where C_p represents the specific heat at constant pressure and C_v the specific heat at constant volume, and allow obtaining these properties from an EoS, C_p has a maximum value at the critical point for water, CO_2, and other fluids [84].

$$\left(\frac{\partial C_v}{\partial V}\right)_T = T\left(\frac{\partial^2 P}{\partial T^2}\right)_V \tag{7}$$

$$\left(\frac{\partial C_p}{\partial P}\right)_T = -T\left(\frac{\partial^2 V}{\partial T^2}\right)_P \tag{8}$$

The C_p and the C_v can be determined experimentally, as for pure CO_2 [85], methanol- CO_2 [86] and ethanol-CO_2 mixtures [87] for some representative examples. It is however to note the lack of exhaustive experimental data for systems concerning hydrogen and supercritical fluids. Calculations from equations of state or Monte Carlo-based models can be performed when data are needed.

2.2.3. Heat transfer

Heat transfer during the flow of compressed gases and supercritical fluids in pipes has been fairly studied in recent years, in particular, the behavior of transport and physicochemical properties at the critical point [88–91]. Some studies have been carried out concerning hydrogenation in compressed and in supercritical phases [8], as the work performed by Häring et al. concerning the development of a model for the hydrogenation of citral (see below Scheme 24, Section 7.3) in a fixed bed reactor and a Pd/alumina catalyst [36]. Mass and heat transfer were taken into consideration together with other relevant parameters for the process such as particle diameter, H_2/citral ratio and CO_2/citral ratio variations among others. The Aspen™ software was successful in the simulation of the reactor [92].

3. Engineering aspects of catalytic hydrogenation reactions in gas-expanded liquids

CO_2-expanded liquids (CXL) are the most used gas-expanded liquids (GXL) [13], maybe because of the abundance, safety and inertness of this gas. If the composition of CO_2 is changed, different liquid media ranging from the neat organic solvent to pure $scCO_2$ can be obtained, and the properties of this medium can be adjusted by pressure changes. As it has been cited before, compressed and $scCO_2$ present enhanced mass transfer and, in many cases, increased gas solubility. CXL can be judicious solvents for separations, particle precipitation, polymer processing, and as reaction media for catalytic reactions [93,94], especially in cases where mass transport hinders the system. The advantages of the processes using CXL include easy separation of the CO_2, enhanced solubility of reactant gases, low flammability and reactivity of CO_2, and lower pressures than processes that use supercritical CO_2.

CXL have been classified according to its expansion behavior [13]. This expansion increases with pressure until the critical point and changes both the solvent character and physical properties of the liquid. The proposed classification that can be found in literature is: i) Class I, liquids that do not expand significantly as the solubility of CO_2 is low; ii) Class II, liquids that dissolve large amounts of CO_2 and therefore expand greatly; iii) Class III, liquids that dissolve moderate amounts of CO_2 and expand moderately in volume. This classification is based on expansion measurements performed on different liquids such as water [95], ethyl acetate [96], some imidazolium-based ILs [97], polyethylene glycol [98] and dimethyl formamide [96] among others. Other gases than CO_2 can form GXL with different degrees of expansion and confer different physicochemical properties to the expanded liquids formed [99].

It is however noticeable that this classification is the first essay to rationalize the different behaviors of CXL; it stays very qualitative and deeper research is needed to increase the database of the behavior of these fluids and then to enlarge the degree of rationalization and prediction of physicochemical properties of these systems. Phase equilibrium determinations are crucial when studying or using GXL; it gives precise data about the solubility of CO_2 in the liquid, together with phase transitions that can be neglected or ignored when no data is available. These determinations can be performed by experiments in equipment

such as high-pressure view cells or by modeling by mainly using equations of state, Monte Carlo methods and Molecular Dynamics [13].

When CO_2 dissolves into the liquid, the polarity and hydrogen-bonding abilities of the expanded liquid are decreased as a result of the inclusion of CO_2 in the interstices of the liquid or its dissolution. However, the clustering phenomenon in the cybotactic region of a solute can be present and, surprisingly, it has been observed that the solvent power changes less than expected compared to simple dilution by CO_2 [100,101]. To show these changes, Table 3 collects data for relative permittivity, density and Kamlet-Taft polarity parameter for some GXL at 0.1 and 5 MPa of pressure.

Other data concerning vapor-liquid equilibrium and other physicochemical properties for different systems such as alkyl acetates and 2-methyltetrahydrofuran can be found in the literature [103,104].

3.1. Mass transfer in gas-expanded liquids

Diffusion coefficients in CXL increased with CO_2 concentration [13]. Zeigermann and Valiullin [105] measured the diffusion properties of CO_2-expanded toluene in bulk and under confinement. These authors found that in the bulk phase, the diffusivity of toluene increased with CO_2 concentration, however, in confined conditions, as in pores sizes below 5 nm, different behavior was observed and attributed to an altered equilibrium phase composition in the pore space, which affects mass transfer rates. In this case, toluene diffusivities decreased at high CO_2 concentrations as compared to the bulk or weakly confined GXL. Unfortunately, mass transfer coefficient determination has been limited to some systems such as CO_2-water and hydrogen and carbon monoxide into CO_2-expanded 1-octene [106]. Catalytic hydrogenation reactions are well present in the literature concerning CO_2-expanded liquids as reaction media since it has been suggested that CO_2 enhances the solubility of hydrogen [107]. Nevertheless, the different studies do not perform reactions in comparable situations, which impedes the rationalization of results and conduct sometimes to contradictory conclusions [106]. Ionic liquids can reduce reaction efficiencies [108,109]. IL and deep eutectic solvents[2] (DES) have attracted increased attention in recent years as neoteric solvents, in particular in reaction media and many scientific documents have reported the study of mass transfer coefficient and solubility of gases in these fluids [110–112]. Zhang et al. have provided insight into gas-liquid mass-transfer properties in CO_2 absorption with IL [113] by determining the external mass transfer coefficient (k_L) of CO_2 in systems formed by IL and water by the pressure drop method in a stirred cell reactor. k_L was also evaluated and analyzed in terms of the nature of the IL, temperature, stirrer speed and concentration of the IL. The authors concluded that the mass transfer coefficient is influenced by the viscosity and the molecular structure of the IL. As the mass transfer coefficient decreases while CO_2 solubility increases with the concentration of IL. They also found that a higher stirrer speed resulted in a higher speed of pressure drop in the reactor, which could be attributed to a higher mass transfer coefficient. These results were coherent with those reported by Sharma et al. who reported that the gas-liquid mass transfer coefficient for H_2 and CO in 1-*n*-butyl-3-methylimidazolium hexafluorophosphate increased with the stirrer speed as well as the temperature [110]. Solinas et al. described how the combination of IL and supercritical CO_2 not only increases the mass transfer but also the solubility of H_2 in the system [114]. This behavior is clearly beneficial to perform effective hydrogenation reactions in IL. Guo et al. [37] have proposed the hydrogenation of levulinic acid in mixtures composed of CO_2, H_2 and ILs to obtain γ-valerolactone in batch reactors (Scheme 2). In this study, the authors observed an increase of the yield in the presence of CO_2 at high pressure, which was attributed to the decrease in viscosity of the IL by CO_2, and the possible increase in solubility of H_2 in the reaction medium. In this case, a [EMIM][Cl]- [EMIM][OAc] mixture (EMIM = ethylmethylimidazolium) gave the lowest viscosity and the highest solubility of H_2.

Kian et al. measured the dynamic viscosity for binary alkane mixtures of n-hexane, n-decane, and n-tetradecane saturated with CO_2, at three different temperatures (298 K, 313 K, and 328 K) under 10.7 MPa [115]. They reported that the viscosity decreased considerably with the pressure of CO_2. According to them, it was not a pressure effect but a large increase in CO_2 solubility in the liquid phase that decreased the viscosity. For example, the system of n-tetradecane/ CO_2 showed the largest absolute and relative drop in viscosity due to the dissolution of CO_2 in the liquid phase. For this system, the viscosity of the liquid phase dropped by 65% (298 K), 76% (313 K) and 87% (328 K) compared to the ambient pressure viscosity, for ca. 55% mole CO_2 solubility. Similarly, Sih et al. determined the viscosity of the CO_2-methanol systems as a function of temperature from 298 K to 313 K, from 0 to 0.85 mol fraction CO_2 and from 0.1 to 7.67 MPa. They reported that the liquid viscosity of the system decreased with CO_2 enrichment and increasing liquid density [116]. Additionally, Jacquemin et al. determined the solubility of eight different gases (CO_2, ethane, methane, O_2, N_2, H_2, argon and CO) in 1-n-butyl-3-methylimidazolium hexafluorophosphate [117]. They found out that CO_2 was the most soluble and H_2 the least soluble of the eight gases. From this data, it can be concluded that CO_2 provides the maximum opportunity for increasing mass transfer and decreasing viscosity issues in GXL.

When data concerning the viscosity of GXL is lacking, which is often the case, they can be obtained by experimental measurements through the use of high-pressure rheometers or by numerical methods using molecular dynamics calculations [103,104,118,119]. The ASOG-VISCO method has been used to obtain the kinematic viscosities for binary mixtures including CO_2 and organic compounds such as paraffins, alcohols and ketones [120]. In this study, the Gibbs free energy has been calculated by group contributions.

Table 3
Relative permittivity (ε), density (ρ), and polarizability (π *) values for some common solvents at atmospheric pressure 0.1 MPa and 5 MPa of CO_2 pressure at 298 K [102].

Pressure (MPa)	ε		ρ (g cm^{-3})		π*	
	0.1	5	0.1	5	0.1	5
Cyclohexane	1.95	1.30	0.773	0.798	0.034	0.067
Toluene	3.00	1.78	0.865	0.885	0.503	0.177
Acetone	20.79	8.20	0.787	0.855	0.677	0.432
Ethanol	25.78	8.86	0.786	0.822	0.537	0.291
Isopropanol	20.62	12.40	0.782	0.794	0.482	0.346
Dimethyl ether	4.86	2.50	0.708	0.793	0.266	0.043
Dichloromethane	7.99	3.64	1.318	1.283	0.812	0.487
Acetonitrile	36.00	13.86	0.777	0.860	0.727	0.530

[2] Deep eutectic solvents are mixtures of different components that in a given composition become liquids at room temperature.

3.2. Heat transfer in gas-expanded liquids

Even if heat transfer properties are crucial in the design of chemical processes, very scarce studies can be found in the literature concerning heat transfer properties of GXL. One of the rare studies has been presented by Kian and Scurto concerning CO_2-tetradecane, CO_2-n-decane and CO_2-n-hexane systems [121]. Thermal conductivities, thermal diffusivities and heat capacities at different temperatures and compositions of CO_2 at pressures up to 10.6 MPa were determined. The Prandtl number was determined and found to decrease with CO_2 concentration while the isothermal compressibility of CXL decreased with pressure and became almost constant after a certain pressure.

Given the increasing interest in IL and in DES, their heat capacity has

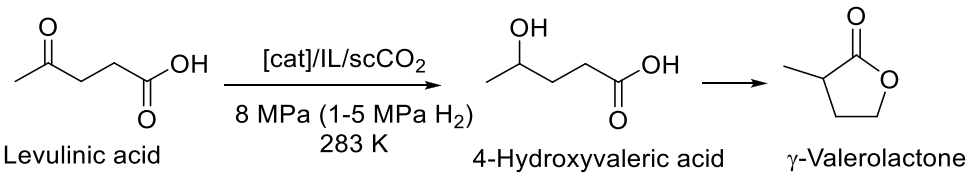

Scheme 2. Hydrogenation of levulinic acid to γ-valerolactone.

been studied in different applications such as refrigerators at low temperature, solar energy collectors or storages at high temperature. IL exhibit high density, high heat capacity and good thermal and chemical stability which make them good candidates as heat transfer fluids in medium and high-temperature heat transfer systems [122]. IL are also known to show large heat storage capacities (up to 50% larger than current heat transfer fluids) [123,124]. França et al. compared the heat capacity of several IL with commercial thermal fluids, observing that the heat capacity per unit volume of IL between room temperature and 403 K was 20–40% higher [124]. Unfortunately, no heat transfer studies could be found concerning CO_2-IL systems. It is also noteworthy that there is a lack of reports describing heat transfer in catalytic hydrogenation reactions in GXL.

Energy consumption during the use of $scCO_2$ in hydrogenation reactions has been evocated by Bourne et al. [38] for the hydrogenation of levulinic acid to γ-valerolactone, the possibility of depressurization to provoke a separation allowed to decrease energy consumption at the end of the process. Damen et al. [40] have designed an intensified process for Levodopa production, where a step of hydrogenation is included, which is the slowest step of the process. The intensified process allowed a decrease in energy consumption of 5.5 MJ/kg product in this step compared to the original process. This decrease was obtained by using $scCO_2$ and an ionic liquid as solvents.

4. Continuous hydrogenation processes under supercritical carbon dioxide flow

Supercritical fluids have emerged as an alternative media for a variety of synthetic reactions. Hark et al. reported hydrogenation of fatty acid methyl esters to fatty alcohols at supercritical conditions, using propane as a solvent over copper catalyst [125]. The productivity of the reaction was increased by decreasing the amount of H_2 used. As H_2 is an antisolvent for the substrate in the reaction mixture of propane/-lipid/H_2, a low H_2 pressure not only improved the selectivity but also improved the lipid solubility. In 2004, Beckman reported the application of CO_2 technology in processes that became cleaner, less expensive and of higher quality [76]. Wandeler et al. on the other hand, reported Pd-catalyzed continuous enantioselective hydrogenation of ethyl pyruvate in supercritical ethane (Scheme 3) by establishing a relation between phase behavior and catalytic performance [126]. They stated that the combination of the catalytic and physicochemical study of ethyl pyruvate hydrogenation permitted to demonstrate that the phase behavior of binary systems is an ideal guide for understanding high-pressure multicomponent reactions [127]. Since the end of the 20th century, continuous hydrogenation reactions under supercritical CO_2 of several alkenes and functional groups have been investigated. In 1998, Poliakoff and coworkers reported one of the first methods for continuous hydrogenation in supercritical CO_2 using heterogeneous noble metal catalyst on Dexlon aminopolysiloxane support [25,128,129].

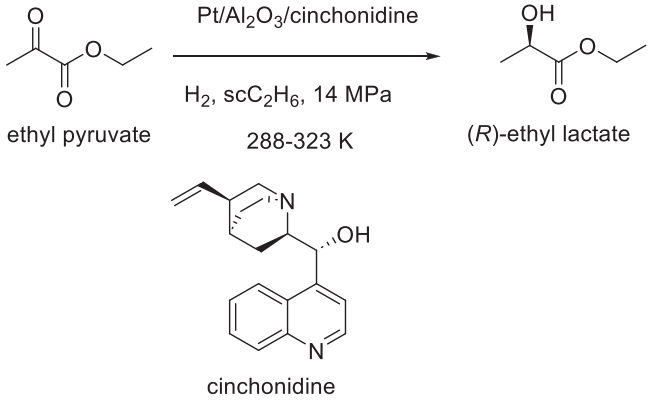

Scheme 3. Enantioselective hydrogenation of ethyl pyruvate over cinchonidine-modified Pt/Al2O3 to afford (*R*)-ethyl lactate [126]. scC_2H_6 = supercritical ethane. Molar ratio C_2H_6/ethyl piruvate/H_2 = 200/1/2,10,20.

The metal-catalyzed hydrogenations involve a wide range of organic functional groups including alkenes, alkynes, aliphatic and aromatic carbonyl derivatives (ketones and aldehydes), epoxides, phenols, oximes, nitrobenzenes, Schiff bases or nitriles [130]. During the process of hydrogenation, substrates and H_2 are commonly dissolved in supercritical CO_2 giving a one-phase system. Consequently, at the end of the reaction, the supercritical fluids mixture is depressurized, and the products and any unreacted starting material can easily be collected, being separated from the gas phase [6]. At industrial scale, it may also be possible to isolate individual heterogeneous catalyst chambers for refilling while avoiding total shutdown and depressurization of the reactor. The dissolution of reactants into one single phase also eliminates the interphase mass transfer limitations. Another important advantage of using continuous process over the batch system is that the reaction conditions can be controlled with considerable precision and high reproducibility of the results.

Additionally, the low solubility of H_2 in the solvent media limits hydrogenation reactions performed in conventional organic solvents. The use of supercritical fluids in hydrogenations can help to increase H_2 transport thus increasing the concentrations of reactants available for reaction [131]. Hark et al. showed that reaction rates for hydrogenation of fats and oils at supercritical conditions can be increased up to 1000 times compared with reactions performed in conventional media; the hypothesis has been emitted that besides an increase in solubility of H_2 in supercritical media, gas-liquid transport resistances in heterogeneous-catalyzed hydrogenations are diminished and thus reaction rates are increased [125].

In 2001, Poliakoff and coworkers described a strategy merging the two technologies, continuous processes and the use of supercritical fluids [132]. Together with Thomas Swan and Co. Ltd., they could scale up the continuous hydrogenation under supercritical CO_2 using heterogeneous catalysts, from laboratory to industrial scale, producing thousand of tons per year [17,132].

Arunajatesan et al. performed Pd/C catalyzed hydrogenation of cyclohexene to cyclohexane in a fixed bed reactor to study the phase behavior of the reaction mixture, the temperature control in the reactor during operation and the effect of operating parameters on catalyst deactivation. They solubilized cyclohexene and H_2 in a single supercritical phase surrounding the solid catalyst [6]. The goal was to develop a fundamental understanding of the underlying physicochemical processes that may help in rationally addressing process feasibility and reactor design issues by considering, for instance, that the conversion of cyclohexene to cyclohexane is an exothermic reaction. Therefore, the maximum adiabatic rise in temperature (ΔT_{ad}) for an equimolar feed of cyclohexene (0.2 mol/h) and hydrogen in 90 mol% CO_2 was described

by using the Eq. 9.

$$\Delta T_{ad} = \frac{F_{A_o}(\Delta H)}{mC_p} \quad (9)$$

where F_{A_o} is the molar cyclohexene flow rate (mol/h), ΔH is the reaction enthalpy, m is the total molar flow rate in the reactor, and C_p is the molar heat capacity (kJ/mol/K) of the reaction mixture at reaction conditions (13.6 MPa and 343 K).

Following the above equation, the maximum adiabatic increase in temperature was only 45 K in a liquid or dense near-critical phase. It was in contrast with the estimated temperature rise in a gas phase that was nearly 170 K. The reason behind this difference in the rise of temperature was the higher heat capacities of the liquid or dense near-critical phase as compared to the gas phase. They demonstrated that for an olefin space velocity of 20 h^{-1}, excellent temperature control around the setpoint (343 K) and stable catalyst activity were observed achieving a cyclohexene conversion exceeding 80% throughout a 22 h run.

Geier et al. performed continuous flow asymmetric hydrogenation of (hetero)aromatic enamides with a Rh/**a** (Scheme 4) catalyst immobilized in a supported IL phase and employing supercritical CO_2 modified with toluene as the mobile phase (modCO_2, Scheme 4) [41]. Their approach allowed the expansion of the scope of the original supported IL phase/supercritical CO_2 system to non-volatile substrates with poor solubility in pure CO_2. In addition, the continuous flow process proposed for this reaction used a 20 times smaller catalytic load than the batch reaction. Bogel-Łukasik et al. showed that the selectivity of the reaction is pressure tunable in a biphasic system where phase equilibrium ratios determine the composition of the liquid phase in contact with the catalyst [133]. By hydrogenation of limonene using Pd/C catalytic system, they showed that when CO_2 in large excess is the solvent and the system is relatively close to the critical line of the mixture but is still biphasic, the partition of the solutes limonene and H_2 between the liquid and the vapor is highly sensitive to pressure. They also showed the effect of the partial pressure of H_2 for the hydrogenation of limonene, keeping the total pressure constant. They reported that an increase in CO_2 when the H_2 pressure decreases the system is closer to the critical pressure and the liquid expands in volume. In these conditions, the higher solubility of H_2 compensates for the lower partial pressure in the gas phase [11].

Continuous hydrogenation in supercritical CO_2 has also overcome one of the major drawbacks of the poisoning of noble metal catalysts that often occur in batch reactors. In hydrogenation reactions, catalyst deactivation can happen due to the formation of CO as a by-product of the reverse water-gas shift reaction (RWGS) even at low temperatures (Scheme 5). Burgerner et al. investigated the reaction between CO_2 and H_2 over Al_2O_3-supported Pt, Pd, Rh and Ru model catalysts by attenuated total reflectance infrared spectroscopy (ATR-FTIR) under high-pressure conditions for both batch and continuous flow reactors. They observed that CO coverage on Pt/Al_2O_3 was less prominent in the

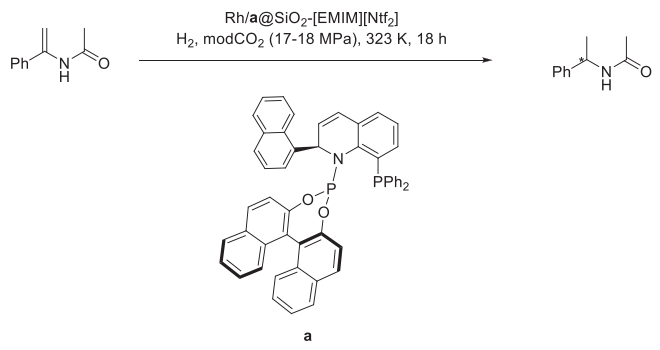

Scheme 4. Asymmetric hydrogenation of *N*-(1-phenylvinyl)acetamide [41]. [EMIM][NTf_2]: 1-Ethyl-3-methylimidazolium bis(trifluoromethyl sulfonyl) imide, modCO_2: scCO2 modified with toluene as the mobile phase.

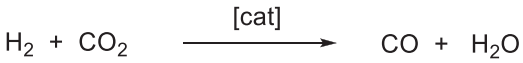

Scheme 5. Reverse Water-Gas-Shift reaction.

continuous flow cell than in the batch reactor cell [134].

Devetta et al. performed the modeling of a trickle bed reactor for catalytic hydrogenation of two double bonds of an unsaturated ketone as a model compound in supercritical CO_2 [135]. Simulations were carried out using a totally predictive model taking into consideration phases equilibria and heat and mass transfers by using the Aspen Plus™ software to accurately understand the reactor behavior; results were in close agreement with experimental data obtained in a pilot unit.

Nevertheless, using the same catalytic system Pt/Al_2O_3 for the hydrogenation of nitrobenzene (Scheme 6) in a batch reactor, the CO generated by RWGS adsorbed on the surface of the catalysts inhibited the full hydrogenation of the intermediate N-phenylhydroxylamine (PHA) to aniline and increased the desired product *p*-aminophenol formed by rearrangement of PHA, which is obtained, thus, with high selectivity in a $scCO_2/H_2O$ medium [39]. Furthermore, the carbonic acid generated in the $scCO_2/H_2O$ media avoided the use of added acids and decreased the by-products formed. Thus the combination of CO_2/H_2O produces changes in the media that influence the product distribution [136].

One of the major concerns, however, in continuous hydrogenation reactions is energy consumption [137]. Stevens et al. proposed different methods to reduce energy consumption, for example, the use of carbon capture and storage [16]. Additionally, another approach was running sequential reactions and/or using lower pressure GXL [138,139].

5. Modeling of reactors, process design and safety issues

Given the multiple chemical and physical phenomena happening at the same time in a chemical reactor, modeling an entire continuous stirred-tank reactor (CSTR), a fixed-bed reactor (FBR) or a plug-flow reactor (PFR) can be a complex task. Transport phenomena and chemical reaction engineering take elements from physics (e.g., transport theories, fluid dynamics or thermodynamics), chemistry (e.g., kinetics or catalysis) and mathematics to treat complex problems arising during chemical process development.

Among the tools that have been developed in this context, computational fluid dynamics combines fluid dynamics and numerical mathematics using modern super calculators, which allow the utilization of complex and extended models difficult to handle before. An example of this, given by Kuipers et al., is the increased use of the Maxwell-Stephan transport model instead of the Fickian model or strongly empirical models used up to now to solve approximately the complex problems encountered in chemical engineering. Thus, the conventional empirical and phenomenological models are being replaced by more fundamental descriptors, based on mass, energy and momentum microbalances [140]. In the simplest cases, an analytical solution can be obtained; however, in almost all the real cases, numerical solutions need to be proposed. In this context, computational fluid dynamics techniques have proved to be accurate and particularly useful [140–143].

Examples of the use of computational fluid dynamics for hydrogenations in supercritical media can be found in the literature, in particular, Guardo et al. have presented a study concerning the catalytic hydrogenation of sunflower oil in a supercritical solvent using a Pd-based catalyst [144]. Firstly, a 2D model of the catalyst pellet and the reacting mixture was used to study the effect of external mass transfer and intra-particle diffusion on the intra-particle concentration profiles. The results from these calculations were used in the modeling of a 3-dimensional packed-bed reactor to transpose the obtained results to an industrial scale. In another example, the catalytic hydrogenation of dimethyl oxalate to ethylene glycol (Scheme 7) in a fluidized-bed reactor was modeled by using a single-particle model and computational fluid

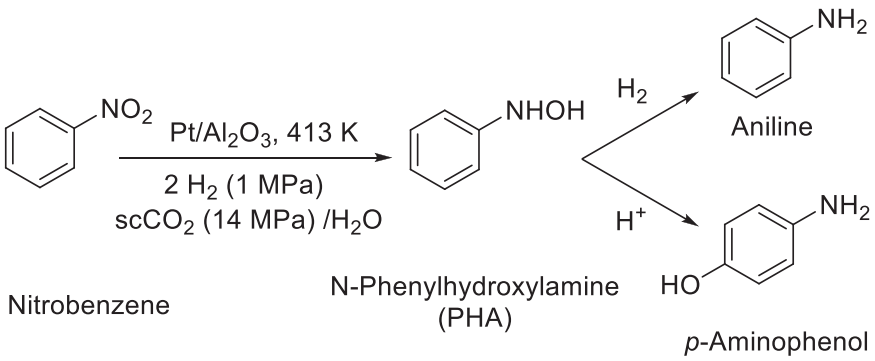

Scheme 6. Possible products from the hydrogenation of nitrobenzene.

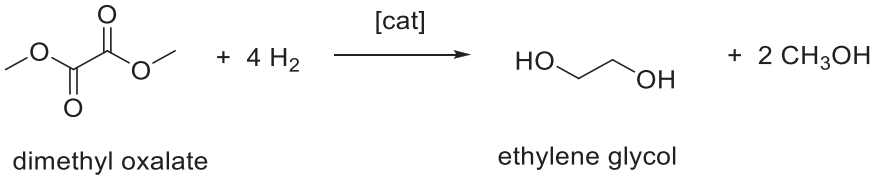

Scheme 7. Hydrogenation of dimethyl oxalate to ethylene glycol.

dynamics by Zhu et al. [145]. The results obtained numerically were compared with experimental results showing that intraparticle transfer resistance increases with particle size and that as the catalyst size becomes smaller, the distributions of the mass fractions of the different species become more uniform.

The development of an entire chemical process, its design and optimization are the ultimate goals of Chemical Processes Engineers, they aim to produce a valuable product safely, at an acceptable cost and low footprint for the environment. In the case of hydrogenation reactions, a great number of chemicals are obtained by catalytic processesby applying mostly heterogeneous catalysis. For example, one of the major concerns in process engineering is the hydrogenation of vegetable oils with low quantities of *trans* fats, as they have been linked to vascular diseases. Efforts to develop new processes to obtain healthier products have passed by the use of systems in a supercritical state. As well, the usage of safer chemicals and chemical processes is a concern more and more present when chemical processes are developed.

Therefore, the group of Recasens conducted continuous hydrogenations of sunflower oil in a gradientless CSTR by using Pd-based catalysts in propane or dimethyl ether as solvents and using CO_2 and hexane as modifiers [81,146,147]. Intrinsic kinetics and intraparticle diffusivity were determined. In these works, it is well shown that the surface of diffusion greatly influenced diffusion mechanisms in the pores. Also, a demonstration plant of 2000 metric tons/year was simulated by using Aspen™ software [148]. The safety of the proposed process was addressed by using the Dow Fire and Explosion Index to compare the different systems studied: 1) process using supercritical propane, 2) co-solvent utilization by using hexane-modified CO_2 and 3) neat liquid hexane. The process using hexane-modified CO_2 was found to present the lowest risk of explosion.

An elegant example of the design of a process including a CSTR and using a GXL was reported by Siougkrou et al. [149]. It is clear from this study that the development of a chemical process by rationally choosing the solvent and focusing on process performances in terms of environmental footprint and operating costs is completely possible. To arrive at the best solvent, the authors took into consideration some of the concepts that we have briefly reviewed in this manuscript: phases equilibrium data, mass-transfer properties, physicochemical parameters concerning solvation, reaction rates, and process design. Besides, a word can be said about process intensification in hydrogenation reactions, where supercritical CO_2 and GXL can provide safer alternative options, for instance, in cases of accidental fires and explosions [115].

Lee et al. [150] worked on a process allowing the simultaneous supercritical transesterification and the partial hydrogenation (SSTPH) of soybean oil in the presence of a catalyst. They presented a kinetic study of the reaction together with the design and the economic analysis of three continuous processes including a conventional supercritical process (CSP), a SSTPH process using a Cu catalyst, and a SSTPH process using Pd/Al_2O_3 catalyst. In comparison, it has been found that the SSTPH processes presented higher total manufacturing costs than the CSP but the total capital investment for the SSTPH using Pd/Al_2O_3 was the lowest because the reaction conditions were the mildest, being the most economically feasible processes among the three studied. For this study, the Aspen HYSYS software was used to simulate continuous packed bed reactors for SSTPH and a continuous PFR for the CSP. Thermodynamic modeling was performed by using Non-Random Two Liquid (NRTL) activity coefficient model, and the economic analysis was done by using the Aspen Process Economic Analyzer.

A review about the equipment used for $scCO_2$ assisted chemical synthesis has been provided by Shi et al. [151], with a comprehensive section concerning hydrogenation reactions; the equipments used are divided into batch, continuous and microfluidic reactors. The key challenge when designing this kind of equipment is the need for a maximal surface contact between the reactants and the catalyst, which can take advantage of the use of $scCO_2$ to decrease mass transfer problems. In particular, the design and use of microfluidic reactors are pointed out as greatly profitable, as temperature control can be precisely performed during the reaction together with the enhancement of contact between reactants and catalysts by $scCO_2$ being able to decrease reaction times down to 1 s.

6. Molecular metal-complex based catalysts

Metal-based molecular catalysts have been used in compressed CO_2 medium due to their high selectivity under mild conditions. Nevertheless, often these metal complexes are polar or ionic species with low solubility in the non-polar CO_2 phase. To overcome this problem different strategies have been proposed: a) the use of so-called " CO_2-*philic*" groups such as perfluorinated fragments; b) the use of CO_2 soluble counter anions in the case of ionic complexes; c) the addition of co-

solvents; d) working at subcritical conditions; and e) working at CO_2 expanded liquid conditions [25]. Furthermore, the problem of the separation of the catalysts at the end of the reaction can be solved by anchoring the metal precursor on a solid support, by membrane separation, extraction of the products by means of CO_2 or running the reaction under biphasic/multiphasic conditions. The use of $scCO_2$ can introduce changes in the activity and selectivity of the catalytic systems that may result from different aspects as identified by Lange et al. [152]; some examples are shown in the following sections.

6.1. Hydrogenation of biomass derived renewable materials

Compressed CO_2 has been used to assist as a catalyst or media for the pretreatment process for the transformation of lignocellulose into value-added commodity chemicals and also in the down-stream reactions such as hydrogenation, to convert this feedstock into valuable platform of chemicals [153]. The use of CO_2 improves the sustainability, energy requirement and cost of the process. Rhodium and ruthenium complexes are the most active catalysts in homogeneous catalytic hydrogenation of unsaturated substrates, therefore most of the molecular catalytic precursors applied in compressed CO_2 are based on them [130].

CO_2 is not always an innocent medium. It can interact with the functionalized substrates, such as those bearing carbonyl groups, or with the catalysts. Additionally, in aqueous systems or in the presence of water, CO_2 forms acidic carbonate species that may interfere with the reaction. Moreover, CO_2 may be eventually reduced in the hydrogen-rich medium to form carbon monoxide which can react with the metal species [154]. In some systems, carbon monoxide may poison the catalyst as discussed in Section 4, but also may favour the formation of active carbonyl species. This is the case of the biomass derived substrate levulinic acid. In the hydrogenation of levulinic acid to γ-valerolactone (Scheme 2) using $[RuCl_2\{P(C_6H_5)_3\}_3]$ as pre-catalyst (0.1 mol%, 4 MPa hydrogen, 423 K), the increase of CO_2 pressure (0–16 MPa) turned in a higher conversion (from 78% to 98%) and selectivity in the lactone (from 92% to 97%) [154]. The reaction proceeded through the intermediate 4-hydroxyvaleric acid (Scheme 2). Analysis by ultraviolet-visible spectroscopy of the reaction of the pre-catalyst $[RuCl_2\{P(C_6H_5)_3\}_3]$ in the presence of CO_2 and hydrogen revealed the formation of the carbonyl species $[RuHCl(CO)\{P(C_6H_5)_3\}_3]$ (Eq. 10). Carbon monoxide was probably formed from RWGS reaction of CO_2 and hydrogen (Scheme 5). By comparison of the catalytic activity of commercial samples of $[RuHCl(CO)\{P(C_6H_5)_3\}_3]$, the authors concluded that this one was a catalytically active species. The formation of carbon monoxide speeded up with the increase of pressure, which explained the positive effect of CO_2 pressure in the conversion [154].

$$[RuCl_2\{P(C_6H_5)_3\}_3] + CO + H_2 \rightarrow [RuHCl(CO)\{P(C_6H_5)_3\}_3] + HCl \quad (10)$$

In the case of the hydrogenation of levulinic acid, an interaction of CO_2 with the carboxylic group was detected by infrared spectroscopy, however there was no evidence that this interaction affected the increase in catalytic activity in $scCO_2$ [154]. On the contrary, in the case of the hydrogenation of cinnamaldehyde (Scheme 8) catalyzed by $RuCl_3$/P$\{(C_6H_5)(C_6F_5)_2\}$ complex, in which the CO_2-*philic* -(C_6F_5) fragment was introduced, the interaction of the substrate with CO_2 was crucial to obtain high selectivity [43]. In this substrate, three functionalities can be reduced, namely the aldehyde, the alkene and the aromatic groups. Using the ruthenium catalytic system $RuCl_3$/P$\{(C_6H_5)(C_6F_5)_2\}$ a mixture of all the possible products was observed (cinnamyl and hydrocinnamyl alcohol and hydrocinnamaldehyde) (Scheme 8), but a fine-tuning of the reaction conditions including the phase behaviour, the loading of pre-catalyst and substrate, together with the CO_2 pressure permitted to selectively obtain cinnamyl alcohol (98%) at good conversion (54%) in CO_2-expanded cinnamaldehyde (CAL) liquid phase.

The authors claimed that under optimized conditions the reaction medium exhibited a high cinnamaldehyde concentration in the CAL phase and the solubility of hydrogen was also enhanced. Furthermore, the analysis by infrared spectroscopy of the cinnamaldehyde/CO_2/hydrogen reaction mixtures revealed the presence of an interaction between the substrate and CO_2 since a red-shift of the absorption band of C═O of ca 50 cm^{-1} from the gas phase to the CAL phase was observed. This was attributed to a hydrogen bond -(O)C-H···O(=C═O) between the substrate and CO_2 [43], which may control the selectivity towards the formation of cinnamyl alcohol by activating the carbonyl group.

Itaconic acid and related compounds are also interesting sustainable starting materials obtained from biomass [42,155]. In addition, the enantiopure 2-alkyl succinates are useful intermediates for the synthesis of peptidomimetics, polyesters and chiral drugs [42]. Catalytic systems based on the successful atropoisomeric Noyori's chiral ligand (±)− 2, 2′-bis(diphenylphosphino)− 1,1′-binaphthalene have been extensively used in the asymmetric hydrogenation of C═C bonds in $scCO_2$ [44]. This ligand has been modified to increase the solubility of the catalytic systems in the non-polar CO_2 medium. The benchmark substrates are often acrylate derivatives like tiglic and itaconic acid.

First approach, developed at Noyori's group, used a partially hydrogenated naphthyl group to increase the lipophilicity of the metal complex in the ruthenium-catalyzed hydrogenation of tiglic acid (TA, Table 4) [44]. Thus, $[Ru(OCOCH_3)_2$(**a**)] (for the structure of **a**, see Fig. 4) catalyzed the hydrogenation of tiglic acid in $scCO_2$ (17–18 MPa) with an enantioselectivity (81% enantiomeric excess, entry 1, Table 4) similar to that obtained in other solvents such as methanol (82% enantiomeric excess) (entries 1–2, Table 4). The addition of a fluorinated alcohol, such as $CF_3(CF_2)_6CH_2OH$, produced an increase in enatioselectivity and yield working at lower hydrogen pressure (entry 3, Table 4) [44].

The combination mixtures of ILs and methanol with compressed CO_2 giving place to CO_2 expanded IL systems increased the enantioselectivity of the hydrogenation of atropic acid (ATA, entries 4 and 5, Table 4) using the Ru/**b** (Fig. 4) catalytic system [156]. In this case, it was related with the fact that atropic acid hydrogenation was hydrogen concentration dependent.

Another example of increasing solubility in $scCO_2$ by introducing long perfluoroalkylated chains in the binaphtyl skeleton of (±)− 2,2′-

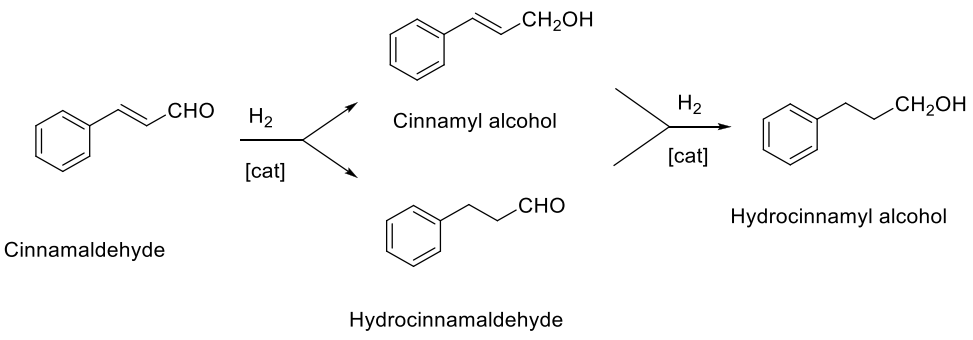

Scheme 8. Schematic reaction pathway of cinnamaldehyde hydrogenation.

Table 4
Hydrogenation of α,β-unsaturated acids using Ru(II) catalytic systems with (±)− 2,2′-bis(diphenylphosphino)− 1,1′-binaphthalene type ligands (see Fig. 4 for the ligand structures).

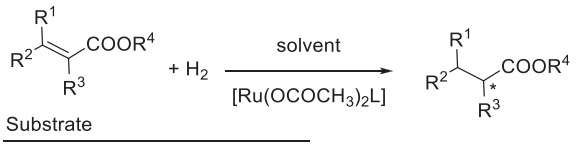

Substrate

TA = R^1,R^2,R^3,R^4 = H,Me,Me,H
DMI = R^1,R^2,R^3,R^4 = H,H,CO_2Me,Me
ATA = R^1,R^2,R^3,R^4 = H,H,Ph,H

Entry	L[a]	Substrate[b]	Solvent	H_2 (MPa)	ee (%)	Reference
1[c]	**a**	TA	$scCO_2$	3.3	81	[44]
2[c]	**a**	TA	CH_3OH	3.0	82	[44]
3[c]	**a**	TA	$scCO_2$/RfOH	0.5	89	[44]
4[e]	**b**	ATA	CO_2/IL/CH_3OH	5.0	87	[156]
5[e]	**b**	ATA	IL/CH_3OH	5.0	54	[156]
6[d]	**c**	DMI	$scCO_2$/MeOH	5.0	93.6	[157]

Reaction conditions: [a] See Fig. 4 for structure of ligands L. [b] TA= tiglic acid; DMI=dimethyl itaconate; ATA= atropic acid, t = 12–15 h, T = 323 K, substrate/catalyst = 150–160. P_{CO2} = 17–18 MPa. R_fOH = $CF_3(CF_2)_6CH_2OH$, 1.5 mmol. [c]Substrate/catalyst = 385. P(total) = 16.6 MPa, T = 298 K, methanol = 1 mL. [d]substrate/catalyst = 29.6; t = 24 h; P_{CO2} = 0 MPa; T = 313 K; IL= 1-n-butyl-3-methylimidazolium hexafluorophosphate methanol = 1.8 g. [e]substrate/catalyst = 29.6; t = 24 h; P_{CO2} = 5 MPa; T = 313 K; IL= 1-n-butyl-3-methylimidazolium hexafluorophosphate, methanol = 1.8 g.

bis(diphenylphosphino)− 1,1′-binaphthalene (**c**, Fig. 4) was reported by Hu et al. [157]. In this case, a C_2H_4 spacer was inserted between the perfluorinated chain and the aromatic ring to reduce the electron-withdrawing negative effect in the catalytic activity. This catalytic system was applied in the asymmetric hydrogenation of dimethyl itaconate (DMI) to dimethyl-2-methyl succinate. The ruthenium-catalyzed hydrogenation of dimethyl itaconate with **c** (Fig. 4) based system required the addition of small amounts of methanol to obtain comparable results to the ones attained in pure methanol. Thus high conversion and enantioselectivity were achieved using [Ru$(OCOCH_3)_2$(**c**)] (Fig. 4) as the catalyst, after carefully optimizing reaction parameters such as the electronic parameters, reaction temperature (295–373 K), addition of co-solvent or CO_2 pressure (entry 6, Table 4) [157].

A second generation of (±)− 2,2′-bis(diphenylphosphino)− 1,1′-binaphthalene chiral ligands very efficient for enantioselective hydrogenations of itaconate and enamide derivatives was developed at the beginning of the 2000s. They consisted of rhodium(I) complexes with chiral monodentate phosphonite, phosphoramidite or phosphite ligands based on (*R*)- and (*S*)-binaphthol skeleton. They provided high asymmetric induction in the hydrogenation of a variety of itaconate and acrylate derivatives (up to 94% ee) [158,159].

Surprisingly, non-fluorinated phosphite ligands such as (4 *R*)− 4-ethoxydinaphtho[2,1-d:1′,2′-*f*][1,3,2]dioxaphosphepine (**d**, Fig. 4) [160], phosphoroamidite 4-(dinaphtho[2,1-d:1′,2′-*f*][1,3,2]dioxaphosphepin-4-yl)morpholine or 1-(dinaphtho[2,1-d:1′,2′-*f*][1,3,2]dioxaphosphepin-4-yl)piperidine (**e** and **f** respectively, Fig. 4) [161], led to more effective catalytic systems in $scCO_2$ than in dichloromethane. Thus, the in situ catalytic system [Rh$(COD)_2$][BF_4]/**d** (molar ratio 1:2) (COD=1,5-cyclooctadiene) at 1 mol% Rh loading in $scCO_2$ (20 MPa) provided full conversion in the hydrogenation of dimethyl itaconate in 2 h at 10 MPa hydrogen pressure. That was seven-fold times higher than in dichloromethane. Moreover, the enantiomeric excess of the product obtained in $scCO_2$ (90%) was similar to that obtained in dichloromethane (97% enantiomeric excess). At the same catalytic conditions, full conversion was reached in 35–50 min with Rh/**f** and Rh/**e** catalytic systems (Fig. 4), with enantiomeric excess of ca. 98% (*R* enantiomer) [161]. The authors attributed this behavior to the high concentration of hydrogen in the $scCO_2$ phase and the high miscibility and diffusivity of hydrogen gas in the supercritical medium [160].

The development of continuous-flow processes in which the metal complexes are immobilized in fixed catalyst bed is essential to apply homogeneous catalysis in industrial processes. The continuous flow $scCO_2$ asymmetric hydrogenation of dimethylitaconate process was reported using a Rh(I) catalyst with a diphosphine chiral ligand immobilized in composites [162,163]. The Rh(I)/bisphosphine catalyst was immobilized on γ-alumina via a phosphotungstic acid linker $H_3O_{40}PW_{12}$ (Fig. 5). The best enantioselective catalyst leading to 83% enantiomeric excess, was the one bearing a chiral bisphosphine from Solvias AG, **a** (Fig. 5), working at low temperature (308 K).

Another interesting approach for the heterogenization of molecular catalysts to facilitate the separation is combining the great efficiency of the IL/$scCO_2$ biphasic system with the immobilization of the catalyst in solid inorganic supports. It is the so-called concept of Supported ILs Phase catalysts in supercritical conditions (Scheme 9) [42]. Leitner's group [42,164] used this approach to develop a continuous-flow system

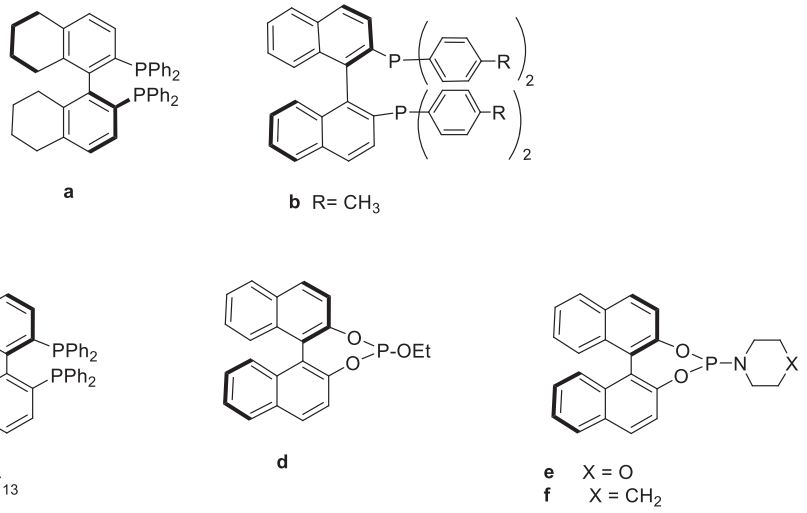

Fig. 4. (±)− 2,2′-Bis(diphenylphosphino)− 1,1′-binaphthalene derivatives **a-f** used as chiral ligands in the asymmetric hydrogenation of prochiral substrates under $scCO_2$.

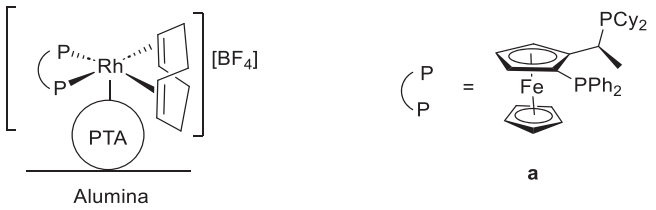

Fig. 5. Rh(I)/**a** catalytic system immobilized in phosphotungstic acid (PTA) over alumina applied in the asymmetric hydrogenation of dimethylitaconate in $scCO_2$ continuous-flow process [162]. **a** = (*R*)− 1-[(S_P)− 2-(diphenylphosphino)ferrocenyl]ethyldicyclohexylphosphine. PTA = phosphotungstic acid $H_3O_{40}PW_{12}$.

for the asymmetric hydrogenation of dimethyl itaconate using the chiral rhodium(I) complex [Rh(COD)(**a**)][NTf_2] (**a** = (2 *R*)− 1-((4 *S*)-dinaphtho[2,1-d:1′,2′-*f*][1–3]dioxaphosphepin-4-yl)− 8-(diphenylphosphaneyl)− 2-(naphthalen-1-yl)− 1,2-dihydroquinoline, NTf_2 = bis(trifluoromethyl sulfonyl)imide, Scheme 9), which was very active (turn over frequency (TOF) 45,000 h^{-1} at 2 MPa hydrogen, 313 K) and highly enantioselective (more than 99% enantiomeric excess (*S*) in dichloromethane). Using 1-ethyl-3-methylimidazolium bis(trifluoromethyl sulfonyl)imide as a solvent, the enantioselectivity was preserved. Solutions of the metal complex [Rh(COD)(**a**,)][NTf_2] (**a** = (2 *R*)− 1-((4 *S*)-dinaphtho[2,1-d:1′,2′-*f*][1,3,2]dioxaphosphepin-4-yl)− 8-(diphenylphosphaneyl)− 2-(naphthalen-1-yl)− 1,2-dihydroquinoline, NTf_2 = bis(trifluoromethyl sulfonyl)imide, Scheme 9) in 1-ethyl-3--methylimidazolium bis(trifluoromethyl sulfonyl)imide were supported over silica gel by wet impregnation (Merck, mean pore diameter 140 Å, Brunauer–Emmett–Teller surface area 298 m^2g^{-1}, mesopore volume 1.02 mLg^{-1}). This system operated in continuous flow in $scCO_2$ as a mobile phase at an initial TOF higher than 3800 h^{-1} (the turnover number TON was more than 100,000). Essentially, enantiopure (*S*)-dimethyl-2-methyl succinate was produced at yields of up to 0.7 $kgL^{-1}h^{-1}$ space-time and productivities of more than 100 kg product per gram of rhodium or 14 kg per gram of ligand [42].

The supported IL phase methodology was also applied to the continuous hydrogenation of C═C in the enol ester 1-(trifluoromethyl) vinylacetate to 1-(trifluoromethyl)ethylacetate (Scheme 10), which is an active ingredient for the treatment of neurological and neuropsychiatric disorders [165]. The supported IL phase Rh-based catalytic system containing **a** (Scheme 10), was very stable in continuous-flow conditions operating during 233 h at high pass-conversions (90–70%), with slight enantioselectivity increasing (80–84% enantiomeric excess) and turn over number higher than the analogous IL/$scCO_2$ batch system [165].

6.2. *Asymmetric hydrogenation of industrial and pharmacological interesting substrates*

Asymmetric hydrogenation of prochiral C═C, C═O and C═N containing compounds catalyzed by chiral metal complex catalysts is an efficient method to obtain chiral compounds with high enantioselective at mild reaction conditions. Many processes to produce optically pure pharmaceutical, agrochemical or cosmetic products include an asymmetric hydrogenation step catalyzed by a metal-based molecular catalyst [166]. In this context, the use of non-toxic alternative solvents such as $scCO_2$ has extensively been studied [3167].

One of the pioneering works on asymmetric hydrogenation of C═C bonds using $scCO_2$ was the hydrogenation of prochiral α-enamines as precursors of α-amino acids (Scheme 11). The chiral catalyst used was

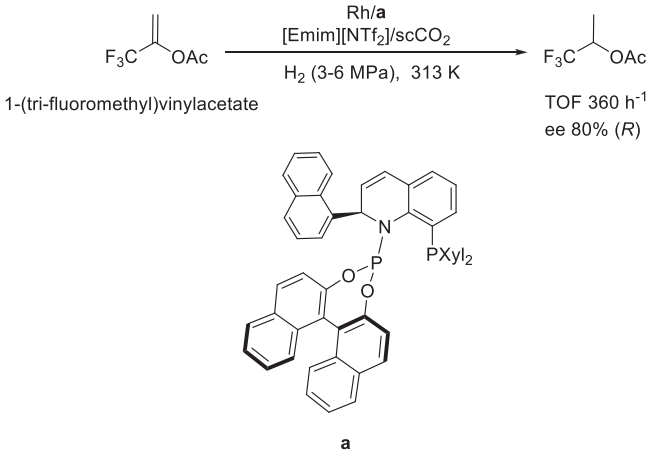

Scheme 10. Rh-catalyzed hydrogenation of 1-(tri-fluoromethyl)vinylacetate with Rh/**a** in IL/scCO2 continuous-flow system [165]. ee = enantiomeric excess, [EMIM][NTf_2] = 1-Ethyl-3-methylimidazolium bis(trifluoromethyl sulfonyl)imide.

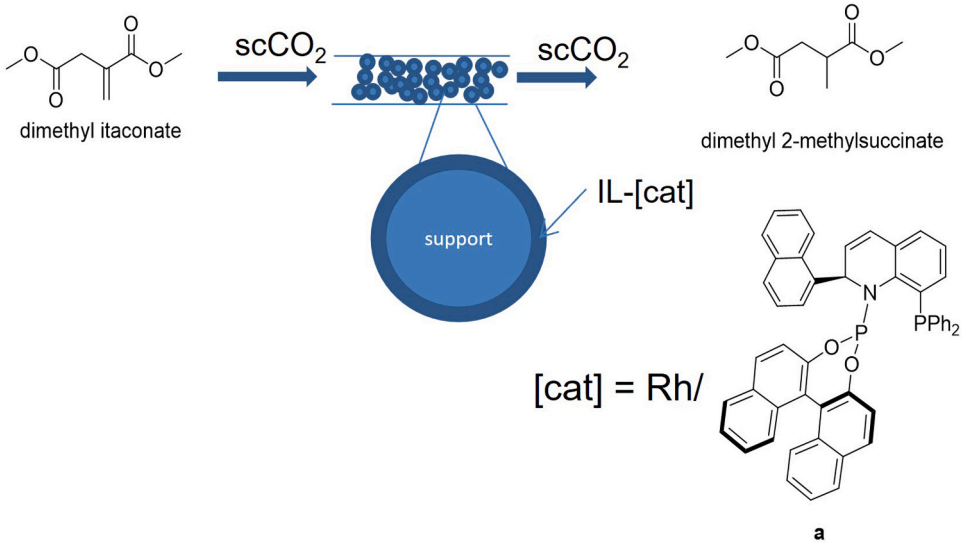

Scheme 9. Continuous-flow system for supported IL phase catalysis in $scCO_2$ for the asymmetric hydrogenation of dimethyl itaconate [42]. IL = 1-ethyl-3-methylimidazolium bis(trifluoromethyl sulfonyl)imide, **a** = (2 *R*)− 1-((4 *S*)-dinaphtho[2,1-d:1′,2′-*f*][1,3,2]dioxaphosphepin-4-yl)− 8-(diphenylphosphaneyl)− 2-(naphthalen-1-yl)− 1,2-dihydroquinoline.

the cationic complex [Rh(COD)(**a**)]X (COD = 1,5-cyclooctadiene; **a,** Scheme 11) containing fluorinated counter anions (X = B(3,5-$(CF_3)_2C_6H_3)_4$ or CF_3SO_3) to render the pre-catalyst soluble in $scCO_2$ [168]. Using organic solvents (hexane or methanol), the same catalytic system hydrogenated the α-enamides leading to more than 98% enantiomeric excess [169]. Substitution of the organic solvent by $scCO_2$ at a hydrogen pressure of 1.4 MPa, total pressure of 34.5 MPa and 313 K (substrate/catalyst = 500/1) showed that the enantioselectivities obtained in $scCO_2$ were as high as the ones obtained for the organic solvents, most of them exceeding the 99% enantiomeric excess (ee) [168]. In the case of β,β-disubstituted enamides (Scheme 11), the ee obtained in $scCO_2$ was clearly higher (84.7–96.8%) than those obtained in organic solvents (62.6–95.0% ee). The authors suggested that the positive effect was not only related to pressure effects rather to the use of $scCO_2$ but it was not further investigated.

An industrial application using the methyl derivative of the chiral bidentate ligand Duphos (R'' = Me, Scheme 11, Me-DuPhos) (−)− 1,2-bis((2 *R*,5 *R*)− 2,5-dimethylphospholano)benzene(cyclooctadiene)-rhodium(I) tetrafluoroborate catalytic system was proposed for the synthesis of the (*S*)− 2-amino-3-(3,4-dihydroxiphenil)propanoic acid (L-DOPA, Scheme 11), a chiral drug used in the treatment of Parkinson disease [40]. The key step is the hydrogenation of the intermediate (*Z*)− 2-acetamido-3-(4-acetoxy-3-methoxyphenyl)acrylic acid (pro-L-DOPA, Scheme 11). In the process, the use of $scCO_2$/IL (1-butyl-3-methylpyrrolidinium octylsulphate) technology to improve the process efficiency by decreasing the costs was proposed. Taking into account the overall process, the use of the $scCO_2$/IL biphasic hydrogenation produced 20 tons of (*S*)− 2-amino-3-(3,4-dihydroxyphenyl)propanoic acid per year, substantially reducing the costs of raw materials and energy consumption (in the $scCO_2$/IL process, 24% lower than the calculated for the conventional process) [40].

The compound (*S*)− 2-(4-fluorophenyl)− 3-methylbutanoic acid is an intermediate in the synthesis of the calcium antagonist Mibefradil (POSICOR®, Scheme 12) [170]. This compound was prepared by asymmetric Ru/**a**-catalyzed hydrogenation of 2-(4-fluorophenyl)− 3-methylbut-2-enoic acid in methanol (Scheme 12), obtaining high enantiomeric excess under high hydrogen pressure (up to 26 MPa) [171]. The use of the $scCO_2$/methanol system reduced the conversion and selectivity (91% yield; 63–84% enantiomeric excess) in comparison with the hydrogenation in methanol (99% yield; 93% enantiomeric excess) probably due to the lower solubility of the catalyst in $scCO_2$ [172].

Enantiopure chiral amines can be obtained by asymmetric

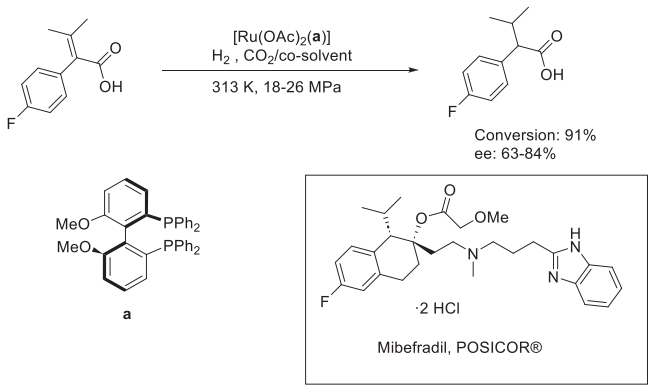

Scheme 12. Hydrogenation of 2-(4-fluorophenyl)− 3- methylbut-2-enoic acid catalyzed by the chiral Ru/**a** catalytic system [172]. **a** = (*R*)-(6,6′-dimethoxy-[1,1′-biphenyl]−2,2′-diyl)bis(diphenylphosphane).

hydrogenation of prochiral imines catalyzed by metal-complexes [173]. The synthesis of the herbicide (*S*)-Metolachlor includes one asymmetric hydrogenation step giving 80% enantiomeric excess on a technical scale [174]. An alternative process in $scCO_2$ was proposed using an Ir complex with a chiral P,N-donor phosphinodihydrooxazol ligand (**a**, Scheme 13) [175]. Cationic complexes with the fluorinated anion BArF [Ir(COD)(**a**)] [BArF] (BArF = tetra-3,5-trifluoro-phenyl borate) were prepared. The activities obtained in the hydrogenation of *N*-(1-phenylethyllidene)aniline at very low catalyst loading (0.078 mol% catalyst), 3 MPa hydrogen and at density of CO_2 0.75 g/mL were higher in $scCO_2$ (TOF up to 2820 h^{-1}) than in dichloromethane (TOF up to 1280 h^{-1}). The enantioselectivy in the (*R*)-enantiomer was comparable (up to 78% enantiomeric excess in $scCO_2$ versus 87% enantiomeric excess in dichloromethane) [175].

At the end of the reaction, the product was selectively extracted with the supercritical fluid CO_2 from the catalyst, which remained in the reactor, and was re-used without loss of catalytic activity. The whole process integrated catalytic reaction and extraction under the same reaction conditions in the so-called "catalysis and extraction using supercritical solutions". The catalyst was selectively separated since analysis by atomic absorption spectroscopy indicated that less than 5 ppm of Ir remained in the extracted product [175]. Nevertheless, the deactivation of the catalyst was detected during the separation process. To overcome this problem, the catalytic system [Ir(COD)(**a**)]PF_6, (**a**, Scheme 13) without fluorinated groups, was immobilized in ILs to

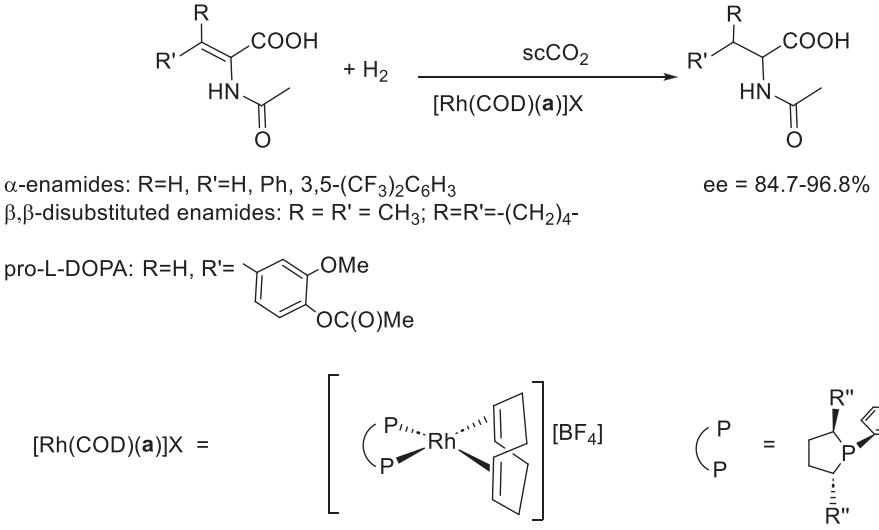

Scheme 11. Asymmetric hydrogenation of α- and β,β-disubstituted enamines with Rh(I) metal complexes [169]. L-DOPA= (*S*)− 2-amino-3-(3,4-dihydroxyphenyl) propanoic acid, **a** = bis-(*2 R,3 R*)− 2,5-diethylphospholanebenzene.

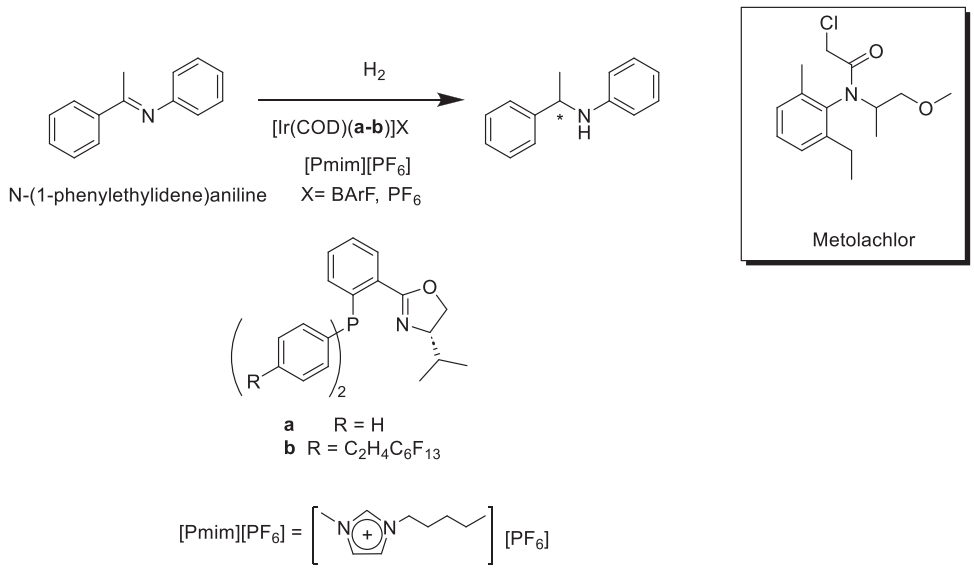

Scheme 13. Ir-catalyzed hydrogenation of *N*-(1-phenylethylidene)aniline as a model for the intermediate of Metolachlor.[175] BArF = $(B(3,5\text{-}(CF_3)_2C_6H_3)_4)^-$.

obtain a more stable and recyclable catalyst. Although the catalytic activity decreased in the biphasic IL/$scCO_2$ medium (turnover frequency up to 327 h^{-1} with the IL 1-pentyl-3-methylimidazolium hexafluorophosphate) compared to the use of neat $scCO_2$, the level of enantioselectivity was comparable (up to 78% enantiomeric excess) [114]. The catalyst was recycled up to seven times without loss of catalytic activity and showed remarkable stability upon exposure to air. The final product was quantitatively extracted from the IL phase with $scCO_2$ under moderate conditions. Further advantages of biphasic systems were that the solubility of hydrogen increased as confirmed by high-pressure ^1H NMR analyses [114]. Also, the catalyst could be formed in situ by the addition of the ligand to $[Ir(\mu\text{-}Cl)(COD)]_2$ (COD = 1,5-cyclooctadiene) into the IL.

Another example of chiral intermediates for the synthesis of flavors and pharmaceuticals are the hydroxyesters obtained by metal-catalyzed hydrogenation of β-ketoesters. Examples are the aliphatic 3-oxobutanoates, which are intermediates for the synthesis of Orlistat (Scheme 14), an inhibitor of intestinal digestion for the treatment of obesity [176]. The catalyst [$RuCl_2$(**a**)] (**a**, Scheme 14) catalyzed the hydrogenation in the $scCO_2$/methanol phase [172]. Under the reaction conditions, the substrate was a liquid and mixed very well in the reaction medium improving the results. Catalytic activity (estimated average turnover frequency 4000–6000 h^{-1}) and enantiomeric excess (98.3–98.8%) increased with the partial pressure of hydrogen (2–6 MPa) and CO_2 pressure (12–16 MPa). The authors proposed that the mass transfer of hydrogen into the reaction phase was the limiting factor of the process [172].

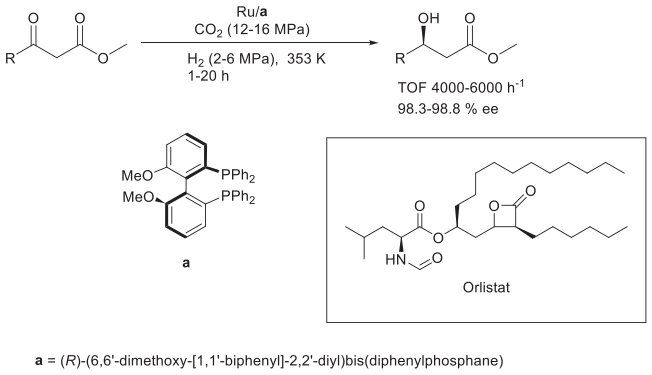

a = (*R*)-(6,6'-dimethoxy-[1,1'-biphenyl]-2,2'-diyl)bis(diphenylphosphane)

Scheme 14. Asymmetric hydrogenation of β-ketoesters with Ru/**a**-based catalyst [172]. TOF = turn over frequency, ee = enantiomeric excess.

Further improvement in the field of hydrogenation of C=O was the application of a continuous-flow process to the hydrogenation of methyl 3-oxo-pentanoate to methyl (*R*)− 3-hydroxypentanoate (Scheme 15), an intermediate of the synthesis of the pharmacological product atorvastatin calcium (Lipitor). The in situ formed $[Ru(C_6H_6)Cl_2]_2$/**a** (Scheme 15) catalytic system immobilized in IL b (Scheme 15) as stationary phase in the presence of an acidic additive c (Scheme 15) provided high single pass conversions (>90%) and good enantioselectivity (80–82% enantiomeric excess) in the first 80 h. The average space-time yielded 149 gL^{-1} h^{-1} in long-term experiments. Furthermore, no ruthenium or phosphorus contamination (below 5 ppm) was detected by inductively coupled plasma-optical emission (ICP-OES) spectrometry in the product stream [177].

7. Metal-based nanoparticles in hydrogen-mediated reactions in supercritical carbon dioxide

Transition-metal based nanoparticles (MNPs) are distinctive objects for applications in catalysis, because of their inherently electronic and geometric properties, in addition to the high specific surface area if compared with usual heterogeneous catalysts [178]. The synthesis of MNPs by bottom-up methodologies frequently involves the reduction of a salt, coordination or organometallic complex in the presence of a stabilizer in different types of media [179]. The nature of the solvent can induce a significant influence on the morphology of the MNPs; moreover, solvent can also participate as a stabilizing agent [180–182]. Supercritical fluid reactive deposition or chemical fluid deposition is a versatile approach to prepare well-defined metal-based nanostructures supported on solids, mainly by hydrogenation of the convenient metal precursor in supercritical conditions. The ensuing high phase homogeneity under these conditions, due to inherently boosted transport (high diffusivity and miscibility favoring mass transfer processes), permits to control of both seeding (formation of nuclei) and particle growth steps [183], and in consequence the morphology of the resulting nanoparticles [184–188]. Thanks to the tunable characteristics of $scCO_2$, numerous nanostructured systems such as supported and unsupported nanoparticles, quantum dots, nanofilms, nanorods, nanofoams, and nanowires have been produced without requiring further purification [188,189]. However, the main issue often encountered is the limited solubility of the metal species basically due to the low polarity of CO_2. To overcome this difficulty, water-in-$scCO_2$ microemulsions generated with (per)fluorinated surfactants have been applied in the synthesis of

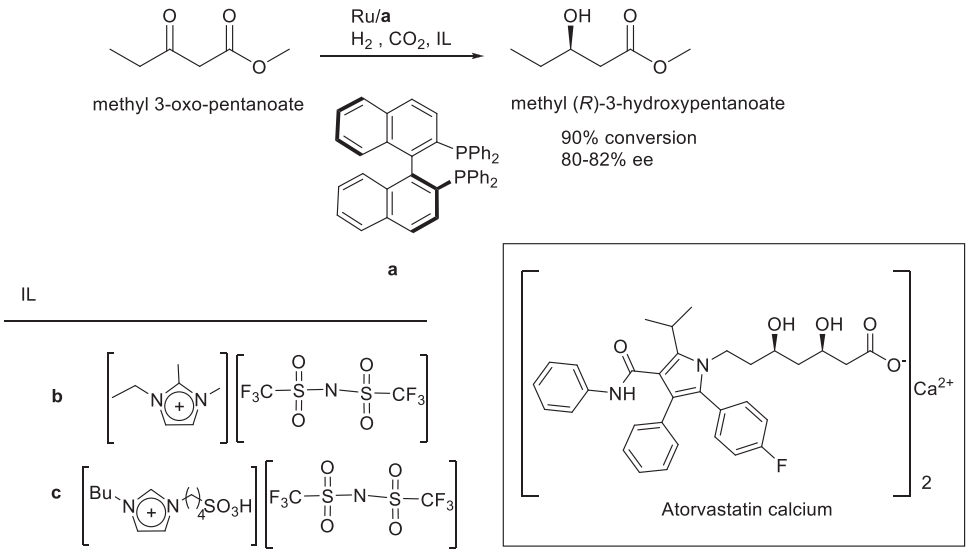

Scheme 15. Asymmetric hydrogenation of methyl 3-oxo-pentanoate catalyzed by Ru/**a** systems [177]. a = (*S*)− 2,2′-Bis(diphenylphosphino)− 1,1′-binaphthalene, ee = enantiomeric excess.

nanoparticles [190,191]. As discussed in Section 6, (per)fluorinated ligands are also employed to increase the solubility of the metal precursors [192], acting as well as efficient nanoparticle stabilizers [193, 194]. In this section, hydrogenation reactions involving metal-based nanocatalysts in $scCO_2$ are discussed, organized by type of substrate.

7.1. Hydrogenation of non-aromatic C═C bonds

In this section, the hydrogenation of C═C bond is discussed, excluding those belonging to an aromatic system. In the first part, non-conjugated systems are described, followed by substrates containing one C═C bond conjugated to aromatic or carbonyl groups.

7.1.1. Hydrogenation of non-conjugated substrates

The hydrogenation of cyclohexene represents a benchmark process for parameter optimization and also for comparison with other reported catalysts. Palladium nanoparticles supported on silica aerogels under $scCO_2$ were successfully applied in cyclohexene hydrogenation under flow, without detecting any metal surface modification after catalysis [195]. Knez's group prepared palladium nanoparticles by one-pot strategy synthesis, using organic modified silica aerogels as support, under $scCO_2$ conditions (313 K, 50 MPa CO_2). The as-prepared catalytic material was active in the reduction of 2,5-dihydro-2,5-dimethoxyfuran, exhibiting higher efficiency when working under flow conditions in comparison to batch ones (batch reactor: 60% conversion; flow reactor: 99% conversion) [45].

RuNPs on supports derived from carbon (single-walled carbon nanotubes-SWCNT; hollow graphitized nanofibers) applied in alkene hydrogenation proved the crucial function of $scCO_2$ concerning the transport of the reactants to the catalyst surface, principally for ruthenium nanoparticles/SWCNT (RuNPs mean diameter: 0.74 ± 0.18 nm) [46]. In fact, ruthenium nanoparticles/hollow graphitized nanofibers exhibited low activity under the same conditions (10 MPa CO_2, 1 MPa hydrogen, 383 K, 0.17 mol% Pd, 24 h) for the hydrogenation of norbornene and benzonorbornadiene (Scheme 16). Both catalytic materials exhibited ruthenium nanoparticles inside the carbon-based support (evidenced by both high-resolution transmission electron microscopy and scanning transmission electron microscopy). Ru/C commercially available material (RuNPs adsorbed at the support surface) was less active than ruthenium immobilized on SWCNT. Aromatic substituents showed high affinity for the inner cavities of carbon-based materials, as proven by competitive experiments which evidenced differences in terms of selectivity (Scheme 16b).

Recently, we prepared PdNPs stabilized by choline tosylalaninate (IL) in glycerol in the presence of $scCO_2$ showing higher catalytic reactivity in the hydrogenation of 4-phenylbut-3-en-2-one in comparison

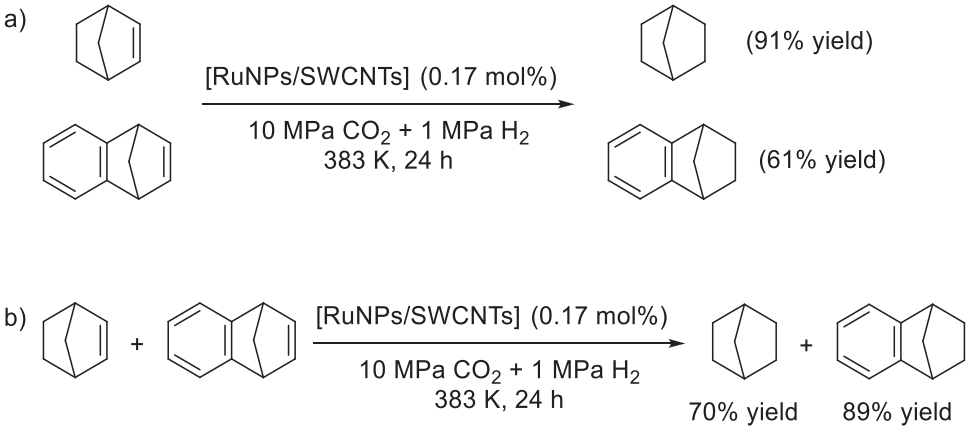

Scheme 16. Ru-based nanocatalysts on single-walled carbon nanotubes (RuNPs/SWCNTs) catalyzed the hydrogenation of non-aromatic C═C bonds: independent reactions (a) and competitive reaction (b) of norbornene and benzonorbornadiene[46].

with those prepared in its absence [47]. In addition, we observed a beneficial effect of CO_2 in the demanding hydrogenation of 4-phenylbutan-2-one (Scheme 17). The positive effect of CO_2 was undoubtedly evidenced when the catalytic hydrogenation took place under the same total pressure (40 bar): using four times less molecular hydrogen, the reactivity was nearly the same than using only hydrogen. But only 40% conversion was achieved. This behavior might be explained by the plausible catalyst deactivation, most likely due to the metal surface poisoning by carbon monoxide, produced by the reverse water-gas shift reaction.

7.1.2. Hydrogenation of conjugated substrates

Crooks and coworkers reported for the first time the use of PdNPs stabilized by dendrimers in catalysis under $scCO_2$, in particular in styrene hydrogenation obtaining ethylbenzene, a model substrate to evaluate the efficiency of new catalysts [196].

MNPs prepared in water-in-CO_2 microemulsions showed well-dispersion in the supercritical phase and relatively high stability [48]. Based on that, Wai and coworkers applied PdNPs in a water-in-CO_2 microemulsion containing the sodium bis(2-ethylhexyl)sulfosuccinate surfactant and perfluoropolyether phosphate or octanol, in the hydrogenation of some aromatic substrates and also maleic acid, proving that both CO_2- and water-soluble substrates can be hydrogenated using this type of catalysts [197,198] (Scheme 18). The catalytic phase was recycled up to 5 times for the hydrogenation of triphenylethylene.

Later on, the same group described the preparation of PdNPs supported on multi-walled carbon nanotubes in $scCO_2$, and then applied in the hydrogenation of *trans*-stilbene (10 MPa CO_2, 0.5 MPa hydrogen, 296 K, 10% weight Pd, 5–10 min), obtaining 96% of 1,2-diphenylethane [199,200] (Scheme 18).

From a sustainable viewpoint, selective hydrogenations avoiding the presence of additives require the design of suitable catalysts. For alkenes bearing a benzyl group, hydrogenolysis reaction (deprotection) can also occur together with C=C bond hydrogenations, frequently prevented by some additives [201]. Byeon, Kim and coworkers reported a selective catalyst based on PdNPs confined on the pores of Santa Barbara Amorphous support (SBA-15, a mesoporous silica); this catalytic material was successfully applied in the chemoselective reduction of 4-methoxycinnamic acid benzyl ester under $scCO_2$ (Scheme 19) [202]. In comparison with other heterogeneous systems (Pd/C, Pd/Al_2O_3), PdNPs on SBA-15 were more selective, leading to 97% selectivity (for quantitative conversion) in contrast to Pd/C (38% selectivity for full conversion) and Pd/Al_2O_3 (64% selectivity for 92% conversion).

The catalytic study of conjugated substrates permits the evaluation of the selectivity induced by the catalyst. AuNPs supported on cubic mesoporous Mobil Composition of Matter named MCM-48, confined inside the porous, which were prepared under different pressures of CO_2 (in the range of 7–12 MPa), led to a high selectivity in the hydrogenation of crotonaldehyde [203]. Under the studied conditions (7–14 MPa CO_2, 4 MPa hydrogen, 323 K, 4 h), the hydrogenation path towards crotyl alcohol was favored (Scheme 20), observing an increase in selectivity with an increase in pressure (from 7 to 14 MPa), which correlates with the density of the medium, and also with the size of nanoparticles (selectivity decreased from 90% to 50% for gold nanoparticles exhibiting 10 nm and 2 nm, respectively).

PdNPs stabilized by a cross-linked polymer and supported on silica allowed in $scCO_2$ the selective hydrogenation of 2,4-dimethyl-1,3-pentadiene into 2,4-dimethyl-2-pentene, observing that polymer-free palladium nanoparticles were more active than those coated by the polymer, but much less selective [204]. As expected, $scCO_2$ enhanced the rate (mainly due to the hydrogen solubility in this medium), increasing the selectivity up to 80%, slightly higher than that obtained under solvent-free conditions (75%).

Bimetallic palladium ruthenium nanoparticles, synthesized by co-reduction of metal salts in reverse micelles under $scCO_2$ conditions, were applied in the selective hydrogenation of (*Z*)− 2-pentenenitrile, being the most catalytically active those exhibiting a Pd:Ru ratio of 1:1 [205]. The presence of the nitrile group enhanced the hydrogenation rate of the C=C bond, as proven by comparing the turnover frequency values for (*Z*)− 2-pentenenitrile (12.05 min^{-1}) and 1-hexene (5.09 min^{-1}). In addition, the turnover frequency obtained for (*Z*)− 2-pentenenitrile hydrogenation using the monometallic counterparts, i.e., PdNPs (1.99 min^{-1}) and RuNPs (5.56 min^{-1}), evidenced the synergy effect between both metals in the bimetallic system; the structure of this bimetallic catalyst was not described. The catalytic system was reused three consecutive times preserving its activity and selectivity (catalytic conditions: 120 MPa CO_2, 20 MPa hydrogen, 348 K, 90 min).

Bimetallic palladium copper nanoparticles stabilized by polyurea, were applied in styrene oxide hydrogenation under $scCO_2$ conditions [206]. This bimetallic catalyst was more selective than the monometallic counterparts, giving up to 65% selectivity towards 2-phenylethanol. A rationale regarding activity and selectivity was proposed by the authors based on the Langmuir–Hinshelwood–Hougen–Watson model for bifunctional catalysts.

7.2. Hydrogenation of nitro-arenes

Haloanilines represent an important type of intermediates in the production of dyes, agrochemicals and drugs; they are usually prepared by metal-catalyzed hydrogenation of the corresponding nitro derivatives [207]. For that, chemoselective catalysts are required, in order to avoid dehalogenation, condensation reactions (leading to the formation of azoxybenzene, azobenzene or hydrazobenzene) and hydrogenation of the aromatic ring [208,209]. Zhao and coworkers developed the synthesis of PtNPs stabilized by polyethylene glycol (PEG) supported on different oxides (γ-Al_2O_3, SBA-15, TiO_2) and also on active carbon [210]. These platinum-PEG/support catalysts were successfully applied in the hydrogenation of chloronitrobenzenes (2-, 3 and 4-chloronitrobenzene, 2-chloro-6-nitrotoluene), 4-bromonitrobenzene and 3-iodonitrobenzene, obtaining selectively the products corresponding to the reduction of NO_2 into NH_2 in $scCO_2$ (less than 0.9% of by-products was observed). For platinum-PEG/γ-Al_2O_3 catalyzed 4-chloronitrobenzene hydrogenation, the catalytic behavior using $scCO_2$ and hexane was compared, concluding that in $scCO_2$ (8 MPa at 333 K) the hydrodehalogenation was suppressed but occurred when organic solvents were used. This process was also avoided in the case of 4-bromonitrobenzene and 3-iodonitrobenzene, although C-Br and C-I bonds are weaker than C-Cl ones, mainly observing the formation of the corresponding haloaniline. The platinum-PEG/γ-Al_2O_3 catalyst was recycled up to 4 consecutive runs for the hydrogenation of 4-chloronitrobenzene, with a decrease in conversion (from 98.7% to 88.9%) but preserving the selectivity (>99.6%); no leaching of Pt was observed by ICP-OES analyses.

Kawanami and coworkers ascertained that palladium nanoparticles supported on mesoporous boron-substituted MCM-41 were also efficient in the selective hydrogenation of nitroarenes in $scCO_2$ [211]. Compared

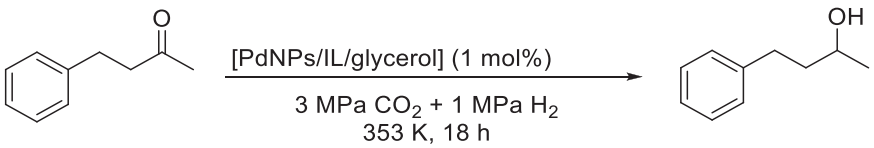

Scheme 17. PdNPs stabilized by choline tosylalaninate (IL) for the catalytic hydrogenation of 4-phenylbutan-2-one in glycerol [47].

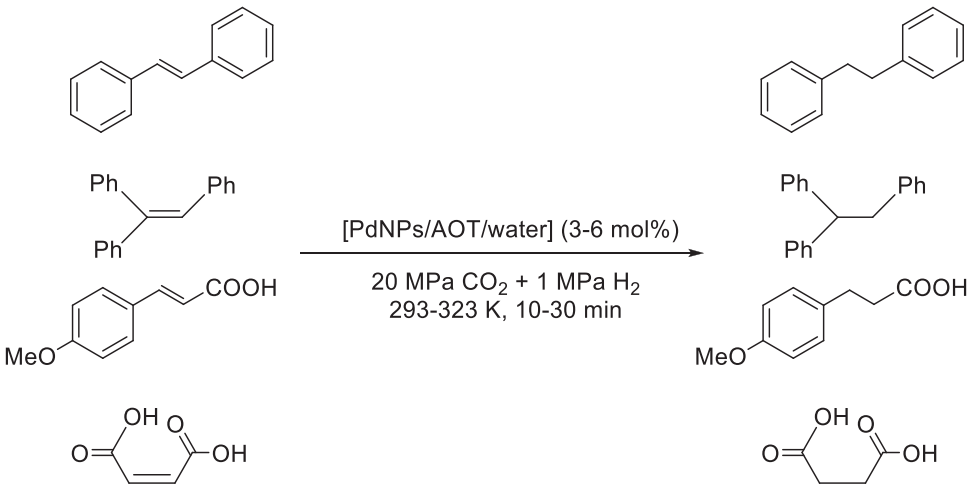

Scheme 18. PdNPs in water-in-CO_2 microemulsions catalyzed hydrogenation of both CO_2- and water-soluble substrates, using sodium bis(2-ethylhexyl) sulfosuccinate (AOT) as surfactant [197].

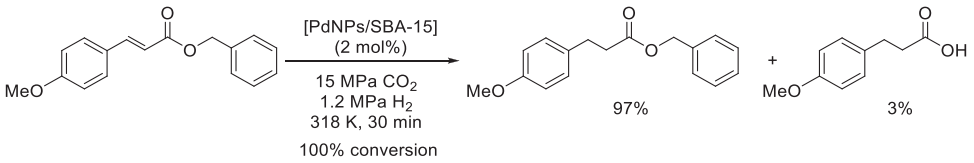

Scheme 19. PdNPs supported on mesoporous silica for chemoselective hydrogenation of an alkene containing a benzyl ester [202].

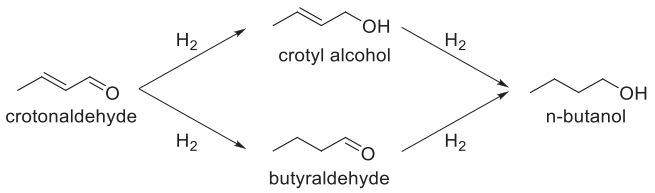

Scheme 20. Hydrogenation pathways for the hydrogenation of crotonaldehyde.

with PdNPs supported on Al-MCM-41 and Ga-MCM-41 materials, PdNPs/B-MCM-41 gave faster hydrogenations. Optimized conditions found for the reduction of nitrobenzene to aniline were applied to different substrates (2-, 3- and 4-chloronitrobenzene), merely obtaining the corresponding aniline (Scheme 21). This catalyst was also efficient for 2-, 3- and 4-nitroanisole starting materials. Other functional groups were also reduced, as observed in the hydrogenation of benzonitrile into benzylamine and phenol into cyclohexanone. Nitrobenzene hydrogenation was carried out in ethanol and hexane for comparative purposes; hexane gave the same selectivity (100%) but lower activity than $scCO_2$ (34% vs 100%, respectively), and ethanol gave the same activity (100%) but lower chemoselectivity leading to the formation of 27% of by-products. The catalyst proved a long-term activity, being recycled up to 7 consecutive runs for the nitrobenzene hydrogenation.

The analogous PdO-based catalysts were also prepared, i.e. PdO NPs/MCM-41 (M = B, Al, Ga) [212]. Similar behavior in relation to the zero-valent PdNPs was observed, that is boron-substituted support led to higher catalytic activity and better selectivity for the hydrogenation of 2-, 3- and 4-chloronitrobenzene in $scCO_2$ (conditions: 10% weight of catalyst, 308 K, 50 min, 12 MPa CO_2, 2 MPa hydrogen). However, the recycling was less efficient with PdO nanoparticles on boron-based MCM-41 (3 runs) than that observed for PdNPs-based catalyst (7 runs, see above [211]), although Pd(0) and not Pd(II) was observed after catalysis by powder X-ray diffraction.

7.3. Hydrogenation of renewable materials

In this section, the biomass valorization through metal-based nanoparticles catalyzed hydrogenation of renewable compounds, such as furfural, limonene, cinnamaldehyde and citral coming from oils of plants, is reviewed.

Furfural is a renewable chemical feedstock occurring in different agricultural by-products (like corncobs, oat or wheat bran), derived from lignocellulosic biomass. It represents a talented platform compound for the production of chemicals and fuels (for a selected review,

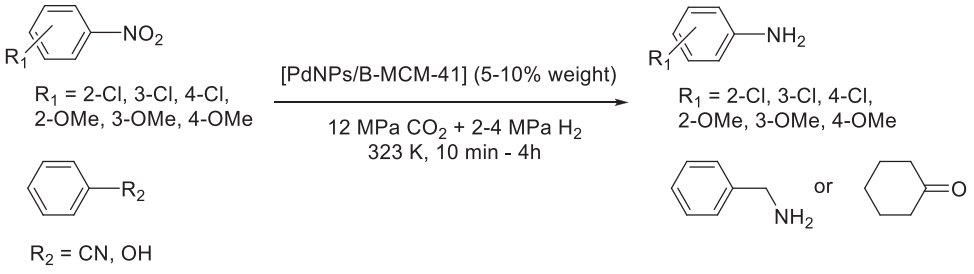

Scheme 21. Selective hydrogenation of aromatic substrates catalyzed by PdNPs/B-MCM-41 in $scCO_2$ [211].

see Li et al. [213]). Furfural can be transformed into a variety of C_4 and C_5 chemicals. Most of C_5 derivatives are generated via sequential methodologies involving hydrogenation and/or hydrogenolysis steps. In particular, the production of furfuryl alcohol represents ca. 65% of the consumption of furfural, which finds applications as solvent, fuel or monomer for the synthesis of polymers, among the most relevant uses. Furfuryl alcohol is industrially produced by catalytic hydrogenation of furfural being bimetallic Cu/Cr-based catalysts the most employed [214–216]. Due to the serious environmental issues of chromium, the development of Cr-free catalysts has been extensively studied.

Cabañas and coworkers have recently prepared mono- Pt, Cu, Ru, and bimetallic, RuPt and CuPt, nanoparticles supported on SBA-15 by reduction of the corresponding metal precursors in $scCO_2$, leading to MNPs homogeneously dispersed on the support. In the case of bimetallic systems, alloy structures were obtained [217]. Both mono- and bi-metallic systems were applied in the hydrogenation of furfural. Bimetallic RuPt/ SBA-15 catalyst was less active than monometallic Pt/SBA-15 one (copper nanoparticles and ruthenium nanoparticles were inactive), but more selective towards furfuryl alcohol. Major products were furfuryl alcohol and tetrahydrofurfuryl alcohol, but 2-methylfuran, 2-methyltetrahydrofuran and 1,5-pentanediol were also identified in small concentrations (Scheme 22).

The same group has investigated the partial hydrogenation of limonene, to compare the selectivity induced by different monometallic MNPs (M = Pt, Ru, Ni) supported on graphene [218] (Scheme 23). Thanks to the ability of $scCO_2$ to penetration and exfoliation, MNPs were deposited on reduced graphene oxide, exhibiting a well-dispersion on the support; for Ni/reduced graphene oxide, large particles were obtained (ca. 15 nm) in contrast to those corresponding to Pt and Ru (mean sizes in the range 2.5 – 4.5 nm). Authors postulate that these differences are related to the lower cohesive energy and diffusion barrier of Ni comparing with Pt and Ru. Pt- and Ru-based catalysts were highly active (conversions ca. 78%) and selective (more than 80%), yielding up to ca. 67% of *p*-menthenes (mixture of both *p*-menth-1-ene and *p*-menth-3-ene); the activity of Ru/C (commercial catalyst) was lower, but also showing a high selectivity (conversion = 42%; yield = 38%). Curiously, almost the same catalytic reactivity as for Ru/C was observed for metal-free reduced graphene oxide. These catalysts did not exhibit efficient recyclability using the Ru-based catalyst; after the first run, a loss of activity was observed, but the selectivity was preserved up to the four runs. Comparing these results with those coming from RuNPs/SBA-15 under the same catalytic conditions, ruthenium nanoparticles/reduced graphene oxide and platinum nanoparticles/reduced graphene oxide were less active but more selective [219]; this fact can be related to the support effect.

Cinnamaldehyde, responsible for the cinnamon flavor, is a representative α,β-unsaturated aldehyde often used to study the chemoselectivity induction by catalysts in hydrogenation processes (Scheme 8). In particular, the formation of cinnamyl alcohol is more challenging and more interesting from an industrial point of view (used in fragrances due to its hyacinth aroma), because the hydrogenation of the conjugated C=C bond to the carbonyl group is both kinetically and thermodynamically straightforward, leading to hydrocinnamaldehyde.

AuNPs and PtNPs exhibited a high selectivity towards the formation of cinnamyl alcohol under $scCO_2$. AuNPs were stabilized by encapsulation on the porous of an amphiphilic copolymer constituted of maleic acid and an alkyl (C_{18}) vinyl monomer [220]. For AuNPs showing sizes in the range 5–15 nm, cinnamaldehyde hydrogenation under $scCO_2$ (20% weight catalyst, 10 MPa CO_2, 4 MPa hydrogen, 323 K, 4 h) led to more than 88% of selectivity towards cinnamyl alcohol, obtaining hydrocinnamyl alcohol as a major byproduct (less than 12%); for bigger nanoparticles, the selectivity dramatically dropped. In all the cases, conversions were low (up to 38%). PtNPs supported on different solids gave from low to moderate conversions, mainly depending on the nature of the support. Therefore, PtNPs on silica or ceria gave comparable activity for hydrogenations in common organic solvents (pentane, isopropanol) and in $scCO_2$ or $scCO_2$-isopropanol mixture (9–22% conversion), but the selectivity towards the formation of alcohol was clearly higher in $scCO_2$ (80–90%) than isopropanol (less than 55%). The highest selectivity was achieved using PtNPs on silica under neat $scCO_2$ (conversion = 12.5%; selectivity = 91.3%). Authors postulated that the C=O turns weaker due to the interaction of cinnamaldehyde with CO_2 under supercritical conditions, favoring, in consequence, its adsorption at the metal surface and subsequent reduction, as discussed in Section 6.1.

Chatterjee and coworkers prepared PtNPs on mesoporous supports MCM-48, Al-MCM-48 and Ti-MCM-48, observing a higher reactivity and selectivity (towards the formation of cinnamyl alcohol) for the PtNPs/Ti-MCM-48 catalytic material, although the mean size of the nanoparticles was practically the same (5.3–5.8 nm) [221]. This behavior was justified by the formation of oxygen sites of Ti-based catalyst at the interface between metal and support favored by $scCO_2$ and in consequence the electronic density on platinum increases, which promotes the C=O hydrogenation. However, the recycling was not satisfactory and an activity decrease was observed after the second run.

Shirai's group applied iridium nanodisks [222] and platinum

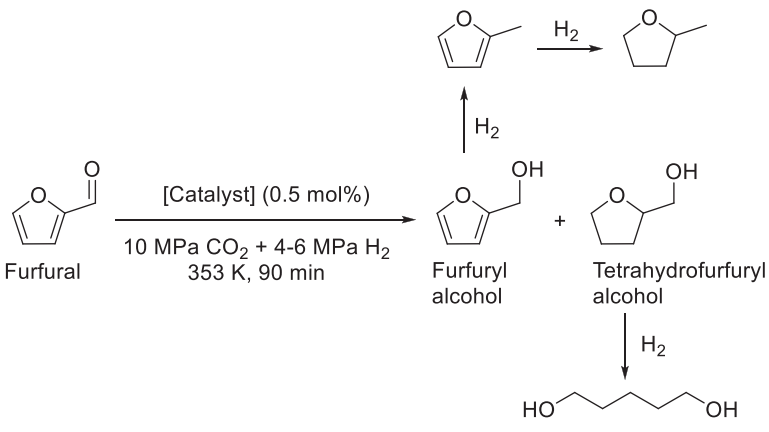

Catalyst = RuPtNPs/SBA-15: conversion = 60%, furfuryl alcohol/tetrahydrofurfuryl alcohol = 53/26
Catalyst = PtNPs/SBA-15: conversion = 70%, furfuryl alcohol/tetrahydrofurfuryl alcohol = 34/40

Scheme 22. MNPs supported on mesoporous SBA-15 catalyzed furfural hydrogenation, mainly leading to the formation of furfuryl alcohol and tetrahydrofurfuryl alcohol [217].

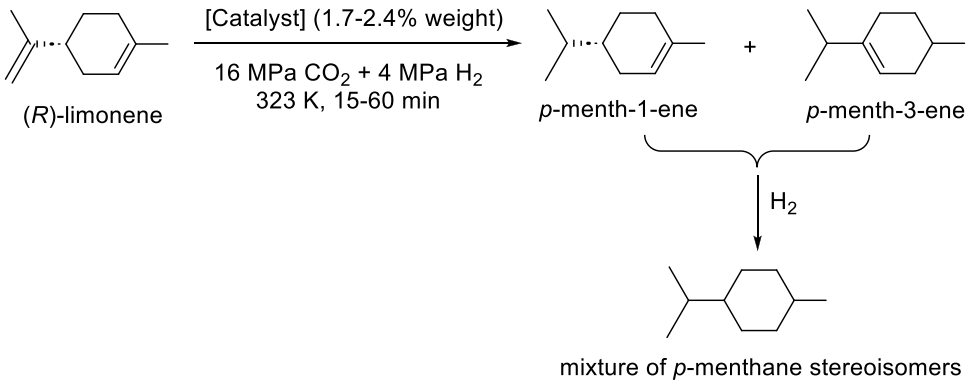

Scheme 23. Reaction pathway for the metal-catalyzed hydrogenation of limonene [218].

nanosheets [223,224] intercalated between graphite layers in cinnamaldehyde hydrogenation under $scCO_2$ conditions. For iridium-based catalytic materials, higher activity and selectivity towards cinnamyl alcohol were observed with respect to Ir nanoparticles immobilized on graphite. In the case of Pt-based catalysts, the authors proved that the chemoselectivity is highly dependent on the graphite surface area; thus, cinnamyl alcohol was selectively obtained for graphite showing a surface area of 20 $m^2.g^{-1}$ while hydrocinnamaldehyde was the main product for graphite with a surface area of 120 $m^2.g^{-1}$. This different behavior was correlated with the different locations of Pt nanosheets depending on the support nature and in consequence resulting in different adsorptions of organic compounds.

In contrast to Au- and Pt-based catalysts, RhNPs supported on ordered MCM-41 and Michigan State University mesoporous silica (MSU-H) led to the formation of hydrocinnamaldehyde with selectivity higher than 85% for the different catalysts (metal nanoparticle mean diameter in the range of 1.6–13 nm), from low to moderate conversions (7–47%) under $scCO_2$ conditions (10 MPa CO_2, 4 MPa hydrogen, 323 K, 3 h) [225].

Citral, present in several oils of plants, is a terpenoid constituted of two stereoisomers (*E*)- and (*Z*)− 3,7-dimethyl-2,6-octadienal, known as geranial and neral respectively. Like cinnamaldehyde, citral represents a benchmark substrate to evaluate the selectivity of a given catalyst in hydrogenation processes (Scheme 24). In particular, the selective reduction of the 2,3 conjugated C═C bond is interesting because led to the formation of citronellal (CIAL) which exhibits insect-repellent properties, giving citronella oil its characteristic lemon scent.

As very well-known, Pd catalysts favor the hydrogenation of C═C bond, but often they are sluggish to hydrogenate carbonyl groups [226]. Thus, PdNPs confined in micro-micelles, which are constituted of a fluorinated ammonium surfactant ($NH_4^+CF_3(CF_2)_{12}COO^-$) in the presence of water [227,228] and under $scCO_2$ were applied in the selective hydrogenation of citral. In the vapor phase and in solution (using hexane as solvent), PdNPs mainly led to the formation of the fully saturated aldehyde (dihydrocitronellal). However, in water-in-$scCO_2$ microemulsions (0.4 mol% Pd, 14 MPa CO_2, 0.4 MPa hydrogen, 313 K), where PdNPs are confined in the core of the micelles, the major product was citronellal (67%) together with the formation of dihydrocitronellal (7%). Authors rationalized this behavior in terms of the steric effect induced by the surfactant around the MNPs, forcing citral to be aligned to penetrate to the micelle and reach palladium, and then favoring the hydrogenation of the conjugated C═C bond. The same group studied the reactivity of RuNPs in water-in-$scCO_2$ microemulsions, observing the same behavior as that shown by palladium for citral hydrogenation [229]. But for the hydrogenation of citronellal, Ru-based catalyst gave the full hydrogenated product 3,7-dimethyloctan-1-ol (93% conversion; selectivity: 81% 3,7-dimethyloctan-1-ol + 19% dihydrocitronellal), while palladium favored the formation of the saturated aldehyde (100% conversion; selectivity: 79% dihydrocitronellal; + 21% 3, 7-dimethyloctan-1-ol).

Zhang and coworkers studied the influence of unsupported monometallic PtNPs (spheres and nanorods) and alloy AuPt nanoparticles [230]. They observed that the activity of the three catalysts was comparable in both solvents, $scCO_2$ and toluene. However, the selectivity was better in $scCO_2$; in particular, using AuPt nanoparticles, at 46% conversion, a mixture of six products was obtained, 60% constituted of geraniol and nerol, meaning that the hydrogenation of the aldehyde group was privileged in relation to both C═C bonds. A mixture of monometallic PdNPs and AuNPs supported on TiO_2 led to higher conversion (69%) and selectivity (90%) towards citronellal than AuPd alloyed system (51% conversion and 61% selectivity); for the monometallic Pd-based catalyst, the selectivity was similar, but the activity

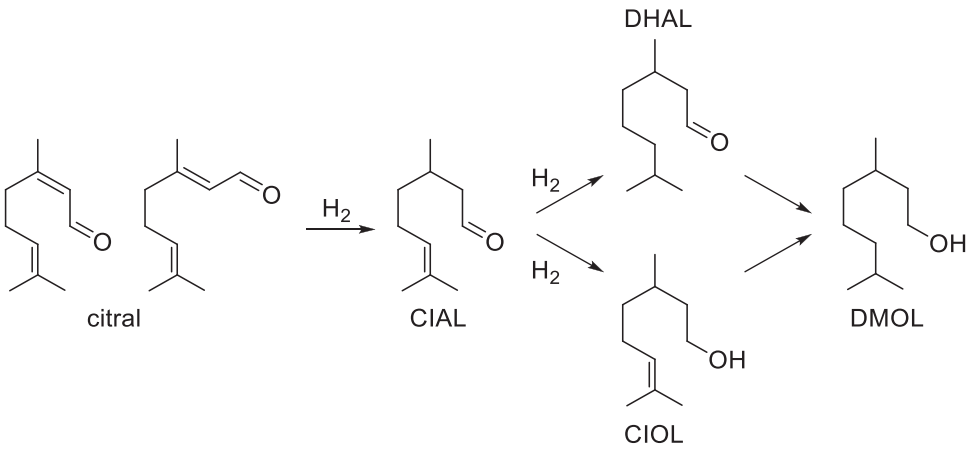

Scheme 24. Simplified pathway of citral hydrogenation. CIAL: citronellal; CIOL: citronellol; DHAL: dihydrocitronellal; DMOL: 3,7-dimethyloctan-1-ol.

drastically dropped (conversion 27%), under the same reaction conditions (8 MPa CO_2, 4 MPa hydrogen, 353 K).

7.4. Hydrogenation of arenes

The selective reduction of phenol to cyclohexanone is an industrial interesting process because it represents a crucial intermediate for the synthesis of adipic acid and caprolactam, starting materials for the production of polyamide resin, Nylon 66 and Nylon 6 [231]. Cyclohexanone is industrially obtained by a two-step methodology, i.e., phenol hydrogenation to cyclohexanol followed by dehydrogenation [232]. In a sustainable development, the direct synthesis of cyclohexanone by selective hydrogenation of phenol is obviously preferred. Gas-phase hydrogenation involving different Pd-based catalysts leads to cyclohexanone, but under harsh conditions which triggers the catalyst deactivation [233,234]. Chatterjee, Kawanami and coworkers evaluated this process using Pd- and Rh-based catalysts supported on Al- MCM-41 (MNPs mean size in the range 10–12 nm) under $scCO_2$ conditions [235]. They observed that for both catalysts the support has an important influence on activity, being more active when supported on Al-MCM-41 than on non-modified substrate. Comparing both catalysts, PdNPs/Al-MCM-41 was much more selective; for a 98% conversion, 97.8% cyclohexanone and 2.2% cyclohexanol, obtaining, for similar activity, nearly equimolar amount of both organic compounds using rhodium nanoparticles/Al-MCM-41 under the same reaction conditions (10% weight of metal, 12 MPa $scCO_2$, 4 MPa hydrogen, 323 K, 4 h). Pd-based catalyst was recycled up to 4 times without efficiency loss. Under comparable conditions but using organic solvents (such as ethanol and hexane), the activity decreased (conversions up to 25%) with low selectivity (65% for hexane; 42% for ethanol). This behavior agrees with the higher solubility of hydrogen in $scCO_2$ and the absence of mass transfer issues (see above Section 2.2). Other hydroxyl aromatic derivatives were also hydrogenated mainly giving the corresponding ketones (Scheme 25).

The support influences the activity and selectivity. Actually, RhNPs supported on carbon nanofibers showed moderate conversions (50–55%) with a low selectivity (cyclohexanone/cyclohexanol = 60/40; reaction conditions: 5 wt% of catalyst, 14 MPa CO_2, 2 MPa hydrogen and 353 K for 10 min) [236]. More active Rh-based catalysts supported on SBA-15 were developed by Kim, Byeon and co-workers [237]. Phenol and 4-methylphenol were efficiently reduced to the corresponding ketone. Wai and co-workers prepared in situ RhNPs in a water-in-CO_2 microemulsion showing high activity and selectivity in the formation of cyclohexanone [238].

Recently, Leitner and coworkers have applied RhNPs immobilized on functionalized silica in the hydrogenation of fluoro-arenes to afford fluorocyclohexane derivatives under $scCO_2$ conditions, suppressing the competitive hydrodefluronation [239].

Lyubimov's group has efficiently prepared Ir [240] and Pd [241] nanoparticles supported on hypercrosslinked polystyrene under hydrogen pressure using $scCO_2$ as a solvent, in both cases obtaining MNPs of ca. 5 nm of mean diameter. These catalytic materials were applied in the hydrogenation of toluene, tetralin, phenol and halo-benzenes, in $scCO_2$ for Pd systems and under neat conditions for iridium ones. Ir-based catalysts favored hydrodehalogenation processes; actually, chloro- and fluorobenzene gave exclusively cyclohexane.

Polycyclic aromatic hydrocarbons are considered as pollutants, exhibiting their derivatives, such as dihydrodiol epoxides, high toxicity (mutagenic and carcinogenic metabolites) [242]. Pd-based catalysts have proven their efficiency in the partial or full hydrogenation of this type of compounds. In fact, PdNPs stabilized by high-density polyethylene polymer, catalyzed the hydrogenation of different aromatic compounds from two to four-fused aromatic rings (naphthalene, anthracene, phenanthrene, pyrene, chrysene, triphenylene, naphthacene; Fig. 6) [243]. For polycyclic aromatic hydrocarbons containing less than four rings, the hydrogenation was complete giving the corresponding saturated compounds. Four-fused derivatives often gave partial hydrogenations, due to their lower hydrogenation kinetics; in general, the partially reduced intermediates were slowly hydrogenated than the starting materials. The same group applied PdNPs embedded in polydimethylsiloxane for the hydrogenation of poly-chloro-biphenyl derivatives and polycyclic aromatic hydrocarbons, obtaining complete hydrogenation and for poly-chlorinated substrates, complete hydrodehalogenation [244].

Pd and Rh nanoparticles supported on plastics (high density polyethylene HDPE and the fluoropolymer, perfluoroalkoxy alkane) and prepared in $scCO_2$, were efficiently applied in the hydrogenation of anthracene to lead to selectively tetralin (PdNPs/HDPE) and benzene (RhNPs/perfluoroalkoxy alkane) [242]. PdNPs/HDPE were recycled up to 10 times, obtaining in each run more than 99% of tetralin. This catalytic system gave also high selectivity in the hydrogenation of phenol, mainly obtaining cyclohexanone.

Shirai and coworkers applied rhodium nanoparticles supported on activated carbon for the hydrogenation of naphthalene and tetralin, evidencing the crucial impact of the MNPs in the hydrogenation under $scCO_2$ due to the different dispersion of the metallic nanoparticles in this medium, which depends on their morphology: better dispersion (smaller nanoparticles), faster hydrogenation [245]. Higher rates were observed comparing the same catalyst in $scCO_2$ than in heptane.

RuNPs and RhNPs stabilized by phosphines were applied in the hydrogenation of arene derivatives (Scheme 26) [246]. Ru-based nanoparticles were more active than rhodium ones, in particular, those containing the phosphine bearing fluorinated groups, in agreement with their higher active surface (RuNPs mean size: 1.30–1.38 nm; RhNPs mean size nanoparticles: 1.70–2.5 nm); after catalysis, RuNPs remained dispersed in contrast to the agglomerates observed for RhNPs. However, the Ru-based catalyst was more active in THF than in $scCO_2$, probably due to its lower solubility in $scCO_2$ medium.

8. Conclusions

To sum up, we have described in this review the remarkable relevance of compressed CO_2 as a medium in metal-promoted hydrogenation processes, analyzing both engineering tools and catalytic applications, involving both metal complexes and metal-based nanoparticles. Selected aspects have been described regarding the engineering aspects concerning advances in hydrogenation reactions in supercritical fluids and gas-expanded liquids. Even if this contribution

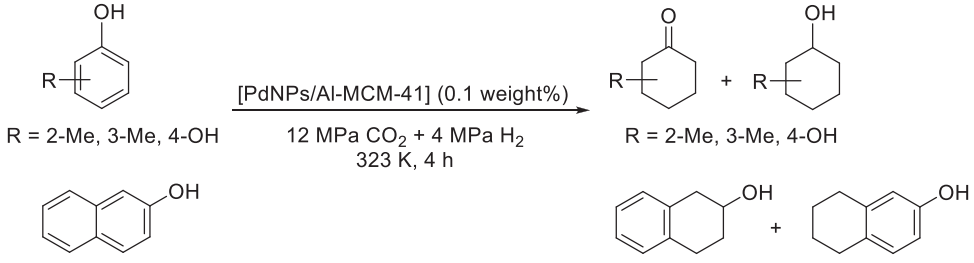

Scheme 25. Hydrogenation of aromatic alcohols catalyzed by PdNPs/Al-MCM-41 [235].

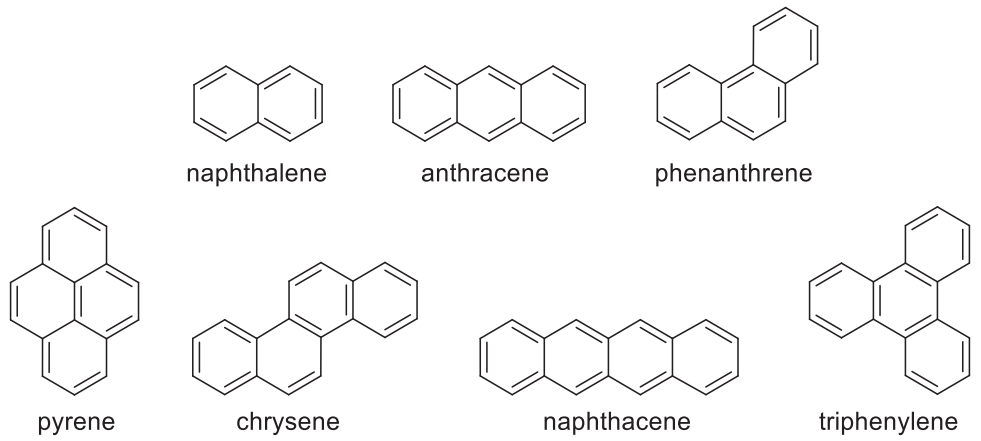

Fig. 6. Structures of the polyaromatic substrates involved in their hydrogenation catalyzed by PdNPs stabilized by high density polyethylene polymer under $scCO_2$ conditions [243].

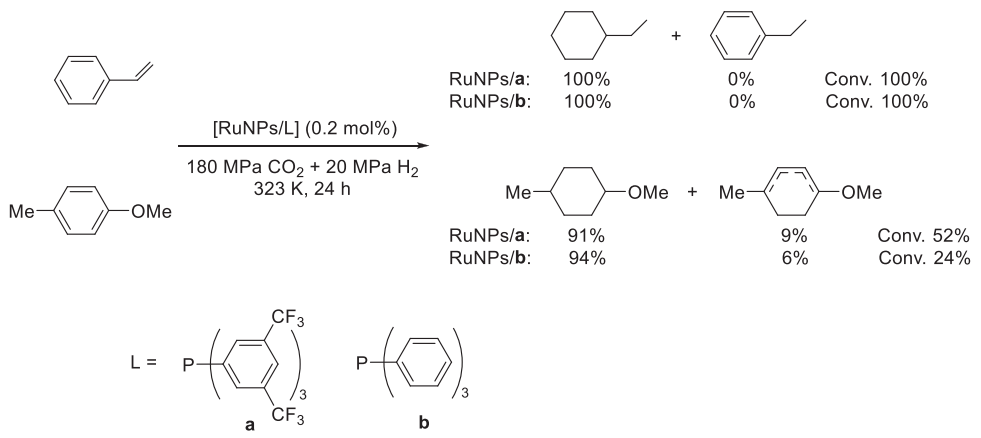

Scheme 26. RuNPs stabilized by fluorinated phosphines (L) applied in the hydrogenation of arenes [246].

does not intend to be exhaustive, it tries to give general notions concerning the current need of process engineers to get data from these systems to develop, design and optimize chemical processes involving these fluids. It is intending to help to foster more sustainable and efficient processes. With this purpose, wide-ranging concepts about phase equilibrium, mass and heat transfer, continuous processes, modeling and process design, together with the latest advances in these fields, have been presented. The lack of studies and data regarding mass and heat transfer is overwhelming and even if modeling tools have been improved in the last years, the scarce experimental data at the micro-scale still represents a difficulty when an entire chemical process is developed. Some successful exemples have been highlighted showing that when a process is carefully and judiciously designed by understanding all of the involved steps, scale-up is possible affording flexible and sustainable processes.

The use of compressed CO_2 as a reaction medium in hydrogenation catalyzed processes has impressively progressed in the last decades. Regarding metal complexes as catalysts, the initial expectations about the possibility of totally replacing organic solvents with $scCO_2$ did not completely succeed, mostly due to the poor solubility of polar/ionic catalyst complexes in the low polar CO_2; the modification of the catalyst to improve the solubility often led to less active systems. Nevertheless, it has achieved a substantial advancement with some modifications of the reaction media such as the addition of co-solvents or the use of ILs and even water as a second phase to facilitate the separation between catalysts and products. Furthermore, the immobilization of molecular catalysts dissolved in ILs on inorganic solids has permitted asymmetric hydrogenation of prochiral substrates with high enantioselectivity in continuous-flow systems. In our opinion, it is in the field of the synthesis of high added-value products such as active pharmaceutical ingredients where selective homogeneous metal-based catalysts in $scCO_2$ can have high catalytic efficiency. The high costs of these catalysts and the supercritical equipment can be overcome by the high value of pharmaceuticals taking into account that low scale reactions (batch or continuous flow) can be performed. Nevertheless, a critical issue here will be the purity of the compressed CO_2. More studies are needed to asses the stability of the metal catalysts in the presence of oxygen or carbon monoxide.

Concerning the applications of catalytic materials containing metal-based nanoparticles, both mono- and bimetallic catalytic systems, this revision evidenced the efficiency of using this type of catalysts in hydrogenation reactions for supported catalysts on solids, but also for those dispersed in a liquid phase, i.e., colloidal dispersions (micro-emulsions confining the nanoclusters, CO_2-soluble ligands capping MNPs, etc.). It is important to highlight that high chemoselectivity is achieved in $scCO_2$ for hydrogenation of multi-functional substrates, often higher than those observed in conventional organic solvents. The recycling can be impeded by catalyst deactivation issues, frequently triggered by the nature of the support and reaction conditions. Actually, catalyst poisoning (carbon monoxide adsorption) and agglomeration of metal-based nanoparticles (decrease of the specific surface) are the foremost factors to cause the catalyst deactivation. Remarkably, MNPs from 3d-transition metals (Fe, Co, Ni) have barely been applied in hydrogenations under $scCO_2$ conditions.

This contribution can help to attract the attention of researchers and motivate them to still increase the data and the studies available on the

properties of supercritical fluids or gas-expanded liquids to develop cleaner, safer and more environmentally friendly catalytic processes.

Declaration of Competing Interest

The authors declare that they have no known competing financial interests or personal relationships that could have appeared to influence the work reported in this paper.

Data Availability

No data was used for the research described in the article.

Acknowledgments

The Université Fédérale de Toulouse (*program IDEX Recherche – [1]Actions Thématiques Stratégiques*), the Centre National de la Recherche Scientifique (CNRS) and the Université Toulouse 3-Paul Sabatier are gratefully acknowledged for their financial support. A. M.-B. thanks the Ministerio de Ciencia e Innovación and AEI/FEDER UE (PID2019-104427RB-100) and Departament d'Economia i Coneixement (2021 SGR 00163) for the financial support. G. G. thanks Université Fédérale de Toulouse for PhD scholarship through the IDEX program.

References

[1] P.T. Anastas, N. Eghbali, Green chemistry: principles and practice, Chem. Soc. Rev. 39 (2010) 301–312, https://doi.org/10.1039/b918763b.
[2] M.A. Abraham, N. Nguyen, "Green engineering: defining the principles"- resdts from the sandestin conference, Environ. Prog. 22 (2003) 233–236, https://doi.org/10.1002/ep.670220410.
[3] D.J. Cole-Hamilton, Asymmetric catalytic synthesis of organic compounds using metal complexes in supercritical fluids, Adv. Synth. Catal. 348 (2006) 1341–1351, https://doi.org/10.1002/adsc.200606167.
[4] R.S. Norhasyima, T.M.I. Mahlia, Advances in CO_2 utilization technology: a patent landscape review, J. CO_2 Util. 26 (2018) 323–335, https://doi.org/10.1016/j.jcou.2018.05.022.
[5] C. Kim, C.-J. Yoo, H.-S. Oh, B.K. Min, U. Lee, Review of carbon dioxide utilization technologies and their potential for industrial application, J. CO_2 Util. 65 (2022), 102239, https://doi.org/10.1016/j.jcou.2022.102239.
[6] V. Arunajatesan, B. Subramaniam, K.W. Hutchenson, F.E. Herkes, Fixed-bed hydrogenation of organic compounds in supercritical carbon dioxide, Chem. Eng. Sci. 56 (2001) 1363–1369, https://doi.org/10.1016/S0009-2509(00)00359-6.
[7] S. van den Hark, M. Härröd, Hydrogenation of oleochemicals at supercritical single-phase conditions: influence of hydrogen and substrate concentrations on the process, Appl. Catal. A Gen. 210 (2001) 207–215, https://doi.org/10.1016/S0926-860X(00)00826-7.
[8] M. Härröd, M.-B. Macher, S. van den Hark, P. Moller, Hydrogenation under supercritical single-phase conditions, in: A. Bertucco, G. Vetter (Eds.), High Pressure Process Technology: Fundamentals and Applications, Elsevier, 2001, pp. 496–508.
[9] K. Burgemeister, G. Franciò, V.H. Gego, L. Greiner, H. Hugl, W. Leitner, Inverted supercritical carbon dioxide/aqueous biphasic media for rhodium-catalyzed hydrogenation reactions, Chem. - A Eur. J. 13 (2007) 2798–2804, https://doi.org/10.1002/chem.200601717.
[10] M.R. Damen, R.W. Brand, S.C. Bloem, E. Pingen, K. Steur, C.J. Peters, G.-J. Witkamp, M.C. Kroon, Process intensification by combining ionic liquids and supercritical carbon dioxide applied to the design of Levodopa production, Chem. Eng. Process.: Process.Intensif. 48 (2009) 549–553, https://doi.org/10.1016/j.cep.2008.08.001.
[11] E. Bogel-Łukasik, R. Bogel-Łukasik, K. Kriaa, I. Fonseca, Y. Tarasenko, M. Nunes da Ponte, Limonene hydrogenation in high-pressure CO_2: Effect of hydrogen pressure, J. Supercrit. Fluids 45 (2008) 225–230, https://doi.org/10.1016/j.supflu.2007.10.001.
[12] E.-K. Shin, B. Lee, E. Section, High-pressure phase behavior of carbon dioxide with ionic liquids: 1-alkyl-3-methylimidazolium trifluoromethanesulfonate, J. Chem. Eng. Data 108 (2009), https://doi.org/10.1021/je8000443.
[13] P.G. Jessop, B. Subramaniam, Gas-expanded liquids, Chem. Rev. 107 (2007) 2666–2694, https://doi.org/10.1021/cr040199o.
[14] M. Herrero, J.A. Mendiola, E. Ibáñez, Gas expanded liquids and switchable solvents, Curr. Opin. Green. Sustain Chem. 5 (2017) 24–30, https://doi.org/10.1016/j.cogsc.2017.03.008.
[15] John R. Rumble (Ed.), Handbook of Chemistry and Physics, in: CRC Handbook of Chemistry and Physics, 104th ed...., CRC Press, Boca-Raton (FL), 2023. ⟨https://hbcp-chemnetbase-com.sabidi.urv.cat/contents/InteractiveTable.xhtml?dswid=-1841⟩. accessed September 4, 2023.
[16] J.G. Stevens, P. Gómez, R.A. Bourne, T.C. Drage, M.W. George, M. Poliakoff, Could the energy cost of using supercritical fluids be mitigated by using CO_2 from carbon capture and storage (CCS)? Green. Chem. 13 (2011) 2727–2733, https://doi.org/10.1039/C1GC15503B.
[17] P. Licence, J. Ke, M. Sokolova, S.K. Ross, M. Poliakoff, Chemical reactions in supercritical carbon dioxide: from laboratory to commercial plant, Green. Chem. 5 (2003) 99–104, https://doi.org/10.1039/b212220k.
[18] L. Fu, Z. Ren, W. Si, Q. Ma, W. Huang, K. Liao, Z. Huang, Y. Wang, J. Li, P. Xu, Research progress on CO_2 capture and utilization technology, J. CO_2 Util. 66 (2022), https://doi.org/10.1016/j.jcou.2022.102260.
[19] L. Soh, Carbon dioxide solvent applications in a biorefinery, in: ACS Symposium Series, American Chemical Society, 2014, pp. 9–35, https://doi.org/10.1021/bk-2014-1186.ch002.
[20] D. Silva, E. Bogel-Lukasik, Valuable new platform chemicals obtained by valorisation of a model succinic acid and bio-succinic acid with an ionic liquid and high-pressure carbon dioxide, Green. Chem. 19 (2017) 4048–4060, https://doi.org/10.1039/C7GC00952F.
[21] E. Bogel-Łukasik, K. Nosol, D. Silva, C.I. Melo, Catalytic hydrogenation for a biomass-derived dicarboxylic acid valorisation with an ionic liquid and CO_2 towards a perspective host guest building block molecule, J. Supercrit. Fluids 133 (2018) 542–547, https://doi.org/10.1016/j.supflu.2017.05.032.
[22] Ž. Knez, M. Pantić, D. Cör, Z. Novak, M. Knez Hrnčič, Are supercritical fluids solvents for the future? Chem. Eng. Process. - Process. Intensif. 141 (2019), 107532 https://doi.org/10.1016/j.cep.2019.107532.
[23] M. Arai, S. ichiro Fujita, M. Shirai, Multiphase catalytic reactions in/under dense phase CO_2, J. Supercrit. Fluids 47 (2009) 351–356, https://doi.org/10.1016/J.SUPFLU.2008.08.012.
[24] P.G. Jessop, T. Ikariya, R. Noyori, Homogeneous catalysis in supercritical fluids, Science 269 (1995) (1979) 1065–1069, https://doi.org/10.1126/science.269.5227.1065.
[25] P.G. Jessop, T. Ikariya, R. Noyori, Homogeneous catalysis in supercritical fluids, Chem. Rev. 99 (1999) 475–494, https://doi.org/10.1021/cr970037a.
[26] R. Amandi, J. Hyde, M. Poliakoff, Heterogeneous reactions in supercritical carbon dioxide, in: Carbon Dioxide Recovery and Utilization, Springer Netherlands, Dordrecht, 2003, pp. 169–179, https://doi.org/10.1007/978-94-017-0245-4_6.
[27] E.S. Alekseev, A.Yu Alentiev, A.S. Belova, V.I. Bogdan, T.V. Bogdan, A. V. Bystrova, E.R. Gafarova, E.N. Golubeva, E.A. Grebenik, O.I. Gromov, V. A. Davankov, S.G. Zlotin, M.G. Kiselev, A.E. Koklin, Y.N. Kononevich, A. E. Lazhko, V.V. Lunin, S.E. Lyubimov, O.N. Martyanov, I.I. Mishanin, A. M. Muzafarov, N.S. Nesterov, A.Yu Nikolaev, R.D. Oparin, O.O. Parenago, O. P. Parenago, Y.A. Pokusaeva, I.A. Ronova, A.B. Solovieva, M.N. Temnikov, P. S. Timashev, O.V. Turova, E.V. Filatova, A.A. Philippov, A.M. Chibiryaev, A. S. Shalygin, Supercritical fluids in chemistry, Russ. Chem. Rev. 89 (2020) 1337–1427, https://doi.org/10.1070/RCR4932.
[28] M. González Prieto, M. Fortunatti Montoya, P.E. Hegel, S. Pereda, Supercritical reactors for the production of advanced bio-fuels: A review, J. Supercrit. Fluids 134 (2018) 106–113, https://doi.org/10.1016/j.supflu.2017.11.020.
[29] W.-H. Wang, X. Liu, M. Bao, Hydrogenation of fats and oils using supercritical carbon dioxide, in: Green Sustainable Process for Chemical and Environmental Engineering and Science, Elsevier, 2020, pp. 347–356, https://doi.org/10.1016/B978-0-12-817388-6.00014-3.
[30] N. Yan, C. Xiao, Y. Kou, Transition metal nanoparticle catalysis in green solvents, Coord. Chem. Rev. 254 (2010) 1179–1218, https://doi.org/10.1016/j.ccr.2010.02.015.
[31] X. Han, M. Poliakoff, Continuous reactions in supercritical carbon dioxide: problems, solutions and possible ways forward, Chem. Soc. Rev. 41 (2012) 1428, https://doi.org/10.1039/c2cs15314a.
[32] E. Brunner, Solubility of hydrogen in 10 organic solvents at 298.15, 323.15, and 373.15 K, J. Chem. Eng. Data 30 (1985) 269–273, https://doi.org/10.1021/je00041a010.
[33] N.U. Din Reshi, M.A. Rizvi, S.K. Moosvi, M. Ahmad, A. Gani, Solubility of organic compounds in scCO2, Green. Sustain. Process Chem. Environ. Eng. Sci.: Supercrit. Carbon Dioxide Green. Solvent (2020) 379–411, https://doi.org/10.1016/B978-0-12-817388-6.00016-7.
[34] A.I. Frolov, M.G. Kiselev, Prediction of cosolvent effect on solvation free energies and solubilities of organic compounds in supercritical carbon dioxide based on fully atomistic molecular simulations, J. Phys. Chem. B 118 (2014) 11769–11780, https://doi.org/10.1021/JP505731Z/SUPPL_FILE/JP505731Z_SI_001.PDF.
[35] M. Shirai, N. Hiyoshi, C.V. Rode, Stereoselective aromatic ring hydrogenation over supported rhodium catalysts in supercritical carbon dioxide solvent, Chem. Rec. 19 (2019) 1926–1934, https://doi.org/10.1002/tcr.201800128.
[36] H. Häring, S. Wilhelm, D. Horn, S. Haase, Development of a robust fixed-bed reactor model for supercritical citral hydrogenation, Chem. Eng. Technol. 40 (2017) 2075–2083, https://doi.org/10.1002/ceat.201700076.
[37] H. Guo, S. Tomoka, R.L. Smith, Catalytic hydrogenation of levulinic acid in ionic liquid mixtures using hydrogen gas in high-pressure CO_2, J. Supercrit. Fluids 164 (2020), 104891, https://doi.org/10.1016/j.supflu.2020.104891.
[38] R.A. Bourne, J.G. Stevens, J. Ke, M. Poliakoff, Maximising opportunities in supercritical chemistry: the continuous conversion of levulinic acid to gamma-valerolactone in, Chem. Commun. (Camb.) 4632–4 (2007) CO2, https://doi.org/10.1039/b708754c.
[39] L. Zhao, H. Cheng, T. Liu, Y. Li, Z. Ying, W. Yang, W. Lin, X. Meng, C. Wang, F. Zhao, A green process for production of p-aminophenol from nitrobenzene hydrogenation in CO_2/H2O: The promoting effects of CO_2 and H2O, J. CO_2 Util. 18 (2017) 229–236, https://doi.org/10.1016/j.jcou.2017.01.012.
[40] M.R. Damen, R.W. Brand, S.C. Bloem, E. Pingen, K. Steur, C.J. Peters, G.-J. Witkamp, M.C. Kroon, Process intensification by combining ionic liquids and supercritical carbon dioxide applied to the design of Levodopa production, Chem.

Eng. Process.: Process.Intensif. 48 (2009) 549–553, https://doi.org/10.1016/j.cep.2008.08.001.
[41] D. Geier, P. Schmitz, J. Walkowiak, W. Leitner, G. Franciò, Continuous flow asymmetric hydrogenation with supported ionic liquid phase catalysts using modified CO 2 as the mobile phase: from model substrate to an active pharmaceutical ingredient, ACS Catal. 8 (2018) 3297–3303, https://doi.org/10.1021/acscatal.8b00216.
[42] U. Hintermair, G. Franciò, W. Leitner, A fully integrated continuous-flow system for asymmetric catalysis: Enantioselective hydrogenation with supported ionic liquid phase catalysts using supercritical CO 2 as the mobile phase, Chem. - A Eur. J. 19 (2013) 4538–4547, https://doi.org/10.1002/chem.201204159.
[43] F. Zhao, S. Fujita, J. Sun, Y. Ikushima, M. Arai, Carbon dioxide-expanded liquid substrate phase: an effective medium for selective hydrogenation of cinnamaldehyde to cinnamyl alcohol, Chem. Commun. 10 (2004) 2326, https://doi.org/10.1039/b408434a.
[44] J. Xiao, S.C.A. Nefkens, P.G. Jessop, T. Ikariya, R. Noyori, Asymmetric hydrogenation of α,β-unsaturated carboxylic acids in supercritical carbon dioxide, Tetrahedron Lett. 37 (1996) 2813–2816.
[45] H.T. Jespersen, S. Štandeker, Z. Novak, K. Schaumburg, J. Madsen, Ž. Knez, Supercritical fluids applied to the sol-gel process for preparation of AEROMOSILS/palladium particle nanocomposite catalyst, J. Supercrit. Fluids 46 (2008) 178–184, https://doi.org/10.1016/j.supflu.2008.04.013.
[46] M. Aygün, C.T. Stoppiello, M.A. Lebedeva, E.F. Smith, M.D.C. Gimenez-Lopez, A. N. Khlobystov, T.W. Chamberlain, Comparison of alkene hydrogenation in carbon nanoreactors of different diameters: probing the effects of nanoscale confinement on ruthenium nanoparticle catalysis, J. Mater. Chem. A Mater. 5 (2017) 21467–21477, https://doi.org/10.1039/c7ta03691d.
[47] G. Garg, A.M. Masdeu-Bultó, N. Farfán, J. Ordóñez-Hernández, M. Gómez, Y. Medina-González, Palladium nanoparticles in glycerol/ionic liquid/carbon dioxide medium as hydrogenation catalysts, ACS Appl. Nano Mater. 3 (2020) 12240–12249, https://doi.org/10.1021/acsanm.0c02706.
[48] M. Ji, X. Chen, C.M. Wai, J.L. Fulton, Synthesizing and dispersing silver nanoparticles in a water-in- supercritical carbon dioxide microemulsion [18], J. Am. Chem. Soc. 121 (1999) 2631–2632, https://doi.org/10.1021/ja9840403.
[49] M.B. King, Chapter 2 - descriptive account of phase equilibria, in: Phase Equilibrium in Mixtures, Elsevier, 1969, pp. 89–173, https://doi.org/10.1016/b978-0-08-012301-1.50007-2.
[50] C.M. Rayner, The potential of carbon dioxide in synthetic organic chemistry, Org. Process Res Dev. 11 (2007) 121–132, https://doi.org/10.1021/OP060165D/ASSET/IMAGES/LARGE/OP060165DF00009.JPEG.
[51] M.T. White, G. Bianchi, L. Chai, S.A. Tassou, A.I. Sayma, Review of supercritical CO_2 technologies and systems for power generation, Appl. Therm. Eng. 185 (2021), 116447, https://doi.org/10.1016/j.applthermaleng.2020.116447.
[52] R. Privat, J.-N. Jaubert, Classification of global fluid-phase equilibrium behaviors in binary systems, Chem. Eng. Res. Des. 91 (2013) 1807–1839, https://doi.org/10.1016/j.cherd.2013.06.026.
[53] S. Pereda, S.B. Bottini, E.A. Brignole, Phase equilibrium engineering of supercritical hydrogenation reactors, AIChE J. 48 (2002) 2635–2645, https://doi.org/10.1002/aic.690481123.
[54] L.J. Rovetto, S.B. Bottini, E.A. Brignole, C.J. Peters, Supercritical hydrogenation processes: experimental results on the fluid phase behavior of binary and ternary mixtures of hydrogen, propane and tripalmitin, J. Supercrit. Fluids 25 (2003) 165–176, https://doi.org/10.1016/S0896-8446(02)00156-0.
[55] S. van den Hark, M. Härröd, Fixed-bed hydrogenation at supercritical conditions to form fatty alcohols: the dramatic effects caused by phase transitions in the reactor, Ind. Eng. Chem. Res 40 (2001) 5052–5057, https://doi.org/10.1021/ie000951l.
[56] G. Brunner, Supercritical Gases as Solvents: Phase Equilibria BT - Gas Extraction: An Introduction to Fundamentals of Supercritical Fluids and the Application to Separation Processes, in: G. Brunner (Ed.), Steinkopff, Heidelberg, 1994: pp. 59–146. https://doi.org/10.1007/978-3-662-07380-3_3.
[57] D. Chouchi, D. Gourgouillon, M. Courel, J. Vital, M. Nunes da Ponte, The influence of phase behavior on reactions at supercritical conditions: the hydrogenation of α-pinene, Ind. Eng. Chem. Res 40 (2001) 2551–2554, https://doi.org/10.1021/ie000859p.
[58] R. Tschan, R. Wandeler, M.S. Schneider, M.M. Schubert, A. Baiker, Continuous semihydrogenation of phenylacetylene over amorphous Pd81Si19 alloy in "supercritical" carbon dioxide: relation between catalytic performance and phase behavior, J. Catal. 204 (2001) 219–229, https://doi.org/10.1006/jcat.2001.3364.
[59] S. Beret, J.M. Prausnitz, Perturbed hard-chain theory: an equation of state for fluids containing small or large molecules, AIChE J. 21 (1975) 1123–1132, https://doi.org/10.1002/aic.690210612.
[60] K. Mejbri, A. Taieb, A. Bellagi, Phase equilibria calculation of binary and ternary mixtures of associating fluids applying PC-SAFT equation of state, J. Supercrit. Fluids 104 (2015) 132–144, https://doi.org/10.1016/j.supflu.2015.05.025.
[61] N.I. Diamantonis, G.C. Boulougouris, E. Mansoor, D.M. Tsangaris, I.G. Economou, Evaluation of cubic, SAFT, and PC-SAFT equations of state for the vapor–liquid equilibrium modeling of CO_2 mixtures with other gases, Ind. Eng. Chem. Res 52 (2013) 3933–3942, https://doi.org/10.1021/ie303248q.
[62] H.P. Gros, S. Bottini, E.A. Brignole, A group contribution equation of state for associating mixtures, Fluid Phase Equilib. 116 (1996) 537–544, https://doi.org/10.1016/0378-3812(95)02928-1.
[63] R.B. Bird, E. Stewart, Warren, N. Lightfoot, Edwin, W.E. Stewart, E.N. Lightfoot. Transport phenomena, 2nd ed..,, Wiley,, New York, NY, 2002.
[64] L.P. Cunico, C. Turner, Chapter 7 Supercritical Fluids and Gas-Expanded Liquids, in: 2019: pp. 155–214. https://doi.org/10.1016/b978–0-12–805297-6.00007–3.
[65] L.M. González, J.L. Bueno, I. Medina, Determination of binary diffusion coefficients of anisole, 2,4-dimethylphenol, and nitrobenzene in supercritical carbon dioxide, Ind. Eng. Chem. Res 40 (2001) 3711–3716, https://doi.org/10.1021/ie010102d.
[66] C.Y. Kong, T. Funazukuri, S. Kagei, Binary diffusion coefficients and retention factors for polar compounds in supercritical carbon dioxide by chromatographic impulse response method, J. Supercrit. Fluids 37 (2006) 359–366, https://doi.org/10.1016/j.supflu.2005.10.006.
[67] C.-C. Lai, C.-S. Tan, Measurement of molecular diffusion coefficients in supercritical carbon dioxide using a coated capillary column, Ind. Eng. Chem. Res 34 (1995) 674–680, https://doi.org/10.1021/ie00041a029.
[68] H. Liu, E. Ruckenstein, Predicting the diffusion coefficients in supercritical fluids, Ind. Eng. Chem. Res 36 (1997) 888–895, https://doi.org/10.1021/ie9604381.
[69] I. Medina, Determination of diffusion coefficients for supercritical fluids, J. Chromatogr. A 1250 (2012) 124–140, https://doi.org/10.1016/j.chroma.2012.04.052.
[70] V.M. Shenai, B.L. Hamilton, M.A. Matthews, Diffusion in liquid and supercritical fluid mixtures, in: Supercritical Fluid Engineering Science, American Chemical Society, 1992, pp. 8–92, https://doi.org/10.1021/bk-1992-0514.ch008.
[71] J.P. Palafox-Hernandez, C.H. Mendis, W.H. Thompson, B.B. Laird, Pressure and temperature tuning of gas-expanded liquid structure and dynamics, J. Phys. Chem. B 123 (2019) 2915–2924, https://doi.org/10.1021/acs.jpcb.8b09826.
[72] T. Voeste, H. Buchold, Production of fatty alcohols from fatty acids, J. Am. Oil Chem. Soc. 61 (1984) 350–352, https://doi.org/10.1007/BF02678794.
[73] H.G.A. Coorens, C.J. Peters, J. De Swaan Arons, Phase equilibria in binary mixtures of propane and tripalmitin, Fluid Phase Equilib. 40 (1988) 135–151, https://doi.org/10.1016/0378-3812(88)80026-8.
[74] P.G. Debenedetti, R.C. Reid, Diffusion and mass transfer in supercritical fluids, AIChE J. 32 (1986) 2034–2046, https://doi.org/10.1002/aic.690321214.
[75] A. López-Padilla, A. Ruiz-Rodriguez, G. Reglero, T. Fornari, Supercritical extraction of solid materials: a practical correlation related with process scaling, J. Food Eng. 222 (2018) 199–206, https://doi.org/10.1016/j.jfoodeng.2017.11.027.
[76] E.J. Beckman, Supercritical and near-critical CO_2 in green chemical synthesis and processing, J. Supercrit. Fluids 28 (2004) 121–191, https://doi.org/10.1016/S0896-8446(03)00029-9.
[77] D. Guha, H. Jin, M.P. Dudukovic, P.A. Ramachandran, B. Subramaniam, Mass transfer effects during homogeneous 1-octene hydroformylation inCO2-expanded solvent: modeling and experiments, Chem. Eng. Sci. 62 (2007) 4967–4975, https://doi.org/10.1016/j.ces.2006.12.029.
[78] Mark E. Davis, R.J. Davis, Effects of transport limitations on rates of solid-catalyzed reactions, in: Fundamentals of Chemical Reaction Engineering, McGraw-Hill Higher Education, New York, NY, USA, 2003, pp. 184–239.
[79] J. Zhou, W. Wang, Adsorption and diffusion of supercritical carbon dioxide in slit pores, Langmuir 16 (2000) 8063–8070, https://doi.org/10.1021/la000216e.
[80] P. Peng, The influence of different diffusion pattern to the sub- and super-critical fluid flow in brown coal, IOP Conf. Ser. Earth Environ. Sci. 128 (2018) 12107, https://doi.org/10.1088/1755-1315/128/1/012107.
[81] E. Ramírez, M.A. Larrayoz, F. Recasens, Intraparticle diffusion mechanisms in SC sunflower oil hydrogenation on Pd, AIChE J. 52 (2006) 1539–1553, https://doi.org/10.1002/aic.10753.
[82] R. Klaewkla, in: M. Arend (Ed.), A Review of Mass Transfer Controlling the Reaction Rate in Heterogeneous Catalytic Systems, IntechOpen, Rijeka, 2011, https://doi.org/10.5772/22962.
[83] P. Beslin, F. Cansell, S. Rey, Thermodynamic aspects of supercritical fluids processing: applications of polymers and wastes treatment, Rev. De. l'Institut Fr. Du Pétrole 53 (1998) 71–98, https://doi.org/10.2516/ogst:1998010.
[84] I. Pioro, in: S.M.E.-A. Belmiloudi (Ed.), Thermophysical Properties at Critical and Supercritical Pressures, IntechOpen, Rijeka, 2011, https://doi.org/10.5772/13790.
[85] C.M. Colina, C.G. Olivera-Fuentes, F.R. Siperstein, M. Lísal, K.E. Gubbins, Thermal properties of supercritical carbon dioxide by monte carlo simulations, Mol. Simul. 29 (2003) 405–412, https://doi.org/10.1080/0892702031000117135.
[86] M.P.E. Ishmael, L.B. Stutzman, M.Z. Lukawski, F.A. Escobedo, J.W. Tester, Heat capacities of supercritical fluid mixtures: Comparing experimental measurements with Monte Carlo molecular simulations for carbon dioxide-methanol mixtures, J. Supercrit. Fluids 123 (2017) 40–49, https://doi.org/10.1016/j.supflu.2016.11.013.
[87] J.R. Boulton, F.P. Stein, The constant pressure heat capacity of supercritical carbon dioxide-methanol and carbon dioxide-ethanol co-solvent mixtures, Fluid Phase Equilib. 91 (1993) 159–176, https://doi.org/10.1016/0378-3812(93)85086-2.
[88] J.H. Song, H.Y. Kim, H. Kim, Y.Y. Bae, Heat transfer characteristics of a supercritical fluid flow in a vertical pipe, J. Supercrit. Fluids 44 (2008) 164–171, https://doi.org/10.1016/j.supflu.2007.11.013.
[89] Q. Zhang, H. Li, X. Kong, J. Liu, X. Lei, Special heat transfer characteristics of supercritical CO_2 flowing in a vertically-upward tube with low mass flux, Int J. Heat. Mass Transf. 122 (2018) 469–482, https://doi.org/10.1016/j.ijheatmasstransfer.2018.01.112.
[90] X. Huai, S. Koyama, Heat transfer characteristics of supercritical CO_2 flow in small-channeled structures, Exp. Heat. Transf. 20 (2007) 19–33, https://doi.org/10.1080/08916150600977424.

[91] Y. Ito, Heat transfer of supercritical fluid flows and compressible flows, in: Heat Exchangers - Advanced Features and Applications, InTech, 2017, https://doi.org/10.5772/65931.

[92] Aspen Tech, (n.d.). https://www.aspentech.com/en/products/engineering/aspen-plus (Accessed July 29, 2019).

[93] M. Wei, G.T. Musie, D.H. Busch, B. Subramaniam, CO_2-expanded solvents: Unique and versatile media for performing homogeneous catalytic oxidations, J. Am. Chem. Soc. 124 (2002) 2513–2517, https://doi.org/10.1021/ja0114411.

[94] A. Zhang, Q. Zhang, H. Bai, L. Li, J. Li, Polymeric nanoporous materials fabricated with supercritical CO 2 and CO 2 -expanded liquids, Chem. Soc. Rev. 43 (2014) 6938–6953, https://doi.org/10.1039/c4cs00100a.

[95] L.W. Diamond, N.N. Akinfiev, Solubility of CO_2 in water from −1.5 to 100 °C and from 0.1 to 100 MPa: evaluation of literature data and thermodynamic modelling, Fluid Phase Equilib. 208 (2003) 265–290, https://doi.org/10.1016/S0378-3812(03)00041-4.

[96] A. Kordikowski, A.P. Schenk, R.M. Van Nielen, C.J. Peters, Volume expansions and vapor-liquid equilibria of binary mixtures of a variety of polar solvents and certain near-critical solvents, J. Supercrit. Fluids 8 (1995) 205–216, https://doi.org/10.1016/0896-8446(95)90033-0.

[97] S.N.V.K. Aki, B.R. Mellein, J.F. Brennecke, High-pressure phase behavior of carbon dioxide with imidazolium-based ionic liquids, J. Phys. Chem. B 108 (2004) 20355–20365.

[98] T. Guadagno, S.G. Kazarian, High-pressure CO_2-expanded solvents: simultaneous measurement of CO_2 sorption and swelling of liquid polymers with in-situ near-IR spectroscopy, J. Phys. Chem. B 108 (2004) 13995–13999, https://doi.org/10.1021/jp0481097.

[99] D.E. Niehaus, R.Mark Wightman, P.A. Flowers, Ionically modified electrodes for use in nonpolar fluids, Anal. Chem. 63 (1991) 1728–1732, https://doi.org/10.1021/ac00017a014.

[100] A.S. Cullick, M.L. Mathis, Densities and viscosities of mixtures of carbon dioxide and n-decane from 310 to 403 K and 7 to 30 MPa, J. Chem. Eng. Data 29 (1984) 393–396, https://doi.org/10.1021/je00038a008.

[101] A.S. Pensado, A.A.H. Pádua, M.J.P. Comuñas, J. Fernández, High-pressure viscosity and density of carbon dioxide + pentaerythritol ester mixtures: Measurements and modeling, AIChE J. 54 (2008) 1625–1636, https://doi.org/10.1002/aic.11473.

[102] A.P. Abbott, E.G. Hope, R. Mistry, A.M. Stuart, Probing the structure of gas expanded liquids using relative permittivity, density and polarity measurements, Green. Chem. 11 (2009) 1530–1535, https://doi.org/10.1039/B915570H.

[103] E. Granero Fernandez, J.-S. Condoret, V. Gerbaud, Y. Medina-Gonzalez, Molecular Dynamics Simulations of Gas-Expanded Liquids, in: A. Espuña, M. Graells, L.B.T.-C.A.C.E. Puigjaner (Eds.), 27 European Symposium on Computer Aided Process Engineering, Elsevier, 2017: pp. 175–180. https://doi.org/https://doi.org/10.1016/B978-0-444-63965-3.50031-3.

[104] E. Granero-Fernandez, D. Machin, C. Lacaze-Dufaure, S. Camy, J.-S. Condoret, V. Gerbaud, P.A. Charpentier, Y. Medina-Gonzalez, CO_2-expanded alkyl acetates: physicochemical and molecular modeling study and applications in chemical processes, ACS Sustain Chem. Eng. 6 (2018) 7627–7637, https://doi.org/10.1021/acssuschemeng.8b00454.

[105] P. Zeigermann, R. Valiullin, Transport properties of gas-expanded liquids in bulk and under confinement, J. Supercrit. Fluids 75 (2013) 43–47, https://doi.org/10.1016/j.supflu.2012.12.011.

[106] G.R. Akien, M. Poliakoff, A critical look at reactions in class I and II gas-expanded liquids using CO_2 and other gases, Green. Chem. 11 (2009) 1083–1100, https://doi.org/10.1039/b904097h.

[107] Z.K. Lopez-Castillo, S.N.V.K. Aki, M.A. Stadtherr, J.F. Brennecke, Enhanced solubility of oxygen and carbon monoxide in CO 2- expanded liquids, Ind. Eng. Chem. Res 45 (2006) 5351–5360, https://doi.org/10.1021/ie0601091.

[108] J. Jacquemin, M.F. Costa Gomes, P. Husson, V. Majer, Solubility of carbon dioxide, ethane, methane, oxygen, nitrogen, hydrogen, argon, and carbon monoxide in 1-butyl-3-methylimidazolium tetrafluoroborate between temperatures 283K and 343K and at pressures close to atmospheric, J. Chem. Thermodyn. 38 (2006) 490–502, https://doi.org/10.1016/j.jct.2005.07.002.

[109] J.L. Anthony, E.J. Maginn, J.F. Brennecke, Solubilities and thermodynamic properties of gases in the ionic liquid 1-n-butyl-3-methylimidazolium hexafluorophosphate, J. Phys. Chem. B 106 (2002) 7315–7320, https://doi.org/10.1021/jp020631a.

[110] A. Sharma, C. Julcour, A.A. Kelkar, R.M. Deshpande, H. Delmas, Mass transfer and solubility of CO and H 2 in Ionic liquid. case of [bmim][PF 6] with gas-inducing stirrer reactor, Ind. Eng. Chem. Res 48 (2009) 4075–4082, https://doi.org/10.1021/ie801584p.

[111] E. Quijada-Maldonado, W.G. Meidersma, A.B. de Haan, Mass transfer in extractive distillation when using ionic liquids as solvents, in: Y. Ren (Ed.), Heat and Mass Transfer - Advances in Modelling and Experimental Study for Industrial Applications, IntechOpen Limited, London, 2018.

[112] X. Zhang, D. Bao, Y. Huang, H. Dong, X. Zhang, S. Zhang, Pyrolysis of heavy oil in the presence of supercritical water: the reaction kinetics in different phases, AICHE J. 61 (2015) 857–866, https://doi.org/10.1002/aic.

[113] X. Zhang, D. Bao, Y. Huang, H. Dong, X. Zhang, S. Zhang, Gas–liquid mass-transfer properties in CO_2 absorption system with ionic liquids, AIChE J. 60 (2014) 2929–2939, https://doi.org/10.1002/aic.14507.

[114] M. Solinas, A. Pfaltz, P.G. Cozzi, W. Leitner, Enantioselective hydrogenation of imines in ionic liquid / carbon dioxide media attractive route to enantiomerically enriched chiral secondary, J. Am. Chem. Soc. 126 (2004) 16142–16147, https://doi.org/10.1021/ja046129g.

[115] K. Kian, A.M. Scurto, Viscosity of compressed CO_2-saturated n-alkanes: CO_2/n-hexane, CO_2/n-decane, and CO_2/n-tetradecane, J. Supercrit. Fluids 133 (2018) 411–420, https://doi.org/10.1016/j.supflu.2017.10.030.

[116] R. Sih, F. Dehghani, N.R. Foster, Viscosity measurements on gas expanded liquid systems—methanol and carbon dioxide, J. Supercrit. Fluids 41 (2007) 148–157, https://doi.org/10.1016/j.supflu.2006.09.002.

[117] J. Jacquemin, P. Husson, V. Majer, M.F.C. Gomes, Low-pressure solubilities and thermodynamics of solvation of eight gases in 1-butyl-3-methylimidazolium hexafluorophosphate, Fluid Phase Equilib. 240 (2006) 87–95, https://doi.org/10.1016/j.fluid.2005.12.003.

[118] H.N. Hoang, E. Granero-Fernandez, S. Yamada, S. Mori, H. Kagechika, Y. Medina-Gonzalez, T. Matsuda, Modulating biocatalytic activity toward sterically bulky substrates in co<inf>2</inf>-expanded biobased liquids by tuning the physicochemical properties, ACS Sustain Chem. Eng. 5 (2017), https://doi.org/10.1021/acssuschemeng.7b03018.

[119] J.P. Palafox-Hernandez, C.H. Mendis, W.H. Thompson, B.B. Laird, Pressure and temperature tuning of gas-expanded liquid structure and dynamics, J. Phys. Chem. B 123 (2019) 2915–2924, https://doi.org/10.1021/acs.jpcb.8b09826.

[120] V.K. Tochigi, K. Funazukuri, T. Matsuda, H. Kurihara, K. Rattan, Estimation of Kinematic Viscosity for CO2 expanded Liquids By Asog-Visco Method, in: AIChE Annual Meeting, 2017: p. 204.

[121] K. Kian, A.M. Scurto, Heat transport properties of CO_2-expanded liquids: n-hexane, n-decane, and n-tetradecane, Ind. Eng. Chem. Res 56 (2017) 12822–12832, https://doi.org/10.1021/acs.iecr.7b03513.

[122] J. Liu, F. Wang, L. Zhang, X. Fang, Z. Zhang, Thermodynamic properties and thermal stability of ionic liquid-based nanofluids containing graphene as advanced heat transfer fluids for medium-to-high-temperature applications, Renew. Energy 63 (2014) 519–523, https://doi.org/10.1016/j.renene.2013.10.002.

[123] S. Aparicio, M. Atilhan, F. Karadas, Thermophysical properties of pure ionic liquids: review of present situation, Ind. Eng. Chem. Res 49 (2010) 9580–9595, https://doi.org/10.1021/ie101441s.

[124] J.M.P. França, C.A. Nieto de Castro, M.M. Lopes, V.M.B. Nunes, Influence of thermophysical properties of ionic liquids in chemical process design, J. Chem. Eng. Data 54 (2009) 2569–2575, https://doi.org/10.1021/je900107t.

[125] S. van den Hark, M. Härröd, P. Møller, Hydrogenation of fatty acid methyl esters to fatty alcohols at supercritical conditions, J. Am. Oil Chem. Soc. 76 (1999) 1363–1370, https://doi.org/10.1007/s11746-999-0151-y.

[126] R. Wandeler, N. Künzle, M.S. Schneider, T. Mallat, A. Baiker, Continuous enantioselective hydrogenation of ethyl pyruvate in “supercritical” ethane: relation between phase behavior and catalytic performance, J. Catal. 200 (2001) 377–388, https://doi.org/10.1006/jcat.2001.3222.

[127] R. Tschan, R. Wandeler, M.S. Schneider, M.M. Schubert, A. Baiker, Continuous semihydrogenation of phenylacetylene over amorphous Pd81Si19 alloy in “supercritical” carbon dioxide: relation between catalytic performance and phase behavior, J. Catal. 204 (2001) 219–229, https://doi.org/10.1006/jcat.2001.3364.

[128] M.G. Hitzler, F.R. Smail, S.K. Ross, M. Poliakoff, Selective catalytic hydrogenation of organic compounds in supercritical fluids as a continuous process, Org. Process Res Dev. 2 (1998) 137–146, https://doi.org/10.1021/op970056m.

[129] A. Bertucco, P. Canu, L. Devetta, A.G. Zwahlen, Catalytic hydrogenation in supercritical CO_2: kinetic measurements in a gradientless internal-recycle reactor, Ind. Eng. Chem. Res 36 (1997) 2626–2633, https://doi.org/10.1021/ie960369q.

[130] J.G. De Vries, C.J. Elsevier (Eds.), The Handbook of Homogeneous Hydrogenation, Wiley-VCH Verlag, Weinheim, 2007.

[131] G. Brunner, C. Saure, D. Buss, Phase equilibrium of hydrogen, carbon dioxide, squalene, and squalane, J. Chem. Eng. Data 54 (2009) 1598–1609, https://doi.org/10.1021/je800926z.

[132] J.R. Hyde, P. Licence, D. Carter, M. Poliakoff, Continuous catalytic reactions in supercritical fluids, Appl. Catal. A Gen. 222 (2001) 119–131, https://doi.org/10.1016/S0926-860X(01)00835-3.

[133] E. Bogel-Łukasik, R. Bogel-Łukasik, K. Kriaa, I. Fonseca, Y. Tarasenko, M. Nunes da Ponte, Limonene hydrogenation in high-pressure CO_2: Effect of hydrogen pressure, J. Supercrit. Fluids 45 (2008) 225–230, https://doi.org/10.1016/j.supflu.2007.10.001.

[134] M. Burgener, D. Ferri, J.-D. Grunwaldt, T. Mallat, A. Baiker, Supercritical carbon dioxide: an inert solvent for catalytic hydrogenation, J. Phys. Chem. B 109 (2005) 16794–16800, https://doi.org/10.1021/jp0521353.

[135] L. Devetta, P. Canu, A. Bertucco, K. Steiner, Modelling of a trickle-bed reactor for a catalytic hydrogenation in supercritical CO_2, Chem. Eng. Sci. 52 (1997) 4163–4169, https://doi.org/10.1016/S0009-2509(97)00258-3.

[136] H. Cheng, F. Zhao, The promoting effects of CO_2 and H2O on selective hydrogenations in CO_2/H2O biphasic system, Curr. Opin. Green. Sustain Chem. 10 (2018) 46–50, https://doi.org/10.1016/J.COGSC.2018.03.001.

[137] X. Han, M. Poliakoff, Continuous reactions in supercritical carbon dioxide: problems, solutions and possible ways forward, Chem. Soc. Rev. 41 (2012) 1428–1436, https://doi.org/10.1039/C2CS15314A.

[138] R. Amandi, J.R. Hyde, S.K. Ross, T.J. Lotz, M. Poliakoff, Continuous reactions in supercritical fluids; a cleaner, more selective synthesis of thymol in supercritical CO_2, Green. Chem. 7 (2005) 288–293, https://doi.org/10.1039/B418983C.

[139] R. Amandi, K. Scovell, P. Licence, T.J. Lotz, M. Poliakoff, The synthesis of o-cyclohexylphenol in supercritical carbon dioxide: towards a continuous two-step reaction, Green. Chem. 9 (2007) 797–801, https://doi.org/10.1039/B618727G.

[140] J.A.M. Kuipers, W.P.M. van Swaaij, Computational Fluid Dynamics Applied To Chemical Reaction Engineering, in: J.B.T.-A. in C.E. Wei (Ed.), Academic Press,

1998: pp. 227–328. https://doi.org/https://doi.org/10.1016/S0065–2377(08)60094–0.
[141] V. Ranade, ComputationaL Flow Modeling for Chemical Reactor Engineering, Academic Press, 2001.
[142] J. Bode, Applications of computational fluid dynamics in the chemical industry, Chem. Eng. Technol. 17 (1994) 145–148, https://doi.org/10.1002/ceat.270170302.
[143] C.K. Harris, D. Roekaerts, F.J.J. Rosendal, F.G.J. Buitendijk, Ph Daskopoulos, A.J. N. Vreenegoor, H. Wang, Computational fluid dynamics for chemical reactor engineering, Chem. Eng. Sci. 51 (1996) 1569–1594, https://doi.org/10.1016/0009-2509(96)00021-8.
[144] A. Guardo, M. Casanovas, E. Ramírez, F. Recasens, I. Magaña, D. Martínez, M. A. Larrayoz, CFD modeling on external mass transfer and intra-particle diffusional effects on the supercritical hydrogenation of sunflower oil, Chem. Eng. Sci. 62 (2007) 5054–5061, https://doi.org/10.1016/j.ces.2007.01.080.
[145] Y.-P. Zhu, G.-Q. Chen, Z.-H. Luo, Iterative multiscale computational fluid dynamics–single-particle model for intraparticle transfer and catalytic hydrogenation reaction of dimethyl oxalate in a fluidized-bed reactor, Ind. Eng. Chem. Res 53 (2014) 110–122, https://doi.org/10.1021/ie403227z.
[146] E. Ramírez, F. Recasens, M. Fernández, M.A. Larrayoz, Sunflower oil hydrogenation on Pd/C in SC propane in a continuous recycle reactor, AIChE J. 50 (2004) 1545–1555, https://doi.org/10.1002/aic.10142.
[147] A. Santana, M.A. Larrayoz, E. Ramírez, J. Nistal, F. Recasens, Sunflower oil hydrogenation on Pd in supercritical solvents: Kinetics and selectivities, J. Supercrit. Fluids 41 (2007) 391–403, https://doi.org/10.1016/j.supflu.2006.12.009.
[148] E. Ramírez, M.J. Mayorga, D. Cuevas, F. Recasens, Fatty oil hydrogenation in supercritical solvents: process design and safety issues, J. Supercrit. Fluids 57 (2011) 143–154, https://doi.org/10.1016/j.supflu.2011.02.009.
[149] E. Siougkrou, A. Galindo, C.S. Adjiman, On the optimal design of gas-expanded liquids based on process performance, Chem. Eng. Sci. 115 (2014) 19–30, https://doi.org/10.1016/j.ces.2013.12.025.
[150] D. Lee, J. Choi, Y.-W. Lee, J.M. Lee, Design and economic analysis of biodiesel production process of simultaneous supercritical transesterification and partial hydrogenation using soybean oil with Pd/Al2O3 catalyst, Chem. Eng. Res. Des. 172 (2021) 264–279, https://doi.org/10.1016/j.cherd.2021.06.010.
[151] J. Shi, X. Kang, L. Mao, Y. Jiang, S. Zhao, Y. Liu, B. Zhai, H. Jin, L. Guo, Supercritical CO_2-applied equipment for chemical synthesis and transformation: Current status and perspectives, Chem. Eng. J. 459 (2023), 141608, https://doi.org/10.1016/j.cej.2023.141608.
[152] S. Lange, A. Brinkmann, P. Trautner, K. Woelk, J. Bargon, W. Leitner, Mechanistic aspects of dihydrogen activation and transfer during asymmetric hydrogenation in supercritical carbon dioxide, Chirality 12 (2000) 450–457, https://doi.org/10.1002/(SICI)1520-636X(2000)12:5/6<450::AID-CHIR26>3.0.CO;2-H.
[153] C. Park, J. Lee, Recent achievements in CO_2-assisted and CO_2-catalyzed biomass conversion reactions, Green. Chem. 22 (2020) 2628–2642, https://doi.org/10.1039/d0gc00095g.
[154] W. Yang, H. Cheng, B. Zhang, Y. Li, T. Liu, M. Lan, Y. Yu, C. Zhang, W. Lin, S. I. Fujita, M. Arai, F. Zhao, Hydrogenation of levulinic acid by RuCl 2 (PPh 3) 3 in supercritical CO 2: The significance of structural changes of Ru complexes via interaction with CO 2, Green. Chem. 18 (2016) 3370–3377, https://doi.org/10.1039/c6gc00019c.
[155] J.C. Serrano-Ruiz, R.M. West, J.A. Dumesic, Catalytic conversion of renewable biomass resources to fuels and chemicals, Annu Rev. Chem. Biomol. Eng. 1 (2010) 79–100, https://doi.org/10.1146/annurev-chembioeng-073009-100935.
[156] P.G. Jessop, R.R. Stanley, R.A. Brown, C.A. Eckert, C.L. Liotta, T.T. Ngo, P. Pollet, Neoteric solvents for asymmetric hydrogenation: supercritical fluids, ionic liquids, and expanded ionic liquidsThis work was presented at the Green Solvents for Catalysis Meeting held in Bruchsal, Germany, 13–16th October 2002, Green. Chem. 5 (2003) 123–128, https://doi.org/10.1039/b211894g.
[157] Y. Hu, D.J. Birdsall, A.M. Stuart, E.G. Hope, J. Xiao, Ruthenium-catalysed asymmetric hydrogenation with fluoroalkylated BINAP ligands in supercritical CO_2, J. Mol. Catal. A Chem. 219 (2004) 57–60, https://doi.org/10.1016/J.MOLCATA.2004.05.009.
[158] A. Gillon, K. Heslop, D.J. Hyett, A. Martorell, A.G. Orpen, P.G. Pringle, C. Claver, E. Fernandez, Biarylphosphonites: a class of monodentate phosphorus(iii) ligands that outperform their chelating analogues in asymmetric hydrogenation catalysis, Chem. Commun. 2 (2000) 961–962, https://doi.org/10.1039/b001638l.
[159] M.T. Reetz, T. Sell, Rhodium-catalyzed enantioselective hydrogenation using chiral monophosphonite ligands, Tetrahedron Lett. 41 (2000) 6333–6336, https://doi.org/10.1016/S0040-4039(00)01099-6.
[160] S.E.E. Lyubimov, E.E.E. Said-Galiev, A.R.R. Khokhlov, N.M.M. Loim, L.N. N. Popova, P.V.V. Petrovskii, V.A.A. Davankov, The use of monodentate phosphites and phosphoramidites as effective ligands for Rh-catalyzed asymmetric hydrogenation in supercritical carbon dioxide, J. Supercrit. Fluids 45 (2008) 70–73, https://doi.org/10.1016/j.supflu.2007.12.003.
[161] S.E. Lyubimov, V.A. Davankov, E.E. Said-Galiev, A.R. Khokhlov, Chiral phosphoramidites as inexpensive and efficient ligands for Rh-catalyzed asymmetric olefin-hydrogenation in supercritical carbon dioxide, Catal. Commun. 9 (2008) 1851–1852, https://doi.org/10.1016/j.catcom.2008.03.001.
[162] P. Stephenson, B. Kondor, P. Licence, K. Scovell, S.K. Ross, M. Poliakoff, Continuous asymmetric hydrogenation in supercritical carbon dioxide using an immobilised homogeneous catalyst, Adv. Synth. Catal. 348 (2006) 1605–1610, https://doi.org/10.1002/adsc.200606172.
[163] P. Stephenson, P. Licence, S.K. Ross, M. Poliakoff, Continuous catalytic asymmetric hydrogenation in supercritical CO 2, Green. Chem. 6 (2004) 521–523, https://doi.org/10.1039/b411955j.
[164] U. Hintermair, T. Höfener, T. Pullmann, G. Franciò, W. Leitner, Continuous enantioselective hydrogenation with a molecular catalyst in supported ionic liquid phase under supercritical CO 2 flow, ChemCatChem 2 (2010) 150–154, https://doi.org/10.1002/cctc.200900261.
[165] Z. Zhang, G. Franciò, W. Leitner, Continuous-flow asymmetric hydrogenation of an enol ester by using supercritical carbon dioxide: ionic liquids versus supported ionic liquids as the catalyst matrix, ChemCatChem 7 (2015) 1961–1965, https://doi.org/10.1002/cctc.201500295.
[166] C.S.G. Seo, R.H. Morris, Catalytic homogeneous asymmetric hydrogenation: successes and opportunities, Organometallics 38 (2019) 47–65, https://doi.org/10.1021/acs.organomet.8b00774.
[167] R. Skouta, Selective chemical reactions in supercritical carbon dioxide, water, and ionic liquids, Green. Chem. Lett. Rev. 2 (2009) 121–156, https://doi.org/10.1080/17518250903230001.
[168] M.J. Burk, S. Feng, M.F. Gross, W. Tumas, Asymmetric catalytic hydrogenation reactions in supercritical carbon dioxide, J. Am. Chem. Soc. 117 (1995) 8277–8278, https://doi.org/10.1021/ja00136a029.
[169] M.J. Burk, C2-symmetric bis(phospholanes) and their use in highly enantioselective hydrogenation reactions, J. Am. Chem. Soc. 113 (1991) 8519–8521, https://doi.org/10.1021/ja00022a048.
[170] Y. Crameri, J. Foricher, U. Hengartner, C.-J. Jenny, F. Kienzle, H. Ramuz, M. Scalone, M. Schlageter, R. Schmid, S. Wang, Asymmetric hydrogenation vs. resolution in the synthesis of POSICOR®, a new type of calcium antagonist, Chim. (Aarau) 51 (1997) 303, https://doi.org/10.2533/chimia.1997.303.
[171] S. Wang, F. Kienzle, Development of a continuous homogeneous metal complex catalyzed, asymmetric hydrogenation under high pressure (270 bar), Org. Process Res Dev. 2 (1998) 226–229, https://doi.org/10.1021/op980007p.
[172] S. Wang, F. Kienzle, The syntheses of pharmaceutical intermediates in supercritical fluids, Ind. Eng. Chem. Res 39 (2000) 4487–4490, https://doi.org/10.1021/ie0001319.
[173] R. Noyori, Asymmetric Catalysis in Organic Synthesis, John Wiley & Sons, New York, 1994.
[174] G. Rothenberg, Catalysis: Concepts and Green Applications, Wiley-VCH, Weinheim, 2008. ⟨https://www.wiley.com/en-us/Catalysis%3A+Concepts+and+Green+Applications%2C+2nd+Edition-p-9783527808908⟩. Accessed September 13, 2023.
[175] S. Kainz, A. Brinkmann, W. Leitner, A. Pfaltz, Iridium-catalyzed enantioselective hydrogenation of imines in supercritical carbon dioxide, J. Am. Chem. Soc. 121 (1999) 6421–6429, https://doi.org/10.1021/ja984309i.
[176] A.E. Meinders, A.C. Toornvliet, H. Pijl, De medicamenteuze behandeling van overgewicht [Drug treatment of obesity], Ned. Tijdschr. Geneeskd. 140 (1996), 1632–164.
[177] J. Theuerkauf, G. Franciò, W. Leitner, Continuous-flow asymmetric hydrogenation of the β-keto ester methyl propionylacetate in ionic liquid-supercritical carbon dioxide biphasic systems, Adv. Synth. Catal. 355 (2013) 209–219, https://doi.org/10.1002/adsc.201200724.
[178] Nanoparticles, Wiley-VCH Verlag GmbH & Co, in: G. Schmid (Ed.), KGaA, Weinheim, FRG, 2003, https://doi.org/10.1002/3527602399.
[179] L.S. Ott, R.G. Finke, Transition-metal nanocluster stabilization for catalysis: a critical review of ranking methods and putative stabilizers, Coord. Chem. Rev. 251 (2007) 1075–1100, https://doi.org/10.1016/j.ccr.2006.08.016.
[180] I. Favier, D. Pla, M. Gómez, Metal-based nanoparticles dispersed in glycerol: an efficient approach for catalysis, Catal. Today 310 (2018) 98–106, https://doi.org/10.1016/j.cattod.2017.06.026.
[181] F. Chahdoura, I. Favier, M. Gómez, Glycerol as suitable solvent for the synthesis of metallic species and catalysis, Chem. - A Eur. J. 20 (2014), https://doi.org/10.1002/chem.201403534.
[182] T. Dang-Bao, D. Pla, I. Favier, M. Gómez, Bimetallic nanoparticles in alternative solvents for catalytic purposes, Catalysts 7 (2017) 207, https://doi.org/10.3390/catal7070207.
[183] Y. Qiao, N. Said, M. Rauser, K. Yan, F. Qin, N. Theyssen, W. Leitner, Preparation of SBA-15 supported Pt/Pd bimetallic catalysts using supercritical fluid reactive deposition: how do solvent effects during material synthesis affect catalytic properties? Green. Chem. 19 (2017) 977–986, https://doi.org/10.1039/C6GC02490D.
[184] E. Reverchon, R. Adami, Nanomaterials and supercritical fluids, J. Supercrit. Fluids 37 (2006) 1–22, https://doi.org/10.1016/j.supflu.2005.08.003.
[185] J.A. Dahl, B.L.S. Maddux, J.E. Hutchison, Toward Greener Nanosynthesis, Chem. Rev. 107 (2007) 2228–2269, https://doi.org/10.1021/cr050943k.
[186] J.M. Patete, X. Peng, C. Koenigsmann, Y. Xu, B. Karn, S.S. Wong, Viable methodologies for the synthesis of high-quality nanostructures, Green. Chem. 13 (2011) 482, https://doi.org/10.1039/c0gc00516a.
[187] F. Cansell, C. Aymonier, Design of functional nanostructured materials using supercritical fluids, J. Supercrit. Fluids 47 (2009) 508–516, https://doi.org/10.1016/j.supflu.2008.10.002.
[188] S.E. Bozbağ, C. Erkey, Supercritical deposition: current status and perspectives for the preparation of supported metal nanostructures, J. Supercrit. Fluids 96 (2015) 298–312, https://doi.org/10.1016/j.supflu.2014.09.036.
[189] S.E. Bozbag, D. Sanli, C. Erkey, Synthesis of nanostructured materials using supercritical CO_2: Part II. Chemical transformations, J. Mater. Sci. 47 (2012) 3469–3492, https://doi.org/10.1007/s10853-011-6064-9.
[190] J.S. Wang, H.-B. Pan, C.M. Wai, Deposition of metal nanoparticles on carbon nanotubes via hexane modified water-in-co2 microemulsion at room temperature,

J. Nanosci. Nanotechnol. 6 (2006) 2025–2030, https://doi.org/10.1166/jnn.2006.367.
[191] J. Eastoe, M.J. Hollamby, L. Hudson, Recent advances in nanoparticle synthesis with reversed micelles, Adv. Colloid Interface Sci. 128–130 (2006) 5–15, https://doi.org/10.1016/j.cis.2006.11.009.
[192] K. Esumi, S. Sarashina, T. Yoshimura, Synthesis of gold nanoparticles from an organometallic compound in supercritical carbon dioxide, Langmuir 20 (2004) 5189–5191, https://doi.org/10.1021/la049415e.
[193] K.P. Johnston, S.R.P. da Rocha, Colloids in supercritical fluids over the last 20 years and future directions, J. Supercrit. Fluids 47 (2009) 523–530, https://doi.org/10.1016/j.supflu.2008.10.024.
[194] E. Castillejos, M. Jahjah, I. Favier, A. Orejón, C. Pradel, E. Teuma, A.M. Masdeu-Bultó, P. Serp, M. Gómez, Synthesis of platinum-ruthenium nanoparticles under supercritical co<inf>2</inf>and their confinement in carbon nanotubes: hydrogenation applications, ChemCatChem 4 (2012), https://doi.org/10.1002/cctc.201100244.
[195] K.S. Morley, P. Licence, P.C. Marr, J.R. Hyde, P.D. Brown, R. Mokaya, Y. Xia, S. M. Howdle, Supercritical fluids: a route to palladium-aerogel nanocomposites, J. Mater. Chem. 14 (2004) 1212–1217, https://doi.org/10.1039/b311065f.
[196] L.K. Yeung, C.T. Lee Jr., K.P. Johnston, R.M. Crooks, Catalysis in supercritical CO_2 using dendrimer-encapsulated palladium nanoparticles, Chem. Commun. (2001) 2290–2291, https://doi.org/10.1039/b106594g.
[197] H. Ohde, C.M. Wai, H. Kim, J. Kim, M. Ohde, Hydrogenation of olefins in supercritical CO_2 catalyzed by palladium nanoparticles in a water-in-CO_2 microemulsion, J. Am. Chem. Soc. 124 (2002) 4540–4541, https://doi.org/10.1021/ja012232j.
[198] M. Ohde, H. Ohde, C.M. Wai, Recycling nanoparticles stabilized in water-in-CO 2 microemulsions for catalytic hydrogenations, Langmuir 21 (2005) 1738–1744, https://doi.org/10.1021/la0482709.
[199] X.R. Ye, Y. Lin, C.M. Wai, Decorating catalytic palladium nanoparticles on carbon nanotubes in supercritical carbon dioxide, Chem. Commun. 3 (2003) 642–643, https://doi.org/10.1039/b211350c.
[200] X.R. Ye, Y. Lin, C. Wang, M.H. Engelhard, Y. Wang, C.M. Wai, Supercritical fluid synthesis and characterization of catalytic metal nanoparticles on carbon nanotubes, J. Mater. Chem. (2004) 908–913, https://doi.org/10.1039/b308124a.
[201] H. Sajiki, K. Hattori, K. Hirota, The formation of a Novel Pd/C−ethylenediamine complex catalyst: chemoselective hydrogenation without deprotection of the *O* -Benzyl and *N* -Cbz Groups, J. Org. Chem. 63 (1998) 7990–7992, https://doi.org/10.1021/jo9814694.
[202] S.S. Lee, B.K. Park, S.H. Byeon, F. Chang, H. Kim, Mesoporous silica-supported Pd nanoparticles; highly selective catalyst for hydrogenation of olefins in supercritical carbon dioxide, Chem. Mater. 18 (2006) 5631–5633, https://doi.org/10.1021/cm061060s.
[203] M. Chatterjee, Y. Ikushima, Y. Hakuta, H. Kawanami, In situ synthesis of gold nanoparticles inside the pores of MCM-48 in supercritical carbon dioxide and its catalytic application, Adv. Synth. Catal. 348 (2006) 1580–1590, https://doi.org/10.1002/adsc.200606137.
[204] T. Wu, T. Jiang, B. Hu, B. Han, J. He, X. Zhou, Cross-linked polymer coated Pd nanocatalysts on SiO2 support: Very selective and stable catalysts for hydrogenation in supercritical CO 2, Green. Chem. 11 (2009) 798–803, https://doi.org/10.1039/b822930a.
[205] K.M.K. Yu, P. Meric, S.C. Tsang, Micelle-hosted bimetallic Pd-Ru nanoparticle for in situ catalytic hydrogenation in supercritical CO_2, Catal. Today 114 (2006) 428–433, https://doi.org/10.1016/j.cattod.2006.02.076.
[206] G.D. Yadav, Y.S. Lawate, Selective hydrogenation of styrene oxide to 2-phenyl ethanol over polyurea supported Pd–Cu catalyst in supercritical carbon dioxide, J. Supercrit. Fluids 59 (2011) 78–86, https://doi.org/10.1016/j.supflu.2011.08.008.
[207] H.K. Kadam, S.G. Tilve, Advancement in methodologies for reduction of nitroarenes, RSC Adv. 5 (2015) 83391–83407, https://doi.org/10.1039/C5RA10076C.
[208] H.-U. Blaser, H. Steiner, M. Studer, Selective catalytic hydrogenation of functionalized nitroarenes: an update, ChemCatChem 1 (2009) 210–221, https://doi.org/10.1002/cctc.200900129.
[209] M. Orlandi, D. Brenna, R. Harms, S. Jost, M. Benaglia, Recent developments in the reduction of aromatic and aliphatic nitro compounds to amines, Org. Process Res Dev. 22 (2018) 430–445, https://doi.org/10.1021/acs.oprd.6b00205.
[210] H. Cheng, X. Meng, L. He, W. Lin, F. Zhao, Supported polyethylene glycol stabilized platinum nanoparticles for chemoselective hydrogenation of halonitrobenzenes in scCO2, J. Colloid Interface Sci. 415 (2014) 1–6, https://doi.org/10.1016/j.jcis.2013.10.011.
[211] M. Chatterjee, T. Ishizaka, T. Suzuki, A. Suzuki, H. Kawanami, In situ synthesized Pd nanoparticles supported on B-MCM-41: an efficient catalyst for hydrogenation of nitroaromatics in supercritical carbon dioxide, Green. Chem. 14 (2012) 3415, https://doi.org/10.1039/c2gc36160d.
[212] M. Chatterjee, T. Ishizaka, H. Kawanami, Preparation and characterization of PdO nanoparticles on trivalent metal (B, Al and Ga) substituted MCM-41: Excellent catalytic activity in supercritical carbon dioxide, J. Colloid Interface Sci. 420 (2014) 15–26, https://doi.org/10.1016/j.jcis.2013.12.061.
[213] X. Li, P. Jia, T. Wang, Furfural: a promising platform compound for sustainable production of C 4 and C 5 chemicals, ACS Catal. 6 (2016) 7621–7640, https://doi.org/10.1021/acscatal.6b01838.
[214] R. Rao, A. Dandekar, R.T.K. Baker, M.A. Vannice, Properties of copper chromite catalysts in hydrogenation reactions, J. Catal. 171 (1997) 406–419, https://doi.org/10.1006/jcat.1997.1832.
[215] D. Liu, D. Zemlyanov, T. Wu, R.J. Lobo-Lapidus, J.A. Dumesic, J.T. Miller, C. L. Marshall, Deactivation mechanistic studies of copper chromite catalyst for selective hydrogenation of 2-furfuraldehyde, J. Catal. 299 (2013) 336–345, https://doi.org/10.1016/j.jcat.2012.10.026.
[216] G. Seo, H. Chon, Hydrogenation of furfural over copper-containing catalysts, J. Catal. 67 (1981) 424–429, https://doi.org/10.1016/0021-9517(81)90302-X.
[217] E. Sánchez-Miguel, M.J. Tenorio, J. Morère, A. Cabañas, Green preparation of PtRu and PtCu/SBA-15 catalysts using supercritical CO_2, J. CO_2 Util. 22 (2017) 382–391, https://doi.org/10.1016/j.jcou.2017.10.018.
[218] J. Morère, E. Sánchez-Miguel, M.J. Tenorio, C. Pando, A. Cabañas, Supercritical fluid preparation of Pt, Ru and Ni/graphene nanocomposites and their application as selective catalysts in the partial hydrogenation of limonene, J. Supercrit. Fluids 120 (2017) 7–17, https://doi.org/10.1016/j.supflu.2016.10.007.
[219] J. Morère, M.J. Torralvo, C. Pando, J.A.R. Renuncio, A. Cabañas, Supercritical fluid deposition of Ru nanoparticles onto SiO 2 SBA-15 as a sustainable method to prepare selective hydrogenation catalysts, RSC Adv. 5 (2015) 38880–38891, https://doi.org/10.1039/C5RA04969E.
[220] C.M. Piqueras, V. Gutierrez, D.A. Vega, M.A. Volpe, Selective hydrogenation of cinnamaldehyde in supercritical CO_2 over Pt/SiO2 and Pt/HS-CeO2: an insight about the role of carbonyl interaction with supercritical CO_2 or with ceria support sites in cinamyl alcohol selectivity, Appl. Catal. A Gen. 467 (2013) 253–260, https://doi.org/10.1016/j.apcata.2013.07.028.
[221] M. Chatterjee, Y. Ikushima, T. Yokoyama, T. Suzuki, Effect of heteroatom substituted mesoporous support on the selective hydrogenation of cinnamaldehyde in supercritical carbon dioxide, Microporous Mesoporous Mater. 117 (2009) 201–207, https://doi.org/10.1016/j.micromeso.2008.06.029.
[222] S. Kato, H. Nanao, M. Shirai, Graphite intercalated iridium nanodisks for cinnamaldehyde hydrogenation, Chem. Lett. 48 (2019) 1262–1265, https://doi.org/10.1246/cl.190527.
[223] H. Amanuma, H. Nanao, M. Shirai, Cinnamaldehyde hydrogenation over platinum nanosheet intercalated graphite layers in supercritical carbon dioxide solvent, Chem. Lett. 47 (2018) 475–478, https://doi.org/10.1246/cl.180037.
[224] M. Sodeno, S. Kato, H. Nanao, M. Shirai, Preparation and structural characterization of platinum nanosheets intercalated between graphite powder with high surface area, Catal. Today 375 (2021) 48–55, https://doi.org/10.1016/j.cattod.2020.04.038.
[225] T. Shimizu, M. Ota, Y. Sato, H. Inomata, Effect of pore structure on catalytic properties of mesoporous silica supported rhodium catalysts for the hydrogenation of cinnamaldehyde, Chem. Eng. Res. Des. 104 (2015) 174–179, https://doi.org/10.1016/j.cherd.2015.08.004.
[226] U.K. Singh, M.A. Vannice, Liquid-phase citral hydrogenation over SiO2-supported Group VIII metals, J. Catal. 199 (2001) 73–84, https://doi.org/10.1006/jcat.2000.3157.
[227] P. Meric, K.M.K. Yu, S.C. Tsang, Micelle-hosted palladium nanoparticles catalyze citral molecule hydrogenation in supercritical carbon dioxide, Langmuir 20 (2004) 8537–8545, https://doi.org/10.1021/la049549s.
[228] P. Meric, K.M.K. Yu, S.C. Tsang, Molecular guided catalytic hydrogenation by micelle-hosted pd nanoparticle in supercritical CO_2, Catal. Lett. 95 (2004) 39–43, https://doi.org/10.1023/B-CATL.0000023719.53121.97.
[229] P. Meric, K.M.K. Yu, A.T.S. Kong, S.C. Tsang, Pressure-dependent product distribution of citral hydrogenation over micelle-hosted Pd and Ru nanoparticles in supercritical carbon dioxide, J. Catal. 237 (2006) 330–336, https://doi.org/10.1016/j.jcat.2005.11.010.
[230] S. Song, R. Liu, Y. Zhang, J. Feng, D. Liu, Y. Xing, F. Zhao, H. Zhang, Colloidal noble-metal and bimetallic alloy nanocrystals: A general synthetic method and their catalytic hydrogenation properties, Chem. - A Eur. J. 16 (2010) 6251–6256, https://doi.org/10.1002/chem.200903279.
[231] B.M. Nagaraja, V. Siva Kumar, V. Shashikala, A.H. Padmasri, S. Sreevardhan Reddy, B. David Raju, K.S. Rama Rao, Effect of method of preparation of copper - Magnesium oxide catalyst on the dehydrogenation of cyclohexanol, in: J Mol Catal A Chem, 2004: pp. 339–345. https://doi.org/10.1016/j.molcata.2003.11.046.
[232] V.Z. Fridman, A.A. Davydov, K. Titievsky, Dehydrogenation of cyclohexanol on copper-containing catalysts: II. The pathways of the cyclohexanol dehydrogenation reaction to cyclohexanone on copper-active sites in oxidation state Cu0 and Cu+, J. Catal. 222 (2004) 545–557, https://doi.org/10.1016/j.jcat.2003.12.016.
[233] S. Narayanan, K. Krishna, Structure activity relationship in pd/hydrotalcite: effect of calcination of hydrotalcite on palladium dispersion and phenol hydrogenation, Catal. Today 49 (1999) 57–63, https://doi.org/10.1016/S0920-5861(98)00408-8.
[234] S. Velu, M.P. Kapoor, S. Inagaki, K. Suzuki, Vapor phase hydrogenation of phenol over palladium supported on mesoporous CeO2 and ZrO2, Appl. Catal. A Gen. 245 (2003) 317–331, https://doi.org/10.1016/S0926-860X(02)00655-5.
[235] M. Chatterjee, H. Kawanami, M. Sato, A. Chatterjee, T. Yokoyama, T. Suzuki, Hydrogenation of phenol in supercritical carbon dioxide catalyzed by palladium supported on Al-MCM-41: A facile route for one-pot cyclohexanone formation, Adv. Synth. Catal. 351 (2009) 1912–1924, https://doi.org/10.1002/adsc.200900144.
[236] H. Wang, F. Zhao, S. Ichiro Fujita, M. Arai, Hydrogenation of phenol in scCO2 over carbon nanofiber supported Rh catalyst, Catal. Commun. 9 (2008) 362–368, https://doi.org/10.1016/j.catcom.2007.07.002.
[237] B. Il Lee, D. Bae, J.K. Kang, H. Kim, S.H. Byeon, Synthesis of SBA-15 supported Rh nanoparticles with high loading density and its catalytic hydrogenation of phenol in supercritical carbon dioxide, Bull. Korean Chem. Soc. 30 (2009) 1701–1702, https://doi.org/10.5012/bkcs.2009.30.8.1701.

[238] M. Ohde, H. Ohde, C.M. Wai, Catalytic hydrogenation of arenes with rhodium nanoparticles in a water-in-supercritical CO2microemulsion, Chem. Commun. 2 (2002) 2388–2389, https://doi.org/10.1039/b205993m.
[239] S. Kacem, Y. Qiao, C. Wirtz, N. Theyssen, A. Bordet, W. Leitner, Supercritical carbon dioxide as reaction medium for selective hydrogenation of fluorinated arenes, Green. Chem. 24 (2022) 8671–8676, https://doi.org/10.1039/D2GC02623F.
[240] S.E. Lyubimov, M.V. Sokolovskaya, A.A. Korlyukov, O.P. Parenago, V. A. Davankov, Iridium nanoparticles deposited on hypercrosslinked polystyrene: synthesis and application in the hydrogenation of aromatic compounds, J. Iran. Chem. Soc. 17 (2020) 1283–1287, https://doi.org/10.1007/S13738-020-01854-W/TABLES/1.
[241] S.E. Lyubimov, A.A. Zvinchuk, A.A. Korlyukov, V.A. Davankov, O.P. Parenago, Palladium nanoparticles in hypercrosslinked polystyrene: synthesis and application in the hydrogenation of arenes, Pet. Chem. 61 (2021) 76–80, https://doi.org/10.1134/S0965544121010084/TABLES/2.
[242] K. Hussain, R.R. Hoque, S. Balachandran, S. Medhi, M.G. Idris, M. Rahman, F. L. Hussain, Monitoring and risk analysis of PAHs in the environment, in: Handbook of Environmental Materials Management, Springer International Publishing, 2019, pp. 973–1007, https://doi.org/10.1007/978-3-319-73645-7_29.
[243] W. Liao, H.W. Liu, H.J. Chen, W.Y. Chang, K.H. Chiu, C.M. Wai, Catalytic hydrogenation rate of polycyclic aromatic hydrocarbons in supercritical carbon dioxide containing polymer-stabilized palladium nanoparticles, Chemosphere 82 (2011) 573–580, https://doi.org/10.1016/j.chemosphere.2010.09.078.
[244] H.J. Chen, H.W. Liu, W. Liao, H. Bin Pan, C.M. Wai, K.H. Chiu, J.F. Jen, Highly active and reusable palladium nanoparticle catalyst stabilized by polydimethylsiloxane for hydrogenation of aromatic compounds in supercritical carbon dioxide, Appl. Catal. B 111–112 (2012) 402–408, https://doi.org/10.1016/j.apcatb.2011.10.025.
[245] N. Hiyoshi, C.V. Rode, O. Sato, Y. Masuda, A. Yamaguchi, M. Shirai, Particle-size effects of activated carbon-supported rhodium catalysts on hydrogenation of naphthalene in supercritical carbon dioxide solvent, Chem. Lett. 37 (2008) 734–735, https://doi.org/10.1246/cl.2008.734.
[246] M.V. Escárcega-Bobadilla, C. Tortosa, E. Teuma, C. Pradel, A. Orejón, M. Gómez, A.M. Masdeu-Bultó, Ruthenium and rhodium nanoparticles as catalytic precursors in supercritical carbon dioxide, Catal. Today 148 (2009), https://doi.org/10.1016/j.cattod.2009.07.112.